The Extragalactic Background Light and the Gamma-ray Opacity of the Universe

Eli Dwek

Observational Cosmology Lab., Code 665, NASA Goddard Space Flight Center,
Greenbelt, MD 20771; e-mail: eli.dwek@nasa.gov

Frank Krennrich

Department of Physics and Astronomy, Iowa State University, Ames, IA 50011;
e-mail: krennrich@iastate.edu

Abstract

The extragalactic background light (EBL) is one of the fundamental observational quantities in cosmology. All energy releases from resolved and unresolved extragalactic sources, and the light from any truly diffuse background, excluding the cosmic microwave background (CMB), contribute to its intensity and spectral energy distribution. It therefore plays a crucial role in cosmological tests for the formation and evolution of stellar objects and galaxies, and for setting limits on exotic energy releases in the universe. The EBL also plays an important role in the propagation of very high energy $\gamma-$rays which are attenuated en route to Earth by pair producing $\gamma-\gamma$ interactions with the EBL and CMB. The EBL affects the spectrum of the sources, predominantly blazars, in the $\sim$ 10 GeV to 10 TeV energy regime. Knowledge of the EBL intensity and spectrum will allow the determination of the intrinsic blazar spectrum in a crucial energy regime that can be used to test particle acceleration mechanisms and VHE $\gamma-$ray production models. Conversely, knowledge of the intrinsic $\gamma-$ray spectrum and the detection of blazars at increasingly higher redshifts will set strong limits on the EBL and its evolution. This paper reviews the latest developments in the determination of the EBL and its impact on the current understanding of the origin and production mechanisms of $\gamma-$rays in blazars, and on energy releases in the universe. The review concludes with a summary and future directions in Cherenkov Telescope Array techniques and in infrared ground-based and space observatories that will greatly improve our knowledge of the EBL and

Preprint submitted to Astroparticle Physics *September 18, 2012*

the origin and production of very high energy $\gamma-$rays.

Keywords: extragalactic background light, cosmic infrared background, cosmology, dark matter, galaxy evolution, gamma-ray astronomy, GeV/TeV sources, blazars, gamma-ray opacity

---

1. Introduction

The extragalactic background light (EBL), defined here as the emission in the 0.1 to 1000 μm wavelength region, is one of the fundamental observational quantities in cosmology. It comprises the integrated light from resolved and unresolved extragalactic sources, and the light from any truly diffuse background, excluding the cosmic microwave background (CMB). It is therefore the repository of all energy released by nuclear and gravitational processes since the epoch of recombination. A significant fraction of this radiation is shifted by cosmic expansion and by absorption and reradiation by dust into infrared (IR) wavelengths. Consequently, its intensity and spectral shape hold key information about the formation and evolution of galaxies and their stellar and interstellar contents throughout cosmic history. A strict lower limit on the EBL intensity is provided by the integrated light from resolved galaxies, hereafter referred to as the integrated galaxy light (IGL).

The EBL plays also an important role in the propagation of high energy $\gamma-$ray rays that are predominantly emitted by blazars, a subgroup of active galaxies hosting active galactic nuclei (AGN), whose relativistic jet is pointed towards the Earth. High energy photons emitted by blazars are attenuated by photon-photon interactions with the EBL, a process that can be used to set important limits on both, the intrinsic spectra of blazars and the intensity of the EBL in select energy and wavelength regions where these interactions are most prominent.

The EBL is intimately connected to the diffuse X-ray, radio, and supernova neutrino backgrounds. Deep X-ray surveys have resolved the X-ray background into point sources, most of which are dust enshrouded AGNs (Mushotzky et al., 2000). Up to 90% of the X-ray energy produced in individual AGN can be degraded and reradiated predominantly at mid-IR wavelengths (e.g. Franceschini et al., 2002; Ballantyne et al., 2006). Consequently, the X-ray background can be used to predict the EBL intensity at at these wavelengths. Current estimates show that about 15% of the 24 μm EBL intensity is powered by AGN activity (Treister et al., 2006; Soifer et al., 2008, and references therein). Conversely, the connection between mid-IR bright sources and AGN can be used to estimate the contribution of obscured AGN to the X-ray background (Gandhi & Fabian, 2003; Soifer et al., 2008, and references therein).

Massive stars that power the IR emission also emit radio free-free emission during the main sequence phase, and radio synchrotron emission during the supernova remnant phase of their evolution. The IR emission from star-forming galaxies is therefore correlated with the radio emission (Lisenfeld et al., 1996; Condon et al., 1991). This correlation can be used to estimate the contribution of star-forming galaxies to the cosmic radio background (Haarsma & Partridge, 1998; Dwek & Barker, 2002; Ponente et al., 2011).

Most of the EBL intensity is powered by massive stars that end their life as core collapse supernovae. The total EBL intensity can therefore be used to derive an estimate of the supernova rate and the resulting flux of supernova neutrinos (Horiuchi et al., 2009; Beacom, 2010). The detectability of these neutrinos can be greatly enhanced by the proposed introduction of gadolinium in existing large water Cherenkov detectors (such as Super-Kamiokande) (Beacom & Vagins, 2004). Gadolinium has a very high capture cross section for neutrons generated in $\bar{\nu}_e + p \rightarrow e^+ + n$ reactions, and can be introduced in the form of soluble trichloride ($GdCl_3$). Following the neutron capture, the Gd emits an 8 MeV $\gamma-$ray which produces relativistic electrons by Compton scattering. The Cherenkov radiation from these electrons is more easily detected than that produced in the cascade of the 2.2 MeV $\gamma-$ray generated by the capture of neutrons by free protons.

Several reviews have appeared in the literature, presenting a historical overview of the importance of the EBL, early estimates of its intensity, the quests for its detection, and its many astrophysical implications (Hauser & Dwek, 2001; Kashlinsky, 2005; Lagache et al., 2005). Since these reviews were written significant advances have been made in studies of the EBL with the launch of UV (*Galex*) and IR space observatories (*Spitzer*, *Herschel*, and *Akari*). These observatories, together with ground-based telescopes, such as 2MASS, have provided new limits on the EBL ranging from UV to submillimeter wavelengths. Deeper galaxy number counts and new data analysis techniques of stacking astronomical images have narrowed the gap between the contribution of resolved galaxies and the true intensity of the EBL.

The *Fermi* Gamma-ray Space Telescope, operating between 200 MeV and 300 GeV, and ground-based air Cherenkov detectors (H.E.S.S., MAGIC, and VERITAS) operating in the $\sim$ 50 GeV to 100 TeV range have broadened the energy window for the studies of $\gamma-$ray sources. These advances have led to the detection of new GeV and TeV $\gamma-$ray sources and provided new data for determining their intrinsic spectra. Reviews of these subjects were presented by Weekes (2008) and Hinton & Hofmann (2009). More recently, Dermer (2012) presented a review of the *Fermi* catalog of $\gamma-$ray sources and the physics of the production of relativistic particles and $\gamma-$rays from these sources. Table 1 presents a glossary to the acronyms of the observatories and instruments referred to in this review.

These developments provide the main impetus for this review. We first present, in §2, the basic formulae describing the attenuation of photons by pair producing interactions with other photons. We then show how this attenuation will affect γ rays traversing a radiation field characterized first by a pure black body, representing the stellar emission component of the EBL, and then by a more realistic EBL that includes the dust emission component. This attenuation can, in principle, be used to determine the intensity of the attenuating radiation field if the intrinsic source spectrum is known. In §3 we survey the type of $\gamma-$ray sources that are used in these studies, their spectral characteristics, the physical mechanisms for generating their spectra, and constraints on their spectral shape imposed by general physical principles. In §4 we summarize measurements and limits on the EBL intensity determined by direct measurements and by adding the light from resolved galaxies. Models for the EBL intensity and its evolution with redshift are summarized in §5. In §6 we summarize the constraints on the EBL intensity derived from $\gamma-$ray observations of blazars, emphasizing the different assumptions made on the intrinsic blazar spectra to derive these limits. EBL models predict the $\gamma-$ray opacity of the universe at different energies, and in §7 we compare these model predictions with blazar observation. Throughout this review it was tacitly assumed that the production of $\gamma-$rays takes place exclusively in the sources. In §8 we consider alternative scenarios of $\gamma-$ray production that could have important implications for EBL limits, namely, that a significant fraction of the observed $\gamma-$rays could be produced en route to Earth. The role of the EBL in setting limits on exotic energy releases in the universe in briefly discussed in §9. A summary and future prospects for the fields of $\gamma-$ray and EBL research is given in §10.

2. The EBL and the Attenuation of Gamma-Ray Photons

2.1. The EBL

The differential specific flux at wavelength λ_0, $\mathrm{d}F_\nu(\lambda_0)$, received from radiative sources within a comoving volume element $\mathrm{d}V_c(z)$ at redshift z at wavelength λ is given by (e.g. Mo et al., 2010):

$$\mathrm{d}F_\nu(\lambda_0) = (1+z)\,\frac{\mathcal{L}_\nu(\lambda, z)\,\mathrm{d}V_c(z)}{4\pi\, d_L(z)^2} \tag{1}$$

where $\mathcal{L}_\nu(\lambda, z)$ is the comoving specific luminosity density of the sources, d_L is their luminosity distance, and the (1+z) factor arises from the decrease in energy of the emitted photons due to the redshift, and $\lambda_0 = (1+z)\lambda$.

The specific comoving intensity of the EBL per unit solid angle, $\delta\Omega$, at redshift z_0 and wavelength λ_0 is given by an integral over all energy releases over cosmic history:

$$\begin{aligned} I_\nu(\lambda_0, z_0) &= \int_{z_0}^{\infty} (1+z)\frac{\mathcal{L}_\nu(\lambda, z)}{4\pi\, d_L(z)^2}\,\frac{\mathrm{d}V_c(z)}{\delta\Omega} \qquad (2)\\ &= \left(\frac{1}{4\pi}\right)\int_{z_0}^{\infty} \mathcal{L}_\nu(\lambda, z)\left|\frac{c\,dt}{dz}\right| dz \end{aligned}$$

where $c|dt/dz|$ is given by (e.g. Mo et al., 2010):

$$c\left|\frac{dt}{dz}\right| = \frac{R_H}{(1+z)E(z)}; \qquad R_H \equiv \frac{c}{H_0} \tag{3}$$

$$\begin{aligned} E(z) &\equiv \left[\Omega_R(1+z)^4 + \Omega_m(1+z)^3 + \Omega_k(1+z)^2 + \Omega_\Lambda\right]^{1/2} \\ &= \left[(1+z)^2\,(\Omega_m z + 1) - z(2+z)\,\Omega_\Lambda\right]^{1/2} \qquad (4)\\ &= \left[\Omega_m(1+z)^3 + \Omega_\Lambda\right]^{1/2} \qquad . \end{aligned}$$

H_0 is the Hubble constant, and Ω_R Ω_m, Ω_k and Ω_Λ are the dimensionless density parameters of the radiation, matter, the curvature, and the cosmological constant Λ, obeying the relation: $\Omega_R + \Omega_m + \Omega_k + \Omega_\lambda = 1$. The second expression for $E(z)$ is for a matter dominated ($\Omega_R << 1$) universe, and the third is for one that is matter dominated and flat ($\Omega_k = 0$). In the concordance cosmology model: $H_0 = 70$ km s^{-1} Mpc^{-1}; $\Omega_m = 0.27$, and $\Omega_\Lambda = 0.73$ (Hinshaw et al., 2009).

2.2. Gamma-ray attenuation by pair production

The interaction between two photons with energies E_γ and $\epsilon_{\rm b}$, will lead to the creation of a particle anti-particle pair when the total $\gamma-$ray energy in the center of momentum of the system exceeds the rest frame energy of the two particles. The threshold for the creation of an $e^+ + e^-$ pair is given by:

$$\epsilon_{th}(E_\gamma, \mu, z) = \frac{2\,(m_e\, c^2)^2}{E_\gamma\,(1-\mu)} \tag{5}$$

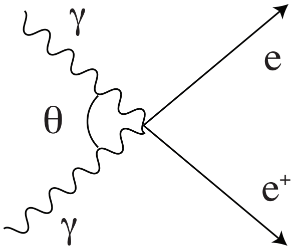

Figure 1: Schematic illustration of the $\gamma - \gamma$ pair production reaction, showing the definition of the angle θ between the interacting photons.

where $\mu \equiv \cos\theta$, and θ is the angle between the two photons, as illustrated in Figure 1.

The cross-section for the $\gamma - \gamma$ interaction is given by:

$$\sigma_{\gamma\gamma}(E_\gamma, \epsilon, \mu, z) = \frac{3\sigma_T}{16}\,(1-\beta^2)\left[2\beta\,(\beta^2-2) + (3-\beta^4)\,\ln\left(\frac{1+\beta)}{(1-\beta)}\right)\right] \tag{6}$$

where

$$\beta \equiv \sqrt{\left(1 - \frac{\epsilon_{th}}{\epsilon}\right)} \tag{7}$$

Figure 2 (left panel) depicts the cross section as a function of β. The cross section peaks at a value of $\beta = 0.70$, providing a relation between the energies E_γ and ϵ (or wavelength λ) at the peak, given by:

$$E_\gamma(TeV) = \frac{1.07}{\epsilon(eV)\,(1-\mu)} = \frac{0.86\,\lambda(\mu m)}{(1-\mu)} \tag{8}$$

The right panel of the figure depicts the cross section as a function of $b \equiv 2(mc^2)^2/E_\gamma\epsilon$ for different values of the angle θ. When the photons are moving in the same direction ($\theta = 0$), the cross section collapses to a delta-function at $b = 0$, and the energy threshold becomes infinite.

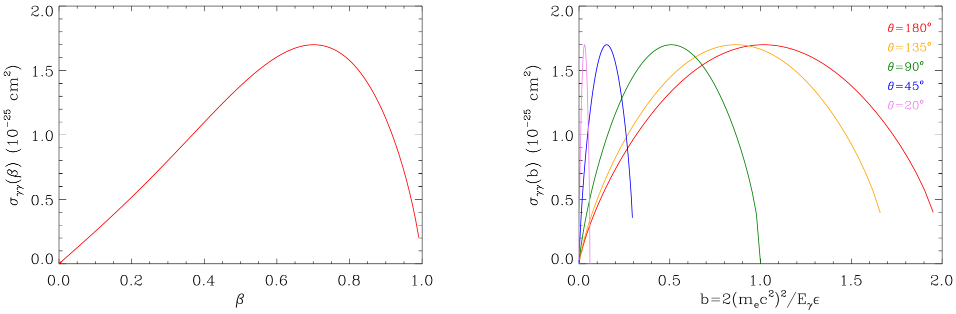

Figure 2: The cross section for the $\gamma-\gamma$ interaction. **Left panel**: its dependence on β [eq. (7)]; **Right panel**: its dependence on b for different angles of incidence.

2.3. The Attenuation of $\gamma-$rays from Cosmological Sources

En route to Earth, $\gamma-$rays from cosmological sources have to pass through the radiation field of the EBL, resulting in their attenuation by pair producing interactions. The optical depth of a $\gamma-$ray photon at an observed energy E_γ, emitted by a source at redshift z due to this process is given by:

$$\tau_{\gamma\gamma}(E_\gamma, z) = \int_0^z dz' \, \frac{d\ell}{dz'} \int_{-1}^{1} d\mu \, \frac{1-\mu}{2} \int_{\epsilon'_{th}}^{\infty} d\epsilon \, n_\epsilon(\epsilon, z')(1+z')^3 \, \sigma_{\gamma\gamma}(\beta', z') \qquad (9)$$

where $n_\epsilon(\epsilon, z) \equiv dn(\epsilon, z)/d\epsilon$ is the specific comoving number density (cm^{-3} eV^{-1}) of background photons with energy ϵ at redshift z, and the $(1+z)^3$ term represents its conversion to a proper number density. The pair-production threshold energy is $\epsilon'_{th} = 2(m_e c^2)^2/E_\gamma(1-\mu)(1+z)$, where the $(1+z)$ factor takes into account that the observed $\gamma-$ray photon had a higher energy at the redshift of the interaction. The parameter $\beta' = (1 - \epsilon'_{th}/\epsilon)^{1/2}$, and $d\ell/dz = c|dt/dz|$, where ℓ is the proper distance.

Calculating the EBL opacity to $\gamma-$rays from cosmological distant sources requires knowledge of the evolution of the comoving specific photon number density $n_\epsilon(\epsilon, z)$ as a function of redshift. The specific number density of photons with energy ϵ at redshift z is related to the specific EBL intensity at a given redshift z by:

$$\begin{aligned} \epsilon^2 \, n_\epsilon(\epsilon, z) &= \frac{4\pi}{c} \, \nu \, I_\nu(\nu, z) \\ &= 2.62 \times 10^{-4} \, \nu \, I_\nu(\nu, z) \end{aligned} \qquad (10)$$

where $\epsilon = h\nu$, $I_\nu(\nu, z)$ is given by eq. (2), and the coefficient in the second line was calculated for ϵ in eV, n_ϵ in cm^{-3} eV^{-1}, and $\nu \, I_\nu$ in nW m^{-2} sr^{-1}.

Finally, we point out that the $\gamma - \gamma$ cross section is wide, so that in calculating the $\gamma-$ray opacity, strong variations in the EBL spectrum are smoothed out over a wide range of $\gamma-$ray energies. The EBL intensity at a given wavelength is therefore effecting $\tau_{\gamma\gamma}$ over a wide range of $\gamma-$ray energies around the peak given by eq. (8).

2.4. A Simple Example: An EBL given by a diluted blackbody spectrum

Of particular interest is the behavior of $\tau_{\gamma\gamma}$ for a background radiation field that is represented by a diluted blackbody. Figure 3 (upper left panel) depicts a local EBL characterized by a Planck function, normalized to an intensity of 10 nW m^{-2} sr^{-1} at 1 μm. The upper right panel of the figure depicts the photon number density. The bottom left panel shows the $\gamma-$ray opacity at redshift $z = 0.2$, assuming a non-evolving EBL, and the right panel shows the source attenuation as a function of $\gamma-$ray energies. Also shown in the figure are the energy regimes in which substantial changes in the slope of the opacity occur (dashed lines).

The rapid rise in the EBL spectrum between 0.5 and 1 μm results in a rise of the $\gamma-$ray opacity, and the onset of substantial source attenuation in the 10 to 500 GeV energy region. This sudden increase in the GeV attenuation creates a break, Γ_{GeV}, in the spectrum, defined as the difference in power law index between the unattenuated and the attenuated region of the spectrum (see Figure 5 in this paper). At higher $\gamma-$ray energies, the spectrum of a blazar characterized by an intrinsic power law will exhibit a second spectral break around $\sim$ 1 TeV. For an evolving EBL, the magnitude and location of this spectral break are expected to evolve with redshift. The substantial decrease in the attenuation at a few TeV is a consequence of the particular choice of the EBL spectrum , which decreases rapidly at wavelengths beyond $\sim$ 2 μm.

2.5. A More Realistic Example: An EBL that includes dust emission

Figure 4 depicts a more realistic presentation of the current EBL spectrum (left panel) and the $\gamma-$ray opacity for different redshifts (right panel), taken from model calculations of Finke et al. (2010). At wavelengths short wards of $\sim$ 5 μm the spectrum represents the stellar and AGN contributions to the EBL. At longer wavelengths the spectrum represents the AGN and starlight energy that was absorbed and reradiated by the dust. The right panel shows the energy dependence of the $\gamma-$ray opacity for sources at different redshifts. The opacity calculations took into account the evolution of the EBL with

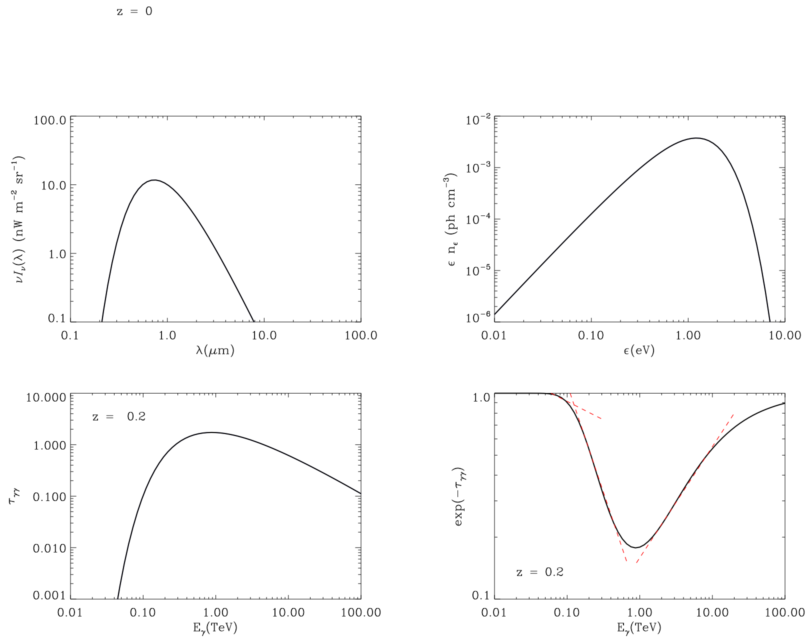

Figure 3: **Top left**: A diluted black body representation of the stellar emission component of the EBL; **Top right**: The corresponding proper photon number density versus energy; **Bottom left**: The $\gamma-$ray opacity versus energy, E_γ; **Bottom right**: The $\gamma-$ray attenuation. The figure illustrates the dramatic change in the attenuation at the $\gamma-$ray energy that corresponds to the wavelength at which the slope of the EBL spectrum changes. The different slopes are depicted as dashed lines in the figure.

redshift. The figure illustrates the relation between the EBL spectrum and the energy dependence of the $\gamma-$ray opacity. The initial rise of the EBL intensity at UV-optical wavelengths causes an increase in the $\gamma - \gamma$ opacity between 10 and 500 GeV. The decline in the EBL intensity between ~ 1 and 15 μm causes $\tau_{\gamma\gamma}$ to rise less rapidly between 1 and 10 TeV. The slope of $\tau_{\gamma\gamma}$ in this region reflects the ratio of the ~ 1 to 15 μm intensities of the EBL. The rise in $\tau_{\gamma\gamma}$ beyond 10 TeV reflects the rise in the EBL towards the peak of the dust emission at $\sim 100 - 200$ μm.

The energy dependence of $\tau_{\gamma\gamma}$ will give rise to several breaks in the spectrum of $\gamma-$ray sources that reflect the changes in the slope of the opacity. The first spectral break, $\Delta\Gamma_{GeV}$ occurs between 10 and 500 GeV. The second, $\Delta\Gamma_{TeV}$ around 1 TeV, and the third around 10 TeV.

The first break has been used in most EBL studies to date with various assumptions on the intrinsic source spectra, and the second break has been most recently explored in the analysis of Orr et al. (2011). A review of studies that utilize the first and second break for constraining the EBL is presented

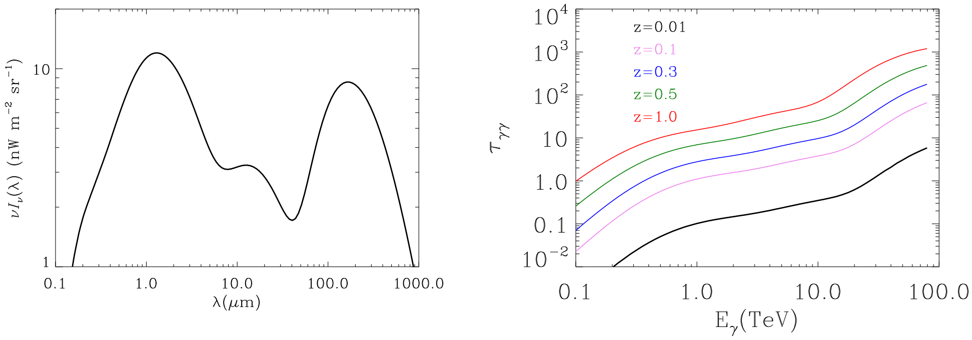

Figure 4: **Left panel**: Calculated EBL intensity versus wavelength at $z = 0$; **Right panel**: The $\gamma-$ray opacity versus energy for sources at different redshift (see labels). The figure illustrates the correlation between the changes in the slope of the EBL intensity with those in $\tau_{\gamma\gamma}$. Model calculations by Finke et al. (2010). Details in §2.5 of the text.

in §6. A break at $\sim$ 10 TeV has yet to be discovered. Starburst galaxies, which have a hard $\gamma-$ray spectrum, are the most promising subject for such analysis.

3. The Types and Spectra of Extragalactic GeV/TeV Sources

Determination of the EBL intensity from GeV–TeV $\gamma-$ray observations requires knowledge of the intrinsic spectrum of the sources. Here we list the different sources, their spectral characteristics, the different proposed mechanisms for their $\gamma-$ray production, and the physical limits on their spectral energy distribution at very high energies.

3.1. The Types of Extragalactic GeV/TeV Sources

The currently available GeV–TeV $\gamma-$ray sources that are being used to derive limits and constraints on the EBL are listed in Table 2. They include the accretion-powered relativistic jets of active galactic nuclei (AGNs), namely BL Lacertae objects (BL Lacs), flat spectrum radio quasars (FSRQs) and a few radio galaxies. The list is complemented by the recent detections of two nearby starburst (SB) galaxies. In contrast to AGNs, their $\gamma-$ray spectrum is generated by the cumulative effects of cosmic-ray acceleration in shocks generated by a large number of supernova remnants (Völk et al., 1996).

Blazars: To date, the most numerous sources used in EBL studies are blazars. Historically, they have been divided into two sub-classes based on their optical properties: FSRQs, characterized by strong emission lines; and BL Lacs, characterized by weak or lack of emission lines. Because of the weakness of their emission lines, the redshift determination of BL Lac blazars has proven difficult or even impossible in many cases. The status of blazars as bright GeV and TeV sources arises from the fact that their relativistic jets are closely aligned with the observers line of sight. Consequently, the luminosity of a $\gamma-$ray emission region moving relativistically along the jet axis in the direction of the observer is strongly beamed, enabling its detection at cosmological distances. Occasional strong flaring activity renders the following BL Lacs: PKS2155 (Aharonian et al., 2007b); Mrk 501 (Catanese et al., 1997; Abdo et al., 2011a), and Mrk 421, (Gaidos et al., 1996; Acciari et al., 2011a; Aleksic et al., 2011) the brightest TeV sources; and the following FSRQs: 3C 454.3 (Donnarumma et al., 2009), and 3C 279, (Wehrle et al., 1998) the brightest GeV emitters in the sky. The flaring has provided high quality $\gamma-$ray spectra and has led to their detection at redshifts as far as $z \approx 0.5$ at TeV energies with IACTs, and as far as $z \approx 3.2$ at ~ 10 GeV energies with *Fermi*.

The combined GeV-TeV observations of blazars makes it possible to study their spectra over a larger range of redshifts, thereby enabling the studies of the EBL over a wider range of wavelengths. GeV photons interact mainly with UV/optical photons, whereas TeV photons probe mainly the near- to mid-IR region of the EBL. Since the intensity of the EBL is much lower at UV energies, the universe is transparent to $\gamma-$rays below 10 GeV, becoming essentially opaque for TeV sources at redshifts of z > 0.5. The *Fermi* Gamma-Ray Space Telescope provides important probes of the UV region of the EBL, and the GeV transparency can be used to test evolutionary models of the EBL to relatively large redshifts ($z > 1$).

Radio galaxies: The jets in radio galaxies are significantly misaligned with respect to the observer's viewing direction, and thereby provide no relativistic Doppler boosting. This limits the detection of radio galaxies with current generation $\gamma-$ray telescopes to the local group and the Perseus galaxy cluster. Deep $\gamma-$ray observations of radio galaxies with CTA combined with spatially resolved studies in the radio, optical and X-ray will play an important role in understanding the physics of relativistic jets. These observations are likely to yield spectra up to $\approx$ 10s TeV which will provide useful constraints on the EBL in the mid- and far-IR wavelength regions (Acciari et al., 2009c, for the VERITAS Collaboration, the VLBA 43 GHz M 87 Monitoring Team, the H.E.S.S. Collaboration, and the MAGIC Collaboration).

With sufficiently high spatial resolution, the $\gamma-$rays produced by IC scattering of CMB and EBL photons off the relativistic electrons of the lobes of radio galaxies can be used to set limits on their energy density in the immediate vicinity of these objects (Georganopoulos et al., 2008, see §6 below).

Starburst galaxies: The detection of starburst galaxies M82 (Acciari et al., 2009b; Abdo et al., 2009) and NGC 253 (Acero et al., 2009), potentially opened a new wavelength regime for studying the EBL. The $\gamma-$rays in starburst galaxies are generated by cosmic rays that are accelerated by a large number of supernova remnants, giving rise to hard $\gamma-$ray spectra that extend to energies of 10s of TeV. The $\sim$ 10 TeV opacity to nearby starburst galaxies is quite small, and about unity at energies of $\sim$ 50 - 100 TeV. Nearby starbursts are therefore important probes of the EBL at far-IR ($\sim$ 100 μm) wavelengths that cannot be probed by other $\gamma-$ray sources because of the relative softness of their spectra compared to those of SB galaxies.

3.2. The Spectra of Extragalactic GeV/TeV Sources

Over a sufficiently small energy range the blazar spectrum can be characterized by a power law, $\mathrm{dN/dE} \propto \mathrm{E}^{-\Gamma}$, with different indices, Γ_{GeV} and Γ_{TeV}, at GeV and TeV energies, respectively. An important characteristic of the observed spectra is the presence of a break, defined as $\Delta\Gamma_{\rm GeV} \equiv \Gamma_{\rm GeV} - \Gamma_{\rm TeV}$, occurring between GeV and TeV energies, the exact location depending on the source's redshift. A source with an intrinsic spectrum characterized by a single power law out to TeV energies will have a value of $\Delta\Gamma_{\rm GeV} = 0$. Without any intergalactic absorption this value will remain constant with redshift.

The spectral index Γ_{GeV} is obtained from a power law fit to the $\sim 1 -$ 10 GeV region of the spectrum which is unaffected by EBL absorption. If the intrinsic blazar spectrum is an extension of this power law to energies of $\sim$ 1 TeV, then any spectral break ($\Gamma_{TeV} > \Gamma_{GeV}$) in the observed spectrum can be regarded as evidence for EBL absorption.

A spectral break analysis of the amount of EBL absorption provides therefore a powerful method for studying the EBL. It is a differential method that replaces knowledge of the intrinsic blazar spectrum with weaker requirement, namely that the power law representing the intrinsic blazar spectrum at GeV energies can be extended to TeV energies as well.

Table 2 lists the values of Γ_{GeV} and Γ_{TeV} and the redshifts for all GeV and TeV detected blazars. Almost all sources exhibit a spectral break ($\Delta\Gamma_{\rm GeV} <$

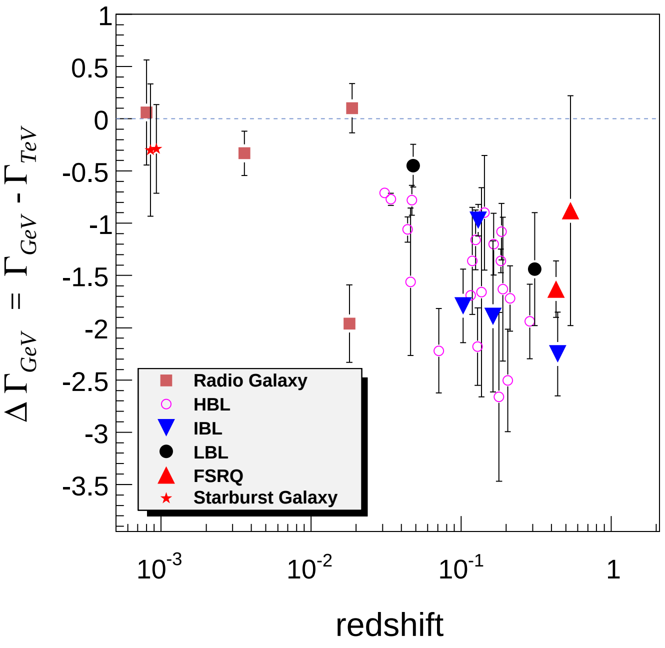

Figure 5: The difference between $\Gamma_{\rm GeV}$, the spectral index at GeV (Fermi) energies, and $\Gamma_{\rm TeV}$, the energy spectral index in the TeV regime (H.E.S.S, MAGIC, VERITAS) is shown as a function of their redshift. Red squares (radio galaxies), red stars (starburst galaxies), empty circles (HBLs, high-frequency peaked BL Lacs), blue downward triangles (intermediate-frequency peaked BL Lacs), filled circles (LBLs, low-frequency peaked BL Lacs), red upward triangles (FSRQs, flat spectrum radio quasars) indicate the different types of $\gamma-$ray sources.

0) at energies between 10 GeV and the 1 TeV. Figure 5 depicts the dependence of $\Delta\Gamma_{\rm GeV}$ on redshift. The figure shows a clear trend of increasing $|\Delta\Gamma_{\rm GeV}|$ with redshift, strongly suggesting that the break is the consequence of the attenuation of the source spectrum by the EBL. As the optical depth increases with redshift, the observed $\gamma-$ray spectrum becomes softer, the position of the break moves to lower energies, and $\Delta\Gamma_{\rm GeV}$ becomes more negative. The detailed redshift dependence of $\Delta\Gamma_{\rm GeV}$ reflects the evolution of the spectrum and proper photon number density of the EBL with redshift (see §7).

Figure 5 also shows that there is significant scatter in $\Delta\Gamma_{\rm GeV}$ at any given redshift. This suggests that some sources have considerable intrinsic hardening/softening in their spectra. Indeed, observations show that sources exhibit a wide range of spectral trends, i.e., spectral softening (3C 279, PKS 1510-08) and spectral hardening (1ES 0502+675) in the GeV regime (Abdo, A. A. et al., 2010), while the spectra of other blazars (Mrk 421, Abdo et al., 2011b), (Mrk 501, Abdo et al., 2011a) extend without any cutoff to 300 GeV (Abdo et al., 2010b), or multi-TeV energies (Krennrich et al., 2002), depending on the flaring state of the source. A lower limit in the scatter of $\Delta\Gamma_{\rm GeV}$ at a given redshift may suggest the combined effects of intrinsic spectral softening of the source spectrum and the effects of EBL absorption. An upper limit in the scatter may simply indicate that the break in the spectral index is only created by EBL attenuation.

Disentangling intrinsic spectral softening from the effects caused by the EBL is complicated, and requires a clear understanding of the physical processes that cause the intrinsic softening or hardening (which is very rare) between the GeV and TeV energy regions of the source spectrum.

Multiwavelength observations are required to solve this problem. Such observations will provide conclusive tests of non-thermal $\gamma-$ray emission models, and constitute an important step towards achieving the ultimate goal of using the radio-optical-X-ray and low energy $\gamma-$ray spectra as a predictor for the TeV spectrum. The application of this approach to different source classes, i.e., blazars, radio galaxies and starburst galaxies could provide additional redundancy to help constrain the EBL.

The current constraints on the UV/optical to mid-IR regions of the EBL have come predominantly from studies of blazars, since the vast majority of the extragalactic GeV/TeV $\gamma-$ray sources are FSRQs and BL Lacs. AGN population studies with *Fermi* reveal only a small number of non-blazar AGNs (Ackermann et al., 2011). Consequently, we will focus in the following sections on EBL limits that were derived from studies of blazar spectra, which have already provided important limits on the near- to mid-IR spectra of the EBL.

3.3. Phenomenology of Blazar Spectra and Models for TeV $\gamma-$ray Production

The non-thermal emission spectra of blazars generally exhibit two emission peaks in νF_ν, the power emitted per unit logarithmic photon energy [see Figure (6), (Abdo et al., 2011b)]. The peak in the radio-UV-X-ray waveband is unequivocally attributed to synchrotron radiation that is produced by ultra-relativistic electrons. The second peak, located at X-rays or $\gamma-$ray

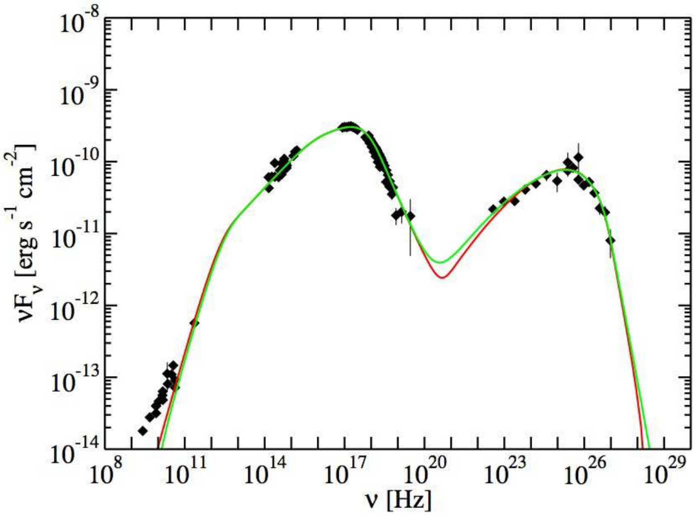

Figure 6: The SED of Mrk 421 depicts the synchrotron peak at X-ray energies, and the inverse Compton peak at TeV energies. The figure was taken from (Abdo et al., 2011b, Figure 11).

energies, is commonly believed to stem from soft photons that were upscattered by the inverse Compton process to X- and $\gamma-$ray energies by the very same electrons responsible for the synchrotron emission. This mechanism for creating the second peak is often referred to as the synchrotron-self-Compton (SSC) mechanism. If the second peak includes upscattered photons drawn from other ambient radiation fields the mechanism is called the external-Compton (EC) mechanism.

Alternatively, the second emission peak can be produced by a hadronic jet containing a significant amount of energy in ultra-high-energy (UHE) protons that subsequently interact with soft photons via $p\gamma \rightarrow \pi^0, \pi^\pm$ interactions. The pions decay giving rise to $\gamma-$rays, electrons, muons, and neutrinos. The strong magnetic fields required to collimate the hadronic jets also lead to the generation of considerable synchrotron radiation by protons and charged leptons in the pair cascade. The electrons from the pair cascade contribute to the lower energy synchrotron peak, whereas the muons together with the secondary photons from neutral pion decay contribute to the higher energy $\gamma-$ray peak. For a recent review of blazar models see Boettcher (2010) and Dermer (2012).

BL Lacs are classified loosely by their synchrotron peak position. They are referred to as low-frequency peaked BL Lacs (LBLs) if their synchrotron peak is at $10^{13} \leq \nu_{peak} \leq 10^{14}$ Hz; as intermediate-frequency peaked BL Lacs (IBLs) if $10^{15} \leq \nu_{\rm peak} \leq 10^{16}$Hz; and as high-frequency peaked BL Lacs (HBLs) if $\nu_{\rm peak} \geq 10^{17}$Hz (Nieppola et al., 2006). The corresponding $\gamma-$ray peak follows a similar pattern, with the peak energy progressively shifting towards higher energy as the synchrotron peak shifts to higher frequencies. LBLs peak at a few GeV (similar to FSQRs), IBLs in the tens of GeV, and HBLs generally peak beyond 100 GeV.

As the $\gamma-$ray peak is found at increasingly higher energy, its luminosity also decreases relative to that of the synchrotron peak, a trend often referred to as the Fossati blazar sequence, (Fossati et al., 1998). As a result, the multi-wavelength spectra of FSRQs and LBLs exhibit a prominent and large $\gamma-$ray luminosity, whereas in IBLs and in particularly HBLs, the $\gamma-$ray peak is typically dwarfed by the synchrotron emission. This makes both FSRQs and BL Lacs very useful and complementary for EBL studies. FSRQs are extremely bright in the GeV regime and despite their low peak energy, some are still detectable in the sub-TeV regime with GeV and TeV telescopes. They are thus becoming increasingly useful for EBL constraints in the UV/optical/near-IR. HBLs are at the other extreme, their $\gamma-$ray peak can extend well into the multi-TeV regime, while their $\gamma-$ray to synchrotron luminosity ratio is much smaller. However, during strong flares some HBLs have been found to show a $\gamma-$ray dominated spectral energy distribution. They are therefore useful for constraining the EBL at near- to mid-IR wavelengths.

In general, HBLs can be well described by basic SSC models where the ultrarelativistic electrons and their target photons are closely linked via synchrotron radiation. IBLs are better described by external Compton (EC) models, that include a strong ambient photon field external to the blazar jet, thereby providing additional target photons for IC scattering (Acciari et al., 2009e). FSRQs, such as 3C 279, are difficult to fit with either model and may require the addition of a hadronic component."

The detailed fitting of blazar spectra with models requires extensive multiwavelength monitoring including optical, X-ray, and $\gamma-$rays. Results from such multi-wavelength campaigns carry the potential to reduce the spread in the $\Delta\Gamma_{\rm GeV}(z)$ relation in figure 5. While numerous successful multiwavelength campaigns have been reported in the literature (Abdo et al., 2011b,a; Aleksić et al., 2010a; Fossati et al., 2008; Abramowski et al., 2011), the unequivocal interpretation of the spectral energy distributions with a clear prediction for the intrinsic TeV spectrum has not been possible.

In spite of the fact that blazar spectra are complex, it is possible to set limits on the behavior of their GeV/TeV spectra that are based on fundamental physical limits imposed by energy losses in the particle acceleration and radiation processes. The most prominent limitation is the maximum hardness of the $\gamma-$ray spectrum which provides an important constraint on the EBL. The energy spectrum of electrons produced in models of diffusive shock acceleration in blazar jets (Malkov & O'C Drury, 2001), strongly constrains the hardness of the resulting $\gamma-$ray spectra produced in SSC and EC models, limiting their power law index to values larger than $\Gamma \approx 1.5$.

Even spectra that obey this limit are difficult to produce at higher energies where the Klein-Nishina effect softens the energy spectra substantially. The detection of relatively hard TeV spectra of blazars with redshift $\approx 0.1 - 0.2$ therefore came as a surprise, since the absorption corrected spectra are already reaching the $\Gamma \approx 1.5$ limit for the minimal EBL imposed by the IGL (Aharonian et al., 2006a; Levenson & Wright, 2008; Krennrich et al., 2008; Ackermann et al., 2011; Abdo et al., 2010a).

To which extent a problem of hard TeV spectra persists depends on theoretical scenarios explaining these hard spectra. A solution to the problem was proposed by Katarzyński et al. (2006). In their model, a high low-energy cutoff in the electron distribution could give the appearance of a hard $\gamma-$ray spectrum for a given energy regime. Other ideas by Aharonian et al. (2008) show that $\gamma - \gamma$ absorption in the source due to narrow band emission from the AGN could lead to unusually hard TeV spectra. The emission produced by proton synchrotron radiation (Aharonian et al., 2007a; Zacharopoulou et al., 2011) combined with internal absorption at lower energies has been shown to produce spectra that exceed the hardness achievable by DSA. Other explanations avoid substantial EBL absorption by introducing axion-like particles that couple with photons in intergalactic magnetic fields thus reducing the $\gamma-$ray opacity of the universe substantially (Sánchez-Conde et al., 2009). Mechanisms that would substantially weaken EBL limits derived from $\gamma-$ray observations are discussed in Section 8.

3.4. Unphysical Blazar Spectra

In spite of the difficulties and the complexity associated with modeling the intrinsic $\gamma-$ray spectra of blazars, models generally predict a common feature of blazar spectra: they follow a power law with curvature and/or exponential cutoff and overall can be described by a concave shape (curvature in energy flux is downward rather than upward). This means that any absorption corrected gamma-ray spectrum showing an exponential rise cannot represent a physical source spectrum, and must have its origin in an over-correction for EBL absorption[1].

The relation between the intrinsic, $(\mathrm{dN/dE})_{\mathrm{int}}$, and observed, $(\mathrm{dN/dE})_{\mathrm{obs}}$, blazar spectrum is given by:

$$\left(\frac{dN}{dE}\right)_{int} = \left(\frac{dN}{dE}\right)_{obs} e^{\tau_{\gamma\gamma}(E_\gamma, z)} \tag{11}$$

The equation illustrates that an overestimate of the $\gamma - \gamma$ opacity will lead to an exponential rise in the inferred intrinsic spectrum of the blazar. Such exponential rise is unphysical. It runs contrary to our basic understanding of blazar models, and is absent in the $\gamma-$ray spectra of blazars at energies below 10 GeV (Abdo et al., 2010a). This behavior can therefore be used to exclude EBL models with optical depths that will result in an exponential rise in the corrected blazar spectrum (Guy et al., 2000; Dwek & Krennrich, 2005).

Similarly, EBL scenarios can lead to an absorption correction for which the reconstructed intrinsic spectra follow a power law with an extremely hard spectral slope. Additional constraints can be derived from the spectral slope itself, however these are model dependent. EBL models leading to slopes of $\Gamma < 1.5$ for the intrinsic spectrum, have been rejected by Aharonian et al. (2006a) on the basis of the diffuse shock acceleration model. Caveats to this approach have been extensively discussed in the literature (Stecker et al., 2007; Katarzyński et al., 2006; Böttcher et al., 2008; Aharonian et al., 2008; Krennrich et al., 2008; Lefa et al., 2011; Zacharopoulou et al., 2011), and while some extreme blazars may exhibit harder spectra with $\Gamma < 1.5$, most GeV energy spectra of blazars obey the $\Gamma = 1.5$ limit, with few exceptions (Ackermann et al., 2011).

These general constraints on the hardness of the intrinsic blazar spectra have been used to derive constraints on the EBL by using few individual objects (Dwek & Krennrich, 2005; Aharonian et al., 2006a), and by using

---

[1] This assumes that no other external effects such as pileups due to pair halos are playing a major role in the modification of blazar spectra. The production of pair halos would require a magnetic field intensity between 10^{-7} and 10^{-12} G, sufficiently large so that electrons are isotropized, and sufficiently small so that IC losses exceed synchrotron losses. Instead of a power law with curvature term, a power law with exponential cutoff or a broken power law is also consistent with the above statement.

samples of blazars (Mazin & Raue, 2007; Orr et al., 2011).

4. The Extragalactic Background Light I: Measurements and Limits

4.1. Spectral Measurements and Limits

The specific intensity of the EBL is usually presented in units of nW $\mathrm{m}^{-2}\ \mathrm{sr}^{-1}$. The conversion between these units and others that are sometimes used in the literature is given by:

$$\begin{aligned} \nu\, I_\nu(\lambda)\, [\mathrm{nW\ m^{-2}\ sr^{-1}}] &= \frac{3000}{\lambda(\mu m)}\, I_\nu(\lambda)\, [\mathrm{MJy\ sr^{-1}}] \\ &= \frac{9.85 \times 10^{-3}}{\lambda(\mu m)}\, I_\nu(\lambda)\, [\mathrm{mJy\ deg^{-2}}] \end{aligned} \tag{12}$$

The EBL intensity can be determined in several ways. The first consists of direct measurements, a method that poses considerable technical and astronomical challenges. Technically, it requires the absolute calibration of the instruments, and the understanding and removal of all measurements uncertainties. Astronomically, it requires the removal of strong foreground emission from interplanetary dust particles (the zodiacal light, ZL) and from stellar and interstellar emission components in the Milky Way. A thorough review of the challenges in determining the EBL was presented by Hauser & Dwek (2001).

A strict lower limit to the EBL intensity can be obtained by adding the light emitted by resolved galaxies. In principle, the integrated galaxy light (IGL) can converge to the total intensity of the EBL. A necessary condition for convergence is that the spectral index α of the differential galaxy number count versus flux S, $dN/dS \sim S^{-\alpha}$, becomes smaller than 2 at lower fluxes, so that the total integrated intensity, $\int S^2\,(dN/dS)\,dS$, is finite. At short wavelengths the intensity of the IGL is limited by the sensitivity of the survey. However, even in deep surveys the convergence of the IGL does not ensure the measurement of the total EBL intensity, since the low surface brightness regions of galaxies may be missed in standard aperture photometry (Bernstein et al., 2002; Levenson & Wright, 2008). Furthermore, a truly diffuse background will always remain undetected in such surveys.

At longer wavelengths and large beam sizes, unresolved galaxies become a source of confusion, limiting the depth of the survey. Below a certain flux (the confusion limiting flux) individual sources become indistinguishable from the variation in the sky brightness caused by statistical fluctuations in the number of faint resolved or unresolved sources (Dole et al., 2004, and references therein). These limitations can be partially circumvented by stacking analysis. Stacking of astronomical images of sources detected at one wavelength enhances their signal relative to the random background fluctuations at some other wavelength (e.g. Dole et al., 2006). The integrated light obtained by this method is thus closer to the EBL intensity than that obtained by integration down to the confusion limit.

Finally, given a model for dN/dS, one can extrapolate the differential source count to very faint fluxes, and evaluate the sensitivity of the integrated intensity to the lower flux limit and functional shape of the extrapolation.

Tables 3-5 list measurements and limits on the EBL intensity derived by the different methods described above with the different satellites, balloons, and ground observatories. Select measurements were used to define the gray area in Figure 7. Absolute measurements and their 1σ uncertainties were used to define the upper limits on the EBL. The integrated light from resolved galaxies and their 1σ uncertainty was used to define the lower limit on the EBL. Lower limits derived from stacking analysis were used when available. At 140 μm the DIRBE detection with the FIRAS calibration (Hauser et al., 1998), and at longer wavelengths the FIRAS detections by (Fixsen et al., 1998) were used to define the limits on the EBL. The measurements used to define the upper and lower limits on the EBL are shown as bold entries in Tables 3-5. The figure shows that the EBL is poorly determined in the $\sim 5 - 60$ μm wavelength region, where the foreground emission from the interplanetary dust cloud is strongest (Kelsall et al., 1998).

4.2. Integral Constraints on the EBL Intensity

The total EBL intensity per unit solid angle is given by:

$$I_{EBL} = \left(\frac{c}{4\pi}\right) \int_0^\infty \mathcal{L}(z) \left|\frac{dt}{dz}\right| \frac{dz}{1+z} \tag{13}$$

where $\mathcal{L}(z)$ is the luminosity density in a comoving volume element at redshift z, and $|\frac{dt}{dz}|$ is given by eq. (3).

The comoving luminosity density is dominated by the radiative output from stars. On a galactic scale, an AGN can dominate the optical to IR output of a galaxy, however, on a global scale AGN make only a small contribution to the total energy releases in the universe. AGN make up most of

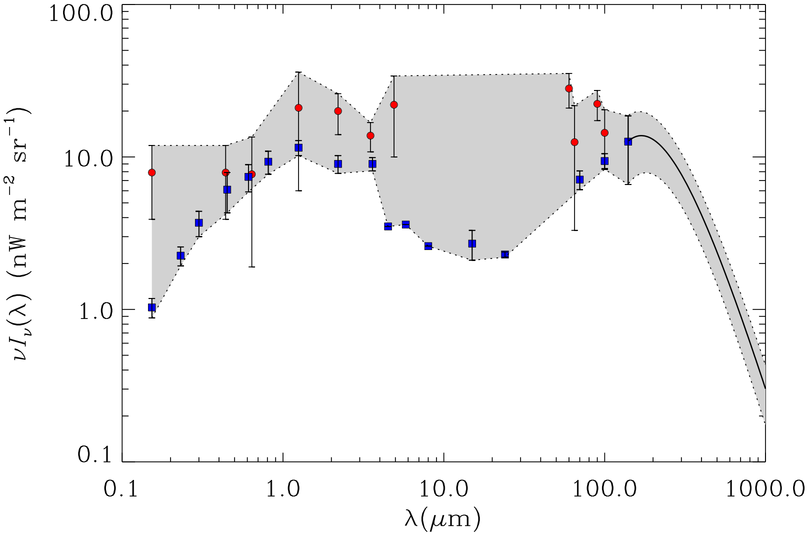

Figure 7: Limits on the EBL intensity. Lower limits (blue squares) are determined by the intensity of the IGL. Upper limits (red circles) are determined by absolute measurements of the EBL. The data used in the figure are listed in Tables 3-5 in bold. The shaded area depicts the range of the allowed EBL intensity as determined by UV to sub millimeter observations.

the X-ray background (Mushotzky et al., 2000; Draper & Ballantyne, 2009), and a significant fraction of the cosmic radio background (Dwek & Barker, 2002). However, they make only a small contribution to the total IR background. Accretion onto a central black hole releases about 10% of the rest mass energy of the accreted matter, significantly more than the 0.7% released in nuclear processes. However, the mass locked up in BH is only $\sim 0.6\%$ of that in stellar objects. Rest frame color-color diagrams generated from *Spitzer* IRAC and MIPS observations covering the 3.6, 4.5, 5.8, 8.0, 24, and 70 μm bands, of radio-detected submillimeter-selected galaxies with spectroscopic redshifts show that AGN constitute a small fraction, between 13 and 19%, of the sample dominating its mid-IR spectrum (Hainline et al., 2009). So with these limits in mind, the total comoving luminosity density is a direct measure of the cosmic star formation rate (CSFR) at a given redshift.

Figure 8 presents the redshift dependence of the CSFR as determined from UV-optical emission lines, [O II], [O III], Lyα, Hα, Hβ, and from mid-IR, submillimeter, and radio observations (Madau et al., 1996; Hopkins & Beacom, 2006; Michałowski et al., 2010). The data in the figure were taken

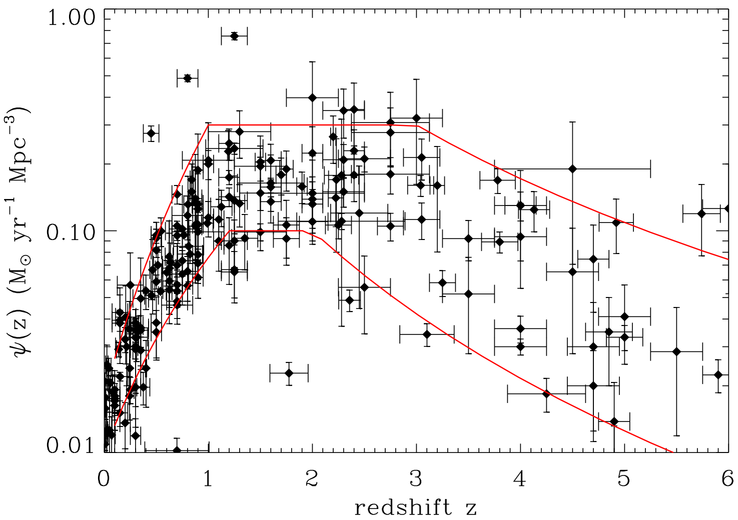

Figure 8: A compilation of the cosmic star formation rate as inferred from UV, H_α, mid-IR, submillimeter, radio, and Lyα observations. Lower limits were excluded from the figure. The red curves are analytical approximations representing the upper and lower limits to the CSFR.

from the compilation of Michałowski et al. (2010), who used the standard ΛCDM parameters to calculate volume densities and the Kennicutt (1998) law with a Salpeter stellar initial mass function (IMF) to convert luminosity densities to star formation rates. The two red lines represent a broken power law approximation to the upper and lower limits lines of the observations. For consistency with the observational determination of the CSFR, the CSFR was converted to a bolometric intensity using the Salpeter IMF and a starburst age of 100 Myr: $L_{bol} = 7.5 \times 10^9 \, \Psi \; M_\odot \; \mathrm{yr}^{-1}$ (Dwek et al., 2011). The integrated intensity of the CSFR is then bounded by:

$$I_{EBL} = 21 - 66 \qquad \mathrm{nW \; m^{-2} \; sr^{-1}} \tag{14}$$

Table 6 presents the current limits on the EBL intensity, separated into its stellar and dust components, and compares them to this predicted by the various EBL models presented in §5.

4.3. Constraints on the EBL from Fluctuation Measurements

Most of the EBL is generated by discrete galactic or primordial stellar sources. Fluctuations in their number and their clustering properties will give rise to spatial fluctuations in the EBL intensity. Studies of the optical region of the EBL via the fluctuations method were first conducted by (Shectman, 1973, 1974), and of the near-IR region using the *COBE*/DIRBE data by Kashlinsky et al. (1996). The fluctuations do not provide a direct measurement of the EBL intensity. The derivation of the EBL intensity from these measurements will require detailed knowledge of the galaxy source counts, their luminosity function, and their clustering properties as a function of redshift. However, spatial fluctuations in the EBL provide a different means of setting limits on its intensity. Fluctuation measurements of the EBL do not require absolute measurements of its intensity, since the removal of foreground emission components is done on the basis of their distinct spatial properties rather than their absolute intensities. At IR wavelengths, these fluctuations can have a spatial signal that is distinctly different from that generated by the interplanetary dust cloud or by interstellar dust. After the removal of all known resolved sources, any residual fluctuations will measure the EBL contribution from sources that may represent a yet unknown or unresolved population of stars or galaxies. Recent fluctuation measurements in the Spitzer 3.6 and 4.5 μm bands (Kashlinsky et al., 2012) show that they are in excess of those that can be attributed to known galaxy populations (Helgason et al., 2012), suggesting an origin in a very faint, yet unknown, population of highly clustered sources. More details and references on the use of fluctuations analysis to constrain the EBL intensity can be found in Hauser & Dwek (2001) and (Kashlinsky, 2005).

EBL fluctuations at far-IR wavelengths were detected at 170 μm (Lagache & Puget, 2000, *ISO* data), at 160 μm (Lagache et al., 2007, *Spitzer* data) and by (Shang et al., 2012), using the *Planck* data. Fluctuation measurements and EBL colors have been used by Pénin et al. (2012) to derive limits on the EBL at 100 and 160 μm (see Tables 4 and 5).

5. The Extragalactic background Light II: Models

The EBL intensity only provides an integral constraint on all the radiative energy releases over cosmic time. In a dust-free universe, it represents the intrinsic stellar or AGN spectra. The EBL intensity and spectral shape depends then on the star formation history, the stellar initial mass function, the evolution of metallicity, the energy released by AGN, and the relative importance of energy releases by nuclear and gravitational processes. In a dusty universe, the comoving luminosity density, $\mathcal{L}(z)$, and total EBL intensity,

I_{EBL} remain unchanged, however the energy is redistributed by absorption and reemission processes over a large spectral range. The resulting spectrum depends on many factors, ranging from the size distribution, composition, and optical properties of the dust grains, the evolution of their abundance and properties over time, and on the morphology of the galaxy which determines the spatial distribution of the dust relative to the radiative sources.

Several distinct approaches have been used to model the intensity and spectral distribution of the EBL at $z = 0$. They all represent different approaches for calculating the evolution of $\mathcal{L}_\nu(\lambda, z)$ with redshift [see eq. (2)]. Backward evolution models start from the local determination of $\mathcal{L}_\nu(\lambda, z = 0)$, evolving it with redshift using observed galaxy number counts at different wavelengths. Forward evolution models use the CSFR to determine $\mathcal{L}_\nu(\lambda, z)$ as a function of redshift, and population synthesis and radiative transfer models to determine the distribution of the energy over wavelengths. Cosmic chemical evolution models are similar to previous models, except that their system is the universe as a whole. Semi-analytic models calculate $\mathcal{L}_\nu(\lambda, z)$ by including the appropriate physical processes in a more general model for the formation and evolution of structure in the universe. In the following we discuss these different models in somewhat more detail. For a more extensive discussion and description we refer the reader to the review by Hauser & Dwek (2001).

5.1. Backward Evolution (BE) Models

BE models start with the construction of a library of the galactic spectral energy distributions (SEDs) representing those of galaxies in the local universe and evolve them back in time in order to fit observed number counts. The EBL intensity and spectral shape is used as an integral constraints on their evolution. The galaxies in such library should represent the range of observed galactic morphologies (spiral elliptical, irregular) and activities (AGN, normal, starburst, mergers) in the local universe. The SEDs of the galaxies comprising such library should also satisfy observed statistical properties of the ensemble of local galaxies, such as: the trend of increasing $S(60\,\mu m)/S(100\,\mu m)/)$ and decreasing $S(12\,\mu m)/S(25\,\mu m)/)$ flux ratios with increasing IR luminosities ((Soifer & Neugebauer, 1991); and the number density of galaxies in the $L + dL$ luminosity interval, represented by the luminosity function (LF), $\Phi(L)dL$.

Many functional forms have been adopted to characterize the local LF. The most commonly one used at optical and near-IR wavelengths is the

Schechter (1976) LF. At wavelengths above $\sim 10\ \mu$m the galaxies' SED is dominated by thermal emission from dust, and their LF cannot be adequately represented by the Schechter LF. Several distinct functional forms have been used to characterize the LF in the different IR wavebands. They are usually characterized by three parameters: a normalization parameter, $\Phi_\star$, a characteristic luminosity, $L_\star$, that determined the transition point between the low and high luminosity behavior of the L; and a power law index, α that determines the behavior of the LF at low luminosities. A list of references to the functional forms derived from the *IRAS* survey can be found in Hauser & Dwek (2001). Of those, the parameters of the Saunders et al. (1990) LF have been recently updated to fit the differential 24 μm number counts obtained by deep *Spitzer* surveys (Rodighiero et al., 2010).

If neither the galaxies' SED nor their comoving number density evolved with time, the spectral luminosity density, $\mathcal{L}_\nu(\lambda, z)$ would be independent of redshift. However, the recent deep surveys with the *Spitzer* and *Herschel* satellites show strong evolution in number counts, compared to predictions made with no evolution models (Lagache et al., 2005; Rodighiero et al., 2010). Evolution in the LF or, equivalently, the spectral luminosity density can be inferred directly from observations if the redshift of the sources is known, and their number counts are complete (e.g. Rodighiero et al., 2010; Dunne et al., 2000). Alternatively, evolution in the LF can be introduced by adding a redshift dependence, usually of the form $(1+z)^\gamma$, to the basic parameters, $\Phi_\star$, $L_\star$, and α, that characterize the LF. The value of γ is then derived by fitting model prediction to the observed galaxy number counts in a given waveband. Evolution in the LF can also be modeled by evolving the relative number of the different type galaxies: quiescent star forming galaxies, starbursts, AGNs, and ellipticals with redshift (Rowan-Robinson, 2001, 2009; Lagache et al., 2003; Domínguez et al., 2011), or by simply evolving the relative number of ultraluminous infrared galaxies (ULIRGs), characterized by IR luminosities in excess of $\sim 10^{12}\ \mathrm{L}_\odot$, relative to the rest of the galaxy population [e.g. Chary & Elbaz (2001)]. Having determined the evolution of the spectral luminosity density with redshift, the EBL is obtained by a simple integration of $\mathcal{L}_\nu(\lambda, z)$ over redshift.

BE models are relatively simple, and their predictions can be easily compared to observed galaxy number counts, their magnitude-color and magnitude number density relations, and their redshift distribution. They are only loosely constrained by physical processes. The predicted dependence of the comoving bolometric luminosity density with redshift should be consistent with that inferred from limits and observations of the cosmic star formation rate.

5.2. Forward Evolution (FE) Models

FE models use the redshift dependence of the cosmic star formation rate (CSFR), inferred from a variety of wavebands and line observation (Madau et al., 1996; Hopkins & Beacom, 2006), as a starting point in their calculations. The CSFR is determined from the UV-optical line and continuum, and IR and radio emission in the various wavebands using statistically determined conversion factors derived from galaxies in the local universe (Kennicutt, 1998; Haarsma et al., 2000). Determination of the CSFR is complicated by extinction effects at UV and optical wavelengths, and by the implicit assumption that the IR luminosity is powered by stars and representative of the total bolometric luminosity of the galaxies. Even if the total bolometric luminosity of a given galaxy is determined, its conversion to a star formation rate requires knowledge of the stellar IMF, a poorly determined quantity at high redshifts, and the duration of the starburst activity at each redshift. Once the CSFR is determined, FE models use population synthesis models such as PÉGASE Fioc & Rocca-Volmerange (1997), Starburst99 Leitherer et al. (1999), Bruzual & Charlot (2003) or Maraston & Strömbäck (2011) to calculate the stellar bolometric and spectral luminosity density as a function of redshift.

The most difficult part of this approach is determining the fraction of starlight that is absorbed by dust, and the spectrum of the reradiated IR emission. The SED of a galaxy can be determined with radiative transfer models, such as GRASIL (Silva et al., 1998), DIRTY (Gordon et al., 2001), or DUSTY (Nenkova et al., 2000). Alternatively, one can use a parametric approach in which the fraction of UV-optical light absorbed by the dust, and the reradiated infrared spectrum are statistically determined from observations. EBL spectra derived from FE evolution models were presented by Dwek et al. (1998), Razzaque et al. (2009), and Finke et al. (2010).

Population synthesis models, combined with simple radiative transfer calculations, are useful for determining the UV to radio SED of individual galaxies. However, the cosmological application of such models assumes that star formation is a monolithic process, in which in all galaxies star formation commenced at the same redshift and evolved quiescently until the current epoch. The models do not allow for galaxy interactions, stochastic star formation histories associated with merger events, or any morphological evolution of galaxies. Any discrepancies between model predictions and galaxy number counts must be introduced in an ad hoc fashion by evolving the stellar IMF, or by introducing a new population of galaxies at the appropriate redshifts.

5.3. Cosmic Chemical Evolution (CCE) Models

CCE models treat the universe as a closed system in which all galaxies within a large comoving volume element are represented by their basic ingredients: stars, interstellar gas, metallicity, and radiation. Chemical evolution equations, analogous to those used to follow the chemical evolution of the Galaxy (e.g. Audouze & Tinsley, 1976; Tinsley, 1981; Pagel, 2001), are used to follow the evolution of the average stellar, gaseous, and radiative contents in each comoving volume in a self consistent manner. CCE models were pioneered by Pei & Fall (1995), and most recently updated by Pei et al. (1999). Inputs parameters for their model are the mean rest frame UV luminosity density as a function of redshift, and the mass of the ISM gas as determined from H I column densities derived from studies of quasar absorption lines through damped Lyα systems. The decrease in the ISM gas with redshift and the UV luminosity density were used to derive a solution for the evolution of the CSFR with redshift which is consistent with that determined from the extinction-corrected Hα, and with SCUBA 850 and *ISO* 15 μm surveys. Similar to FE models, population synthesis models were then used to calculate the stellar SED at each redshift, and an LMC extinction law was adopted to calculate the fraction of starlight absorbed by the dust. A power-law distribution in dust temperature was used to calculate the spectrum of the reradiated IR emission. The model reproduced various observational constraints, including the comoving rest-frame 0.44, 1.0, and 2.2 μm spectral luminosity densities in the $\sim 0 - 2$ redshift interval, the 12, 25, 60, and 100 μm local luminosity densities; and the mean abundance of metals in damped Lyα systems in the $\sim 0.4 - 3.5$ redshift interval.

5.4. Semi-analytical (SA) Models

SA models follow the formation and evolution of galaxies in a cold dark matter Lambda dominated (ΛCDM) universe using the cosmological parameters derived from the 5-year *Wilkinson Microwave Anisotropy Probe* (*WMAP5*) observations (Hinshaw et al., 2009) as the initial conditions. SA models then follow the growth and merger of dark matter halos, and the emergence of galaxies which form as baryonic matter falls into the potential wells of these halos. The fate of the infalling gas is determined by many different processes: the formation of stars in a multiphase interstellar medium, AGN and supernovae feedback processes that quench their formation, the evolution of the stellar radiation field, the heating and cooling of the interstellar medium and its chemical enrichment, the exchange of material with the intergalactic medium through infall and galactic winds, and the growth of the central black hole. A description of recent developments and references to previous work can be found in Somerville et al. (2011). Model prediction are compared to a basic set of observational constraints such as the observed characteristics of galaxies: their morphology, colors, and spectral energy distribution, and morphology; and their integrated cosmological properties: their number counts and luminosity function in different wavebands and redshifts, their mass function, the cosmic star formation rate, and the EBL generated by them. As in all EBL models, determination of the galaxies' SED is complicated by the detailed microscopic and large scale parameters needed to calculate the amount of starlight that is absorbed by dust, and the spectrum of the reradiated emission. Recent SA models have combined the models for galaxy formation with radiative transfer models to determine the galaxies' SED (Fontanot et al., 2009; Fontanot & Somerville, 2011; Somerville et al., 2011; Younger & Hopkins, 2011).

SA models are inherently complex, incorporating a large number of physical processes, some poorly known, to derive galaxy properties. However, they are the most physically motivated models, and quite successful in reproducing a large number of observational constraints.

5.5. Comparison of Model Predictions with Observations

A detailed comparison of all model types with EBL limits and observations was presented by Hauser & Dwek (2001). Here we will represent mostly the models that have been developed since then: BE models by Stecker & Scully (2006), Franceschini et al. (2008), and Domínguez et al. (2011); The FE model of Finke et al. (2010); and the SA model of Gilmore et al. (2011). Figure 9 compares the various models to the current limits and observations of the EBL. In general, all models, except for the BE models of Stecker et al. provide adequate fits to the EBL.

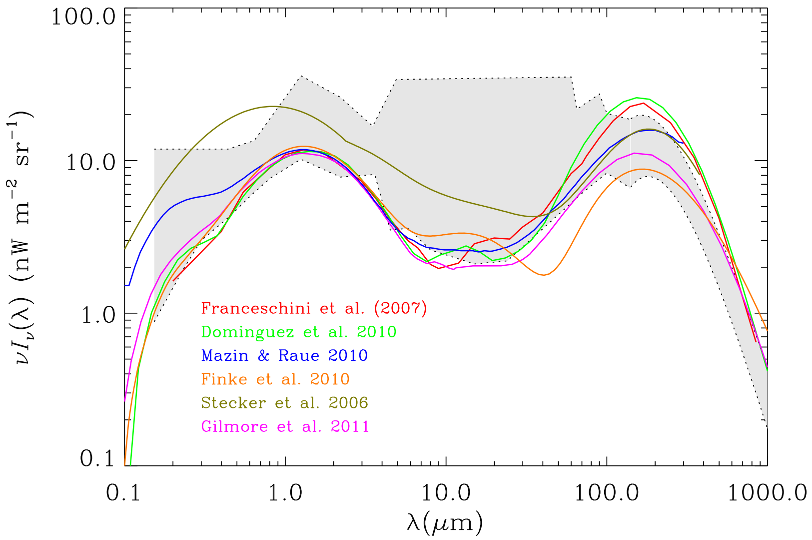

Figure 9: Models of the EBL are compared to observational limits on the EBL.

6. EBL Constraints from $\gamma-$ray Observations of Blazars

The attenuation of $\gamma-$rays by the EBL can in principle be used to determine the EBL intensity at wavelengths corresponding to the $\gamma-$ray observations. Neglecting the possible scattering or production of second generation $\gamma-$ray photons along the line of sight to the blazar, the intrinsic $\gamma-$ray flux from the blazar, $F_{Int}(E_\gamma)$, can be related to the observed one, $F_{obs}(E_\gamma)$ by:

$$F_{obs}(E_\gamma) = F_{Int}(E_\gamma)\, \exp[-\tau_{\gamma\gamma}(E_\gamma)] \tag{15}$$

where the optical depth, $\tau_{\gamma\gamma}$, is given by eq. (9). Determination of the EBL assumes that all the attenuation is caused by interaction with the EBL, instead of photons in or around the vicinity of the blazar. Furthermore, it requires knowledge of the intrinsic blazar spectrum. Assuming that all the attenuation is attributed to the EBL, several upper limits have been derived on the EBL intensity by making various assumptions on the intrinsic blazar spectrum. The $\gamma-$ray derived EBL limits are compared to those derived from UV to sub millimeter observations in Figure 10, and described below.

Fixed power law: Early observations of blazars (Mrk 421 Punch et al., 1992) suggested that the ∼ GeV–TeV spectrum could be approximated by a single power law. If so, then any deviations of the observations from the extrapolated power law to higher energies should be attributed to EBL attenuation. Stecker & de Jager (1993) derived an upper limits at 1-5 μm of 10 nW m^{-2} sr^{-1}, assuming that a straight power law extrapolation of the spectrum of Mrk 421 from GeV energies obtained from the EGRET (Lin et al., 1992) with an index of $\Gamma = 1.96 \pm 0.14$ holds up to the TeV regime, where the index was measured by the Whipple collaboration to be $\Gamma = 2.25 \pm 0.19$. Biller et al. (1995) included the statistical uncertainties of the GeV spectrum, and demonstrated vastly different extrapolations with significantly higher upper limits, thereby yielding conservative upper limit to the EBL in the mid-IR at 10μm.

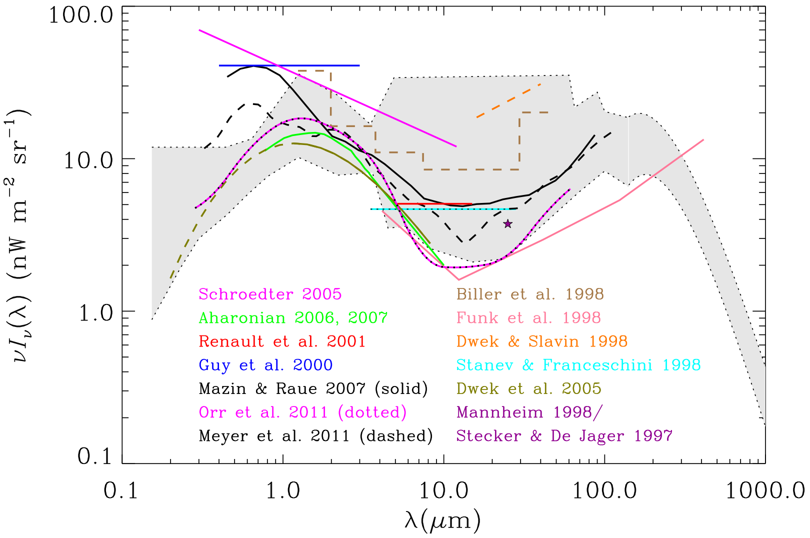

Figure 10: Limits on the EBL as determined from $\gamma-$ray observations of blazars. Details in text.

Strong flaring activity of Mrk 501 provided a well measured TeV spectrum from 0.2 - 24 TeV (Aharonian et al., 1999; Samuelson et al., 1998; Djannati-Atai et al., 1999). Stanev & Franceschini (1998) calculated limits by fitting the energy spectrum of Mrk 501, with a range of possible absorption scenarios assuming intrinsic power law spectra and varying levels of EBL intensity by scaling the lower limits from galaxy counts. This provided strong EBL limits in the near- and mid-IR. Funk et al. (1998) followed a similar approach, except that they used an EBL model by MacMinn & Primack (1996) as the basis for scaling the EBL intensity, yielding similar results in the mid-IR.

Mannheim (1998) argued that the observed spectra would deviate from a power law, if the primary $\gamma-$ray spectrum were substantially attenuated by the EBL. An upper limit in the mid-IR that is based on this hypothesis and an energy spectrum of Mrk 501 from the HEGRA collaboration is also shown in Figure 10. Later on, Vassiliev (2000) demonstrated that the absence of deviations from a power law does not preclude the presence of substantial absorption in the observed spectra.

The obvious drawback of the method is that the assumption of a single power law for the intrinsic blazar spectrum does not hold true over a wide range in energy. Blazar spectra generally exhibit a concave $\gamma-$ray peak over a sufficiently large energy range. Most blazar spectra measured by *Fermi* or by Cherenkov telescopes can be represented by a power law over the energy range covered by the instrument.

Synchrotron Self-Compton (SSC) Spectrum: The SSC model is a popular model explaining the existence of the two peaks in the blazar spectrum: the synchrotron peak at radio-UV-X-ray energies and the inverse Compton (IC) peak at $\gamma-$ray energies. The spectrum of the IC peak can be modeled using parameters that produce the synchrotron peak and the unabsorbed part ($E < 10$ GeV) of the IC spectrum (see review by Dermer, 2012).

Such models for the intrinsic blazar spectrum have been used by Guy et al. (2000) to determine the intensity of the EBL in the 1-5 μm and 20-80 μm wavelength region. They applied a multiwavelength fit to the X-ray and TeV data of Mrk 501 in the framework of a standard homogeneous SSC model to derive the level of absorption present in the TeV spectrum. As a result, they obtained an absolute upper limit on the EBL of 60 nW m^{-2} sr^{-1} and a most likely value of 20 nW m^{-2} sr^{-1} at 1 μm. They also pointed out that the lack of an absorption signature in the spectrum of Mrk 501, as suggested by the HEGRA telescopes, does not necessarily imply a lack of EBL absorption. They emphasized that in the transition region from the near-IR to the mid-IR EBL, the opacity could be nearly constant. This is a consequence of the large width of $\gamma-\gamma$ cross section (see Figure 2). So when $\sigma_{\gamma\gamma}$ is convolved with the number density of background photons, any strong wavelength variations in the EBL are smoothed out. As a result, the observed TeV spectrum at 1 - 10 TeV would corresponds to the intrinsic blazar spectrum since the observed spectrum is now described by $(\mathrm{dN/dE})_{\mathrm{int}} \times \mathrm{e}^{\tau}$ with τ a slowly varying function of energy.

The drawback of using $\gamma-$ray emission models to constrain the EBL is the uncertainty in the many parameters that determine the IC spectrum. Furthermore, while HBLs generally can be well fit by SSC models, IBLs require the inclusion of additional ambient radiation fields that make a contribution to the $\gamma-$ray IC component.

Additional complications arise from the fact that basic one-zone SSC models are not applicable for sources exhibiting ”orphan flares”, where only the TeV flux is enhanced while the synchrotron emission remains unchanged (Krawczynski et al., 2004). Finally, the biggest challenge for the SSC/multi-wavelength approach to constraining the EBL is to get simultaneous measurements for large sets of blazars.

The $\Gamma > 1.5$ limit on the hardness of the blazar spectrum: A more relaxed assumption on the intrinsic blazar spectrum is that it cannot produce too many hard photons, so that the $\gamma-$ray spectrum, expressed as $E^2dN/dE \sim E^{-\Gamma}$ cannot be flatter than one with $\Gamma = 1.5$ (Malkov & O'C Drury, 2001). In the spirit of this limit to the spectral index, Renault et al. (2001) explored a range of EBL scenarios based on measurements with the minimal assumptions that the intrinsic power of Mrk 501 is concave, effectively requiring a decreasing energy flux distribution above 4 TeV ($\Gamma > 2.0$). They derived an upper limit of 5 nW/m^2/sr at 10 μm.

The strict assumption of $\Gamma > 1.5$, was used by Aharonian et al. (2006a) to derive upper limits on the 1–5 μm on the EBL which are close to the lower limits determined by the IGL, suggesting that the EBL has been largely resolved at these wavelengths. A comprehensive study by Mazin & Raue (2007) is based on eleven blazars over a redshift range from 0.03 - 0.18, and explores a large number (8 million) of hypothetical EBL scenarios to set upper limits on the EBL, again with the requirement that the source spectra cannot be harder than $\Gamma = 1.5$ or $\Gamma = 2/3$. The lower value arises from the extreme scenario of a mono-energetic energy distribution of ultra-relativistic electrons in which the resulting IC $\gamma-$ray spectrum could be as hard as $\gamma = 2/3$, leading to two conditional upper limits. The first condition yielded limits that are slightly above that of Aharonian et al. (2006a). The second, more relaxed condition, yielded limits that were higher by about 30%.

The theoretical validity of a strict hardness limit of $\Gamma > 1.5$ has been discussed by a number of authors, with no unanimous verdict (Katarzyński et al., 2006; Stecker et al., 2007; Böttcher et al., 2008; Aharonian et al., 2008; Lefa et al., 2011; Zacharopoulou et al., 2011). Observational evidence, e.g. Levenson & Wright (2008), have provided lower EBL limits from galaxy counts that are higher than previous ones derived by Madau & Pozzetti (2000). If these new limits are correct, they imply $\gamma-$ray spectra that are slightly harder than $\Gamma = 1.5$ (Krennrich et al., 2008).

Unphysical exponential rise of the blazar spectrum: Less model dependent, and therefore more robust limits on the hardness of the intrinsic blazar spectra arise from the notion that an exponential increase of their luminosity with energy is unphysical. All current blazar models produce a concave spectrum, rendering intrinsic blazars spectra with an exponential rise in energy flux theoretically unfeasible. The paradigm of concave intrinsic energy spectra was used by Dwek & Krennrich (2005) to reject many different realization of the EBL. Furthermore, Dwek et al. (2005b) ruled out the extragalactic origin of the near-IR sky brightness observed by Matsumoto et al. (2005), since it would lead to an exponential rise in the spectrum of the blazar PKS 2155-304, which is ruled out by observations (Aharonian et al., 2005b). An EBL spectrum close to the IGL limits yielded a blazar spectrum consistent with the SSC model, suggesting that the EBL was mostly resolved at near-IR wavelengths (Dwek et al., 2005b,a).

Spectral break analysis due to EBL spectrum: Orr et al. (2011) developed a novel approach to set limits on the EBL intensity by studying the effects of the spectral shape of the EBL on the sub– to multi–TeV spectra of blazars. The $\gamma-$ray opacity around 1 TeV is sensitive to the EBL intensity at ~ 1 μm (see Fig. 3). Its subsequent energy dependence hinges on the rate at which the stellar UV, optical, and near-IR emission decreases towards mid-IR wavelengths. The near- to mid-IR intensity ratio of the EBL determines the relative ~ 1 to 10 TeV opacity. This is illustrated in Figure 5 which shows the energy dependence of $\tau_{\gamma\gamma}$. A large near- to mid-IR ratio in the EBL intensity would cause the $\gamma-$ray opacity to be relatively flat in the $\sim 1 - 10$ TeV region, resulting in a hard $\gamma-$ray spectrum. Conversely, a low near- to mid-IR ratio would result in an increase in the ~ 10 TeV opacity relative to that at ~ 1 TeV, resulting in a softer blazar spectrum.

The spectral shape of the EBL in the $\sim 1 - 15$ μm region can be related to the break $\Delta\Gamma_{TeV} \equiv \Gamma(< 1\ TeV) - \Gamma(> 1\ TeV)$ in the blazar spectra. A study of 12 blazars spanning a redshift range from 0.03 to 0.186, showed a trend of increasing $|\Delta\Gamma_{TeV}|$ with redshift with a statistical significance of 3.6σ (Orr et al., 2011). This strongly suggests that the trend is caused by EBL absorption, providing strong constraint on the near-IR to mid-IR EBL intensity ratio. Combined with $\gamma-$ray-derived upper limits on the EBL (Orr et al., 2011) derived correlated constraints between the near-IR and mid-IR intensity ratio of the EBL and the EBL intensity at mid-IR wavelengths.

$\gamma-$ray inverse Compton emission from radio lobes: A new method for

determining the local EBL intensity was described by (Georganopoulos et al., 2008). The method relies on the detection of $\gamma-$rays produced by IC scattering of CMB and EBL photons off the relativistic electrons of the lobes of radio galaxies. Since the lobes have to be clearly resolved with the $\gamma-$ray telescope, the method is presently limited to the nearby radio galaxy Fornax A. With the normalization and maximum electron energy in the lobes determined by their synchrotron spectra (measured by WMAP), the $\gamma-$ray spectrum of the lobes is determined by the intensity of the radiation field in the radio lobes, which is dominated by the CMB and EBL. The resulting $\gamma-$ray spectrum comprises distinct contributions by the CMB and EBL photons: The CMB contribution peaks at energies ~ 40 MeV, while that of the EBL appears as an excess above steeply dropping CMB contribution at higher energies. This excess emission is relatively flat, and extends to energies of ~ 50 GeV. Its magnitude provides a direct measurement of the EBL intensity at mid- and far-IR wavelengths.
Combined $\gamma-$ray limits: Figure 11 shows select limits on the EBL derived from TeV observations. All limits were adjusted to a common Hubble constant of 70 km s^{-1} Mpc^{-1}. Strict convergence of the different limits is not expected, since each limit was derived from different assumptions on the intrinsic blazar spectra and the EBL spectrum. The bold horizontal lines and the Orr et al. (2011) limit represent the most recent limits on the EBL. The 1 μm and 10μm upper limits derived in these studies agree within 20%. It is important to emphasize that different methods were used, i.e., the $\Gamma > 1.5$ limit on the hardness of the blazar spectrum and the spectral break analysis due to EBL spectrum, yet they reached similar conclusions.

In general, much improved upper limits are now available from the observations with the new generation of atmospheric Cherenkov telescopes (H.E.S.S., MAGIC, VERITAS). Both the near-IR and the mid-IR intensity levels are now constrained to much lower values than was possible with early results from the first few TeV blazars, and make only minimal assumptions on the intrinsic blazar spectra. Extreme EBL scenarios, with 70 nW m^{-2} sr^{-1}at 1.5 μm, as suggested by Matsumoto et al. (2005) are clearly ruled out. Minimal assumptions on the blazar spectra such as the absence of exponential rises or applying the $\Gamma > 1.5$ limit, reject such high EBL intensities in the near-IR (Dwek et al., 2005b; Aharonian et al., 2006a).

Mazin & Raue (2007) provide upper limits that are comparable to the former two in the near-IR, while in the mid-IR their upper limits are much higher. For this work the spectrum of 1ES 0229+200, a blazar with a redshift

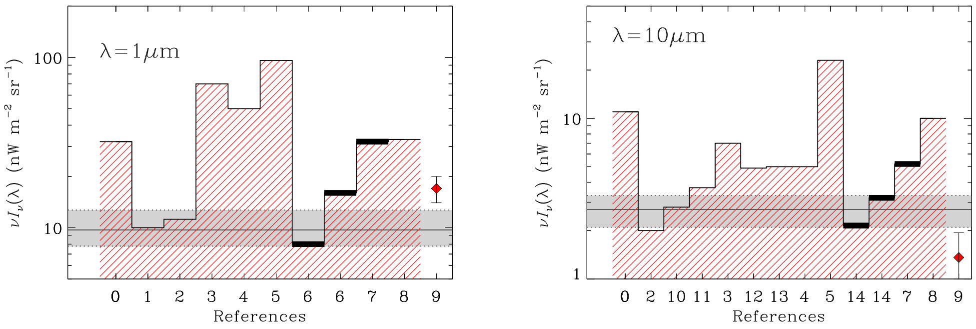

Figure 11: The EBL constraints as derived from $\gamma-$ray observations to the EBL are shown for 1 μm (left) and for 10 μm (right). The horizontal line represents the intensity of the integrated galaxy light (IGL), which provides a strict lower limit on the EBL intensity. The most recent limits are represented by bold lines. The shaded area represents the 1σ uncertainty in the IGL intensity. References to the $\gamma-$ray limits are: (0) Stecker & de Jager (1993); (1) Stanev & Franceschini (1998); (2) Biller et al. (1998); (3) Guy et al. (2000); (4) Dwek et al. (2005b); (5) Schroedter et al. (2005); (6) Aharonian et al. (2006a); (7) Mazin & Raue (2007); (8) Finke & Razzaque (2009); (9) Orr et al. (2011); (10) Funk et al. (1998); (11) Mannheim (1998); (12) Dwek & Slavin (1994); (13) Renault et al. (2001); (14) Aharonian et al. (2007a).

of z=0.129 and a spectrum up to 10 TeV was not available, while it is the basis for strong mid-IR limits in Aharonian et al. (2007b) and Orr et al. (2011). This emphasizes the importance of extending the TeV energy spectra of distant (z$\geq$ 0.1) blazars into the multi-TeV regime, where $\gamma-$rays reach their maximum cross-section with photons in the mid-IR. Furthermore, energy spectra between 100 GeV and 10 TeV are sensitive to the spectral shape of the EBL, thereby linking the upper limits in the near- and mid-IR; a given mid-IR intensity level combined with the EBL spectral shape limits the range of near-IR EBL intensities, i.e., by excluding EBL intensities that are either too high or too low in the near-IR based on the spectral shape constraint.

There are now in the order of 30 extragalactic objects with redshifts up to $z \approx 0.5$ available for constraining the EBL. Limits derived from the recent generation of experiments (H.E.S.S., MAGIC, VERITAS) suggest a low mid-IR, such as the results from Aharonian et al. (2007b) and Orr et al. (2011).

In summary, it should also be noted that all of the most recent TeV constraints are well within the boundaries set by direct measurements and their uncertainties (see shaded area in Figure 10). However, given the debate about some of the assumptions about the blazar spectra, namely, the $\Gamma > 1.5$

limit on the hardness of the blazar spectrum, claims that the EBL has been resolved are premature.

7. The $\gamma-$ray Opacity of the Universe

With blazars being detected at increasingly large redshifts, it becomes possible to use them to discriminate between different EBL models. The $\gamma-$ray opacity to a blazar at redshift z, is given by:

$$\tau_{\gamma\gamma}(E_\gamma, z) = -\log\left[\frac{F(E_\gamma, z)_{obs}}{F(E_\gamma)_{int}}\right] \tag{16}$$

The opacity can be determined from models of the EBL if its evolution with redshift is known and, independently, from $\gamma-$ray observations if the intrinsic blazar spectrum is known. Concordance between these two independent determinations of $\tau_{\gamma\gamma}$ can serve as a test for the validity of the underlying assumptions in each method.

Figures 12 and 13 depict the evolution of the comoving intensity of the EBL, the corresponding evolution of the proper number density of background photons, the optical depth to blazars at various redshift, and the corresponding attenuation factor. Results are plotted for the BE evolution model of Franceschini et al. (2008) and the BE evolution model of Domínguez et al. (2011).

Determining the $\gamma-$ray opacity from observations requires knowledge of the intrinsic blazar spectrum. Differences between the observed and expected flux at a given energy E_γ would then be simply attributed to EBL attenuation. Figures 12 and 13 show that the sharp drop of the EBL intensity at UV and shorter wavelengths renders the universe almost transparent to GeV photons. Consequently, the observed $\sim 1-50$ GeV spectrum is very likely the intrinsic blazar spectrum. So instead of assuming a theoretical limit on the spectral index, one can use the GeV - 10s of GeV energy spectral slope from Fermi data as a proxy for the intrinsic spectra at TeV energies.

Assuming that this power law can be extrapolated from GeV to TeV energies, one can derive the TeV optical depth to the observed blazar. This approach was used by Georganopoulos et al. (2010) and in method 1 in Orr et al. (2011) to set firm upper limits on EBL models using the GeV to TeV spectra of PKS 2155-304 ($z = 0.116$) and 1ES 1218+304 ($z = 0.182$). Assuming that the GeV spectrum is unattenuated by the EBL, Mankuzhiyil et al. (2010) used optical, X-ray and GeV data to model the TeV flux of

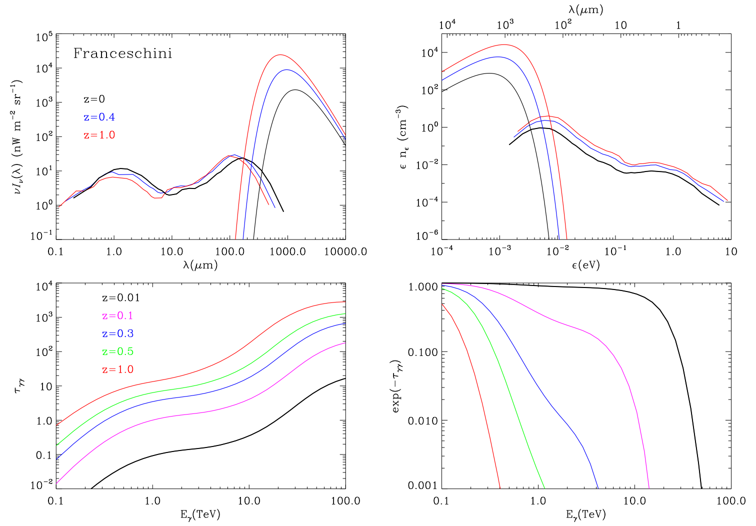

Figure 12: Basic EBL model results by Franceschini et al. (2008): **Top left**: The comoving EBL and CMB intensities versus wavelength for different redshifts; **Top right**: The proper number density of EBL and CMB photons versus energy for the same grid of redshifts as the previous panel; **Bottom left**: The $\gamma-$ray opacity versus energy, E_γ for different redshifts; **Bottom right**: The amount of attenuation versus energy for the same grid of redshifts as the previous panel. The figure illustrates the change in the slope of $\tau_{\gamma\gamma}$ at energies corresponding to the wavelength at which the slope of the EBL spectrum changes.

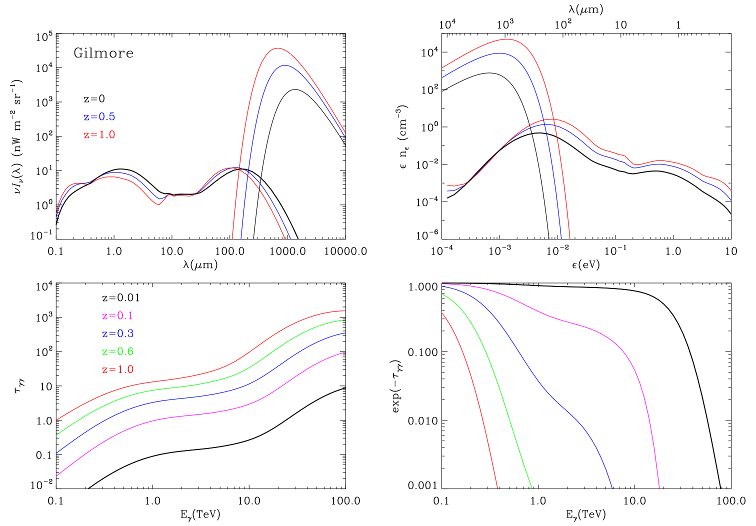

Figure 13: Same as Figure 12 for the Gilmore et al. (2011) model.

PKS2155-304 using a one-zone SSC model. Comparison of the model results with observations, they derived the TeV opacity to this blazar, and found it to be consistent with most EBL models.

Figure 14 compares the dependence of the optical depth derived from EBL models (hatched curves) to that derived for select blazars: Mrk 501, 1ES 1218+304, and 3C 66A. Each hatched band spans the range of optical depths predicted by the EBL models of Franceschini et al. (2008), Finke et al. (2010), Domínguez et al. (2011), and Gilmore et al. (2011). The colored dots represent the optical depths derived from the $\gamma-$ray observations of the three blazars. The intrinsic blazar spectrum was assumed to be a power law determined by the observed flux at 1 GeV and the spectral index, Γ_{GeV}. The observed flux in the TeV range was assumed to be a power law with a spectral index Γ_{TeV} (see Table 2). The $\gamma-$ray opacity in the TeV range was then derived from eq. (9). The band of opacities for each blazar was obtained by performing 100 Monte Carlo simulations of the intrinsic and observed spectra using the uncertainties in the spectral indices and $\gamma-$ray energies into account.

The figure shows that the $\gamma-$ray derived optical depths of Mrk 501 and 1ES 1218-304 are in general agreement with model prediction. The discrepancy between the the EBL and the $\gamma-$ray derived optical depth for 3C 66A is typical of most blazars listed in Table 2. The convergence between observational limits on the EBL and models suggests that the origin of the discrepancy can be mostly attributed to our still incomplete knowledge of the intrinsic spectra of blazars.

8. Is the Blazar Spectrum Determined in the Source?

In deriving upper limits on the EBL from TeV observations, it was tacitly assumed that blazar spectra are produced in the sources and attenuated en route to Earth. The detection of medium redshift blazars at $z \sim 0.2$ with hard $\gamma-$ray spectra has revived alternate models for the origin of their spectra. Since hard photons from these redshifts are easily attenuated, one of these models proposes that the observed blazar spectra contains secondary photons that are produced close to the observer, and therefore more likely to survive.

High resolution optical spectra of the blazars PKS 0447-439 and PMN J0630-24 obtained with the CTIO and NTT observatories show a clear absorption line around 6280 Å which, when attributed to the Mg II 2795.5 Å and

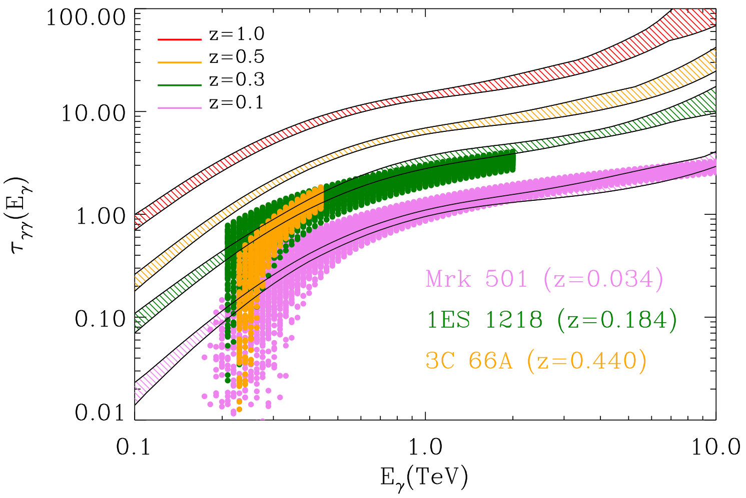

Figure 14: Limits on the optical depth at $z = 0.1$, 0.3, 0.5, and 1.0 as determined by the EBL models are compared to observationally determined optical depths for select blazars. The optical depth to 3C 66A is still uncertain. See §7 for more details.

2802.7 Å doublet, places them at redshifts $z \gtrsim 1.246$ and $z \gtrsim 1.238$, respectively (Landt, 2012). PKS 0447-439 was detected as a very-high energy $\gamma-$ray source with H.E.S.S., showing an energy spectrum from 200 GeV - 1.5 TeV (Zech et al., 2011).

The optical depth of 1 TeV photons at such large redshift is about 20 (see Figures 12 and 13), so that any flux of ~ 1 TeV photons is attenuated by a factor of $\sim 10^{-9}$. This would suggest that the intrinsic 1 TeV luminosity of this blazar is about 10^{10} larger than that of Mrk 421! Any attempts to solve this problem by lowering the $\gamma - \gamma$ opacity of the intervening intergalactic medium will require the unrealistic reduction of the EBL intensity below the lower limits determined by the IGL (see Figure 7).

It is therefore unlikely that primary $\gamma-$rays could have reached the Earth from such distance, suggesting that most of the $\gamma-$rays from this object must be secondary photons created by the interaction of cosmic-ray protons at relatively close distances to the observer (Kusenko, 2012; Aharonian et al., 2012). The secondary photons are generated by the interactions of the protons with the CMB and the EBL. For the secondary photons to be detected, they have to be produced within a distance λ_γ, the mean-free-path of the secondary $\gamma-$rays, of the Earth, and be deflected into the viewing angle of the telescope (e.g Stanev et al., 2000). For these photons to account for part of the energy spectra in blazars, their angular deviation from the primary source direction has to be smaller than the point spread function of the telescope ($\sim 0.1^\circ$). This requires the protons to travel on a "straight" trajectory until the interaction region, which sets a range $\sim 10^{-17} - 10^{-15}$ G on the line-of-sight intensity of the intergalactic magnetic field (Aharonian et al., 2012). While this value is significantly smaller than commonly accepted upper limits for the intergalactic magnetic field (Kronberg, 1994, 2010), weak fields are not ruled out.

Generally, leptonic models (SSC and EC) are capable of explaining the spectral energy distributions of most blazars. However, hadronic particle acceleration lies at the origin of the cascade model, potentially holds the key to understanding blazar jets, and may have far reaching consequences for their role in high energy astrophysics. Hadronic jet models are attractive for explaining the origin of ultra-high energy (UHE: $E \geq 10^{17}$ eV) cosmic rays that are detected by air shower arrays such as AUGER and HiRes (Kampert, 2012; Sokolsky & for the HiRes Collaboration, 2010). Hadronic jet emission models were brought forward (Mannheim, 1993) around the time of the first detection of TeV photons from a blazar (Punch et al., 1992). Protons at energies of $10^{18} - 10^{19}$ eV are capable of reaching the threshold for photopion production with ambient photons, and generate a subsequent cascade inside the jet, and thereby make a substantial contribution to primary $\gamma-$ray emission from blazars. Furthermore, proton synchrotron radiation and synchrotron emission from secondary particles contribute to the $\gamma-$ray spectrum.

Those $\gamma-$ray emission models have been put to test through TeV $\gamma-$ray observations of nearby blazars for which EBL absorption is negligible. The acceleration of UHE protons along relativistic jets requires large magnetic fields, typically several 10s of Gauss. Upper limits to the size of the $\gamma-$ray emission region can be derived from the observation of TeV flares. The first big flare reported from Mrk 421 exhibited sub-hour scale flux variability (Gaidos et al., 1996). Assuming a Doppler factor of 10, the short flux variations set a limit to the size of the gamma-ray emission region ($\leq 10^{13}$ m) in the comoving frame of the relativistic jet (Gaidos et al., 1996). Following Dermer (2012), a magnetic field strength of at least ~ 50 G is required to prevent 10^{19} eV ions and protons from escaping the small emission region. Such large magnetic fields are still consistent with the substantial but plausible power requirements for the magnetic field energy (less than 0.1% of the Eddington luminosity). Therefore, the observation of short flares does not pose a major obstacle to the viability of hadronic models.

A consequence of hadron induced pair cascades in intergalactic space is a contribution to the diffuse $\gamma-$ray background (DGB). Recent measurements of the DGB by *Fermi* (Abdo et al., 2010d) extent up to 100 GeV. Further measurements extending up to 1 TeV would provide important feedback to the presence of secondary $\gamma-$rays from blazars. If indeed the intergalactic magnetic field strength is small, protons can travel cosmological distances and thus dissipate significant amounts of non-thermal energy into secondary $\gamma-$rays locally, and enhance the DGB well into the TeV regime. If the magnetic fields are relatively strong, distant sources would not contribute much to pair cascades initiated within the observer's transparency zone, and one would expect the spectrum of the DGB to fall steeply above several 10s of GeV.

However, the need to resort to hadronic acceleration model to explain the observed flux of PKS 0447-439 is probably premature. The redshift determination to this blazar has recently been challenged by Fumagalli et al. (2012) who independently obtained the PKS 0447-439 spectrum using the 6.5 m Magellan Telescopes with a high S/N ratio of ~ 150 in the 6270–6300 Å region of interest. They point out the existence of an atmospheric telluric absorption line at the wavelength of the claimed Mg II absorption line, which they showed was also present in the spectrum of two standard stars. As a result the redshift of PKS 0447-439 is still undetermined.

9. EBL Limits on "Exotic" Energy Releases in the Universe

The intensity and spectral shape of the EBL contain the memory of all energy releases in the universe since the epoch of recombination. The *COBE*/DIRBE limits on the UV to near-IR regions of the EBL proved useful in ruling out various "exotic" sources of energy in the early universe, such as decaying particles, exploding stars, or very massive objects (Dwek et al., 1998, and references therein).

Primordial (Population III) stars were suggested by Salvaterra & Ferrara (2003) as the source of the excess 1-5 μm diffuse emission above the IGL intensity detected by Matsumoto et al. (2005). However, (Dwek et al., 2005b) ruled out an extragalactic origin for the excess emission, since it would have produced a physically unrealistic intrinsic $\gamma-$ray spectrum of the blazar PKS 2155-304. Furthermore, Dwek et al. (2005a) showed that such origin

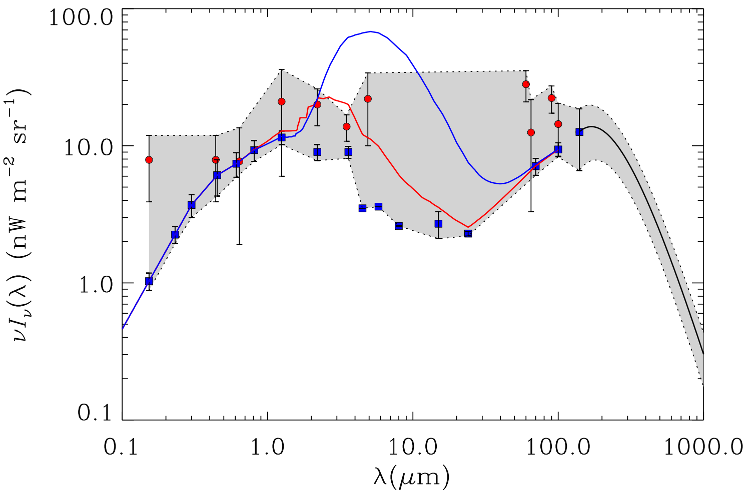

Figure 15: The contribution of dark stars to the EBL for two different Limits on the EBL intensity. Lower limits, blue squares) are determined by the intensity of the IGL. Upper limits (red circles) are determined by absolute measurements of the EBL. The data used in the figure are listed in Tables 3-5 in bold. The shaded area depicts the range of the allowed EBL intensity as determines by UV to sub millimeter observations.

would have required a Pop III star formation rate and energy output to be significantly higher than that predicted by hierarchical models for structure formation in a ΛCDM universe (Bromm & Loeb, 2002). Using theoretical limits on their formation rate, (Dwek et al., 2005a) concluded that Pop III stars can contribute only a fraction of the EBL intensity.

A more detailed study of the contribution of Pop III stars to the EBL intensity was conducted by Raue et al. (2009). Using $\gamma-$ray derived constraints on the EBL intensity they set a limit of 0.3 to 3 $M_\odot$ Mpc^{-3} yr^{-1} on the formation rate of Pop III stars in the $z = 7 - 14$ redshift interval.

More recently, (Maurer et al., 2012) used EBL limits to constrain the properties of dark stars (DS) in the early universe. Dark stars are objects that have either accreted or captured weakly interacting massive particles (WIMPs, a dark matter candidate), which by annihilating inject energy into the stars before their radiative output is dominated by standard nuclear fusion processes. The formation rate of these stars, their luminosity and spectrum, and their effective lifetime are all free parameters of the model. Figure 15 depicts the EBL, to which the contribution of dark stars was added to the IGL intensity, for two different sets of parameters. The blue curve represents the EBL with a contribution of 106 $M_\odot$ DS with a surface temperature of 5,000 K, and the red curve that with the added contribution of 690 $M_\odot$ DS with a surface temperature of 7,500 K. The colder dark stars are obviously ruled out, but the hotter ones are marginally consistent with current EBL limits, dominating the intensity of the IGL in the $\sim 2 - 10\ \mu$m wavelength region.

10. Summary and Future Direction

Very high energy $\gamma-$rays emitted from extragalactic sources are attenuated en route to earth by $\gamma - \gamma$ interaction with EBL photons. $\gamma-$ray observations can therefore be used to set limits on the EBL intensity, provided that the intrinsic $\gamma-$ray spectrum of the sources is known. Conversely, knowledge of the EBL can be used to determine the intrinsic $\gamma-$ray spectrum of the different sources, thereby provide important constraints on mechanisms for their production. The main issues and results discussed in this review can be briefly summarized as follows:

1. The EBL spectrum consists of two broad peaks, one at $\lambda \approx 1\ \mu$m, representing the cumulative gravitational and nuclear energy releases by stars and AGNs over cosmic history. Their energy has been partially absorbed by dust and reradiated at IR wavelengths. This thermal dust emission component generates a second peak at $\sim 100 - 200\ \mu$m. Current limits and detections of the EBL were presented in Figure 7, and the partitioning of its total intensity into the different emission components was presented in Table 6;
2. The cross section for the $\gamma-\gamma$ interaction is broad and peaks at energies $E_\gamma(TeV) \approx 0.86\ \lambda(\mu\ \mathrm{m})$. Consequently, the energy dependence of the $\gamma-$ray opacity, a product of the cross section with the number density of EBL photons, reflects the spectral variation in the EBL. We identified three potential breaks in the spectrum of $\gamma-$ray sources, one occurring between 10 and 500 GeV, a second break at 1 TeV and third at 10 TeV (see Figures 3 and 4);
3. The spectral breaks at GeV and TeV energies have been used to set limits on the EBL intensity at near-IR wavelengths, and on the relative intensities of the peak of the stellar emission and the trough between the stellar and dust emission components of the EBL;

4. $\gamma-$ray derived limits on the EBL vary as different studies used different assumptions on the intrinsic $\gamma-$ray source spectra (see Figure 10). The strictest limits on the EBL are around the 1 and $\sim 10\ \mu$m wavelength regions of the EBL, with some approaching the lower limit on the EBL intensity set by the IGL (see Figure 11);
5. Recent IR space and ground-based observations have resulted in closer agreement between the EBL limits and detections derived from measurements of the absolute sky brightness and lower limits set by the integrated light from galaxies. A summary of the recent observational status of the EBL is presented in Tables 3–5. The major gap in our knowledge of the EBL is in the $\lambda \approx 10-70\ \mu$m wavelength region, where the thermal emission from interplanetary dust (the zodiacal light) dominates the brightness of the sky;
6. Models of the EBL, employing various methods for determining the evolution of the galaxies' spectral energy density with redshift seem to agree on the intensity and spectral shape of the UV to near-IR component of the EBL. However, there are considerable differences in their treatment of the redistribution of the intrinsic stellar and AGN output at IR wavelengths (see Figure 9);
7. The discovery of TeV blazars with alleged redshifts $z \gtrsim 1$ has revived an alternative model for the creation of these high energy photons. In this model hadronic jets produce a cascade of $\sim$ TeV $\gamma-$ray photons en route to earth, circumventing the attenuation problem from such high redshift sources (see §8). However, the redshift of these sources has been disputed, so the need to resort to such hadronic model is highly premature;
8. Dark matter has been invoked to postulate the existence of a new class of primordial stars, powered by dark matter annihilation, instead of nuclear fusion. The energy release from these so-called dark stars could, in principle, lead to an observable signature in the EBL spectrum (see Figure 15); and finally
9. Observations suggest that the universe is essentially transparent to $\gamma-$rays with energies $\lesssim 2$ TeV up to $z \approx 0.2$, and energies of $\lesssim 400$ GeV up to $z \approx 0.4$ (see Figure 14).

The future prospects of intensified EBL studies with $\gamma-$rays are promising, especially when considering the progress made over the last 5 years through the operation of *Fermi* and the current generation of atmospheric

Cherenkov telescopes. These instrument yielded combined energy spectra for at least 3 dozen extragalactic sources that cover up to 5 orders of magnitude in energy. These data have provided a first glimpse of the transition region from a transparent universe at 1 GeV, to TeV energies at which the universe gradually turns opaque with increasing redshift.

Furthermore, *Fermi* detected a large set of blazars (Ackermann et al., 2011) including 310 FSRQs, 395 BL Lacertae objects and 156 candidate blazars, raising the specter for EBL studies with sizable source samples and different sources classes with CTA. Large samples of blazars have the potential to constrain the EBL in the optical/near-IR and mid- IR through a better understanding of the blazar subclasses (FSRQs, LBL, IBL, HBL) and their intrinsic spectra, and better photon statistics for the measurement of the redshift dependence of any spectral feature attributable to the EBL.

Recent discoveries of TeV emission from nearby radio- and starburst galaxies also gives rise to future prospects of extending the reach of $\gamma-$ray constraints up to the far-IR through energy spectra spanning a few GeV up to 100 TeV. These will be important to extend measurements of the $\gamma-$ray opacity imposed by the EBL all the way from UV/optical/near-IR/mid-IR to the far-IR and thus provide additional constraints to the intensity ratios between the different wavelength regimes of the EBL.

Limitations of precision EBL studies with $\gamma-$rays arise from technical reasons, but are not unsurmountable. First, systematic uncertainties in the measurements of $\gamma-$ray spectra with atmospheric Cherenkov telescopes arise from uncertainties in modeling the Earth's atmosphere, which translates into uncertainties in the attenuation of Cherenkov light from electromagnetic cascades. To first order this affects the absolute energy scale of the measured $\gamma-$ray energies and is typically quoted at a level of 15% to 20%. Effects on the spectral index and shape are generally of second order but require detailed studies. Additional uncertainties lie in the absolute instrument calibration of Cherenkov telescopes, e.g., mirror reflectivity, light losses in the focal plane, and uncertainties in the quantum efficiency of the photodetectors, affecting the light throughput and absolute energy scale. Uncertainties in the spectral indices and spectral shape are typically quoted at the level of $\Delta\Gamma = 0.05 - 0.1$ or better, and depend mostly on the $\gamma-$ray selection efficiency derived from Monte Carlo simulations and detailed detector modeling. Currently most energy spectra published (except for few flaring sources) are dominated by statistical uncertainties and leave much room for improvement through a more sensitive instrument such as CTA with a collection area of

$\sim km^2$. At the same time calibration techniques are continually improving to provide a better handle on systematics as well.

Astrophysical challenges facing EBL studies with $\gamma-$rays arise from the fact that currently only 55% of all Fermi detected BL Lacs have reliable redshift measurements (Ackermann et al., 2011). Attempts to increase the redshift identifications through dedicated optical follow-up observations of the host galaxies of Fermi detected blazars during low flaring states are promising to increase the fraction of blazars with known redshift. The redshift distribution for FSRQs detected by *Fermi* peaks at z = 1 extending to z = 3.1, while BL Lacs peak at z = 0.2 reaching up to a redshift of z = 1.5. As already indicated, GeV/TeV detections of FSRQs are promising to allow constraints to the EBL in the UV/optical. Furthermore, the first detection of FSRQs by atmospheric Cherenkov telescopes out to redshifts of $z = 0.5$ provides the potential to complement EBL studies with a different class of sources, with different intrinsic spectral properties than BL Lacs and, most importantly, whose redshifts are known.

Detection and limits on the EBL have been obtained by direct absolute measurements, and by galaxy number counts that provided lower limits on its intensity. Direct measurements are aided by ground-based or space-based observations that resolve the foreground emission from Galactic stars. Future observations can considerably improve direct absolute measurement of the EBL by determining the absolute brightness of the zodiacal light from high resolution observations of reflected solar Fraunhofer lines, or by making absolute sky measurements from the outer solar system, thus effectively removing any foreground contribution from the zodiacal cloud. Lower limits on the EBL can converge to the EBL itself with observations of sufficient depth and resolution to resolve all the galaxies that contribute to its intensity.

The James Webb Space Telescope (JWST) is a large (6.6 m) IR space observatory, passively cooled to temperatures below 50 K, that will be launched into orbit at the second Earth-Sun Lagrange point (L2). The wide band observations with NIRCam at 2 - 5 μm and MIRI at 6 - 25 μm will fill in crucial gaps in our knowledge of the EBL intensity at these wavelengths. NIRCam will cover a 10 arcmin^2 field of view (FOV) and will resolve galaxies down to a 10σ flux limit of 11 nJy at 2 μm in 10,000 s, making it about 10^3 more sensitive than the Spitzer/IRAC 3.6 μm filter. With unparalleled resolution and sensitivity, the JWST (Gardner et al., 2006) will resolve the EBL at near-IR wavelengths. The MIRI instrument operating in its broadband imaging mode at 10 and 21 μm will have a smaller FOV of $\sim$2.6 arcmin^2, and sensitivities of 700 nJy and 9 μJy, respectively. It will resolve galaxies down to the confusion limit which, because of its large telescope size, will be significantly fainter than that of the Spitzer/MIPS instrument at 24 μm.

Absolute measurements of solar absorption line profiles in the zodiacal light, for example the Fraunhofer Mg I line at 1.182819 μm or the Si I line at 1.210354 μm can be used to determine and remove the contribution of the ZL to the total sky brightness in the J (1.25 μm) band (Kutyrev et al., 2004, 2008). High resolution (R $\sim$ 20,000) observations of these lines using the ground-based spectrometer ZEFIR (Zodiacal Emission determination through Fraunhofer IR lines) will determine their equivalent width (EW) in the ZL spectrum. The continuum contribution of the ZL in the J-band can then be determined from knowledge of the EW of these lines in the solar spectrum. The DIRBE instrument provided absolute measurements of the sky brightness in this band, and ground-based sky surveys (2MASS) have removed most of the contribution of Galactic stellar emission from this band. Measurements of the absolute brightness of the ZL will thus provide the absolute intensity of the EBL in the DIRBE 1.25 μm waveband. Similar measurement could also be made from the ground in the 2.2 μm band.

Finally, the contribution of the ZL to the observed sky brightness can be largely eliminated by mapping the absolute intensity of the diffuse emission from the sky from beyond the zodiacal cloud. A satellite mission conducting such EBL measurements from the outer solar system will be an important step in that direction (Cooray, 2011).

The next decade will see significant improvement in γ-ray technology, and measurements of the EBL, providing new insights into the spectrum of the different γ-ray sources and the mechanism that generate them, and into the spectrum of the EBL which will provide new constraints on the history of all nuclear and gravitational energy releases in the universe. The synergy between TeV γ-ray astronomy and EBL research will ensure that any development in each field will greatly benefit both.

Acknowledgements

ED and FK gratefully acknowledge the support from the NASA Fermi Guest Investigator grant NNX11AO38G. FK also acknowledges the support from the U.S. Department of Energy Office of Science. We thanks C.D. Dermer, J.D. Finke, A. Dominguez, R.C. Gilmore, A. Franceschini, and J.R. Primack for providing their model results in digital format. We thank D. Kazanas and R.G. Arendt for their comments on parts of the manuscript, and an anonymous referee for his/her thorough reading of and helpful comments on the manuscript.

Table 1: Glossary of Abbreviations of Spacecrafts[1], Telescopes, and Instruments

Abbreviation	Full Name
Akari	Infrared imaging satellite (ASTRO-F)
BLAST	Balloon-borne Large-Aperture Submillimeter Telescope
COBE	Cosmic Background Explorer
DIRBE	Diffuse Infrared Background Experiment
FIRAS	Far Infrared Absolute Photometer
CTIO	Cerro Tololo Inter-American Observatory
GALEX	Galaxy Evolution Explorer
Herschel	Herschel Space Observatory
PACS	Photodetector Array Camera
SPIRE	Spectral and Photometric Imaging Receiver
HST	Hubble Space Telescope
WFPC2	Wide Field Planetary Camera
NICMOS	Near IR Camera and Multi-Object Spectrometer
IRTS	Infrared Telescope in Space
ISO	Infrared Space Observatory
ISOCAM	ISO Camera
JCMT	James Clerk Maxwell Telescope
SCUBA	Submillimeter Common User Bolometer Array
NTT	New Technology Telescope
Spitzer	Spitzer Space Telescope
IRAC	Infrared Array Camera
MIPS	Multiband Imaging Photometer
Subaru	Optical, near-IR telescope
Pioneer	Interplanetary spacecraft
WMAP	Wilkinson Microwave Anisotropy Probe
2MASS	Two Micron All Sky Survey
CTA	Cherenkov Telescope Array
Fermi	Fermi Gamma-Ray Space Telescope
H.E.S.S.	High Energy Stereoscopic System
IACT	Imaging Air Cherenkov Telescope
MAGIC	Major Atmospheric Gamma-Ray Imaging Cherenkov Telescope
Milagro	Gamma-ray and cosmic-ray telescope
VERITAS	Very Energetic Radiation Imaging Telescope Array

[1] Spacecraft names are presented in italics, and their instruments are indented.

Table 2: Extragalactic $\gamma-$ray sources with GeV and TeV spectral information.

Name	Class	redshift	Γ_{GeV}	Γ_{TeV}	Range [TeV]	References
Centaurus A	Radio	0.0008	2.76±0.05	2.7±0.5	0.2 - 5	[1], [2]
M82	SB	0.00085	2.2±0.2	2.5±0.6	0.7 - 4	[3], [4]
NGC253	SB	0.00093	1.95±0.4	2.24±0.14	0.3 - 50	[3], [5]
M87	Radio	0.0036	2.17±0.07	2.5±0.2	0.2 - 10	[6], [7], 8], [9]
NGC 1275	Radio	0.018	2.00±0.02	3.96±0.37	0.1 - 0.3	[10], [11]
IC 310	Radio	0.0188	2.10±0.19	2.0±0.14	0.1 - 7	[12], [13], [14]
Markarian 421	HBL	0.031	1.77±0.01	$2.48\pm0.03^{\star}$	0.1 - 5	[15]
Markarian 501	HBL	0.034	1.74±0.03	$2.51\pm0.05^{\triangle}$	0.1 - 10	[16]
1ES 2344+514	HBL	0.044	1.72±0.08	$2.78\pm0.09^{\triangle}$	0.3 - 2	[6], [17]
Markarian 180	HBL	0.046	1.74±0.08	3.3±0.70	0.2 - 1	[6] [18]
1ES 1959+650	HBL	0.047	1.94±0.03	2.72±0.14	0.2 - 2	[6], [19]
AP Lib*	LBL	0.048	2.05±0.04	2.5±0.2	0.3 - 2	[6], [20]
BL Lacertae	LBL	0.069	2.11±0.04	3.6±0.5	0.2 - 1	[6], [21]
PKS 2005-489	HBL	0.071	1.78±0.05	4.0±0.4	0.2 - 2	[6], [22]
W Comae	IBL	0.103	2.02±0.03	3.81±0.35	0.3 - 1	[6], [23]
PKS 2155-304	HBL	0.116	1.84±0.02	3.53±0.05	0.4 - 5	[6], [24]
B3 2247+381	HBL	0.119	1.84±0.11	3.2±0.5	0.2 - 1	[6], [25]
RGB J0710+591	HBL	0.125	1.53±0.12	2.69±0.26	0.3 - 4.6	[6], [26]
H 1426+428	HBL	0.129	1.32±0.12	3.50±0.35	0.3 - 10	[6], [27]
1ES 1215+303	IBL	$0.13^{\heartsuit}$	2.02±0.02	2.99±0.15	0.1 - 1	[6], [28]
1ES 0806+524	HBL	0.137	1.94±0.06	3.6±1.0	0.3 - 0.7	[6], [29]
1RXS J101015.9-311909	HBL	0.143	2.24±0.14	3.14±0.53	0.3 - 1	[6], [20]
1ES 1440+122	IBL	0.163	1.41±0.18	3.3±0.7	0.3 - 1	[6], [30]
H 2356-309	HBL	0.165	1.89±0.17	3.09±0.24	0.3 - 2	[6], [31]
VER J0648+152	HBL	0.179	1.74±0.11	4.4±0.8	0.3 - 0.8	[6], [32]
1ES 1218+304	HBL	0.184	1.71±0.07	3.07±0.09	0.2 - 2	[6], [33]
1ES 1101-232	HBL	0.186	1.80±0.21	2.88±0.17	0.16 - 3.3	[6], [31]
RBS 0413	HBL	0.19	1.55±0.11	3.18±0.68	0.25 - 1	[6], [33]
PKS-0447-439	HBL	0.205	1.86±0.02	4.36±0.49	0.25 - 1	[6], [34]
1ES 1011+496	HBL	0.212	1.72±0.04	4.0±0.50	0.25 - 0.6	[6], [35]
1ES 0414+009	HBL	0.287	1.98±0.16	3.44±0.27	0.25 - 1.2	[6],[36]
S5 0716+714	LBL	0.31	2.01±0.02	3.45±0.54	0.25 - 1.2	[6], [37]
1ES 0502+675	HBL	$0.416^{\clubsuit}$	1.49±0.07	3.92±0.35	0.25 - 1	[6], [38]
4C 21.35	FSRQ	0.43	2.12±0.02	3.75±0.27	0.07 - 0.4	[6], [39]
3C 66A	IBL	$0.44^{\clubsuit}$	1.85±0.02	4.1±0.4	0.22 - 0.45	[6], [40]
3C 279	FSRQ	0.536	2.22±0.02	3.03±0.9	0.1 - 0.35	[6], [41]

$\star$ Spectrum is not well fit by a powerlaw. $\triangle$ Spectrum shows variations. $\clubsuit$ redshift uncertain. $\heartsuit$ redshift recently given by Abdo et al. arXiV:1108.1420v1, different redshift was considered viable by Colin et al. 2011

References: [1]Abdo et al. (2010c); [2] Aharonian et al. (2009); [3] Abdo et al. (2010b); [4] Acciari et al. (2009b); [5] (Abramowski et al., 2012, for the H.E.S.S. collaboration); [6] Ackermann et al. (2011); [7] Berger et al. (2011a); [8] Acciari et al. (2010b); [9] Aharonian et al. (2006b); [10] Abdo et al. (2009); [11] Hildebrand et al. (2011); [12] Neronov et al. (2010) ; [13] Aleksić et al. (2010b); [14] Ackermann et al. (2011); [15] Abdo et al. (2011b); [16] Abdo et al. (2011a); [17] Acciari et al. (2011b); [18] Albert et al. (2006a); [19] Albert et al. (2006b); [20]Cerruti, M. for the H.E.S.S. Collaboration (2011); [21] Albert et al. (2007a); [22] Aharonian et al. (2005a); [23] Acciari et al. (2008); [24] Aharonian et al. (2007b); [25] Berger et al. (2011b); [26] Acciari et al. (2010a); [27] Petry et al. (2002); [28] Colin et al. (2011); [29] Acciari et al. (2009a); [30] Benbow (2011); [31] Aharonian et al. (2006a); [32] Errando, M. et al. (2011) [33] Acciari et al. (2010c); [33] Şentürk et al. (2011); [34] Zech et al. (2011); [35] Albert et al. (2007b); [36] Volpe et al. (2011); [37] Anderhub et al. (2009); [38] Benbow, W. et al. (2011); [39] Aleksić et al. (2011a); [40] Acciari et al. (2009d); [41] Aleksić et al. (2011b).

Table 3: Limits and detection of the extragalactic background light (EBL).

λ		$\nu\, I_\nu$(nW m^{-2} sr^{-1})		Comment	Reference
(μm)	IGL	EXT	ABS		
0.1530	0.68 ± 0.10	$\mathbf{1.03 \pm 0.15}$		*Galex*	[1]
0.1595	3.75 ± 1.25			*HST*/STIS	[2]
0.2	0.6			FOCA/balloon	[3]
0.2310	0.99 ± 0.15	$\mathbf{2.25 \pm 0.32}$		*Galex*	[1]
0.2365	$3.6^{+0.7}_{-0.5}$			*HST*/WFPC2	[2]
0.30			18 ± 12	*HST*/WFPC2	[4]
	2.7 ± 0.3	$\mathbf{3.7 \pm 0.7}$		*HST*+ground	[5]
0.36	$2.9^{+0.6}_{-0.4}$			*HST*+ground	[6]
0.40			$< 36\,(26 \pm 10)$	dark cloud	[7]
0.44			$\boldsymbol{7.9 \pm 4.0}$	Pioneer 10/11	[8]
0.45	$4.6^{+0.7}_{-0.5}$			*HST*+ground	[6]
	4.4 ± 0.4	$\mathbf{6.1 \pm 1.8}$		*HST*+ground	[5]
0.5115			$< 39\,(30 \pm 9)$	ground	[9]
0.55			55 ± 27	*HST*/WFPC2	[4]
0.61	6.0 ± 0.6	$\mathbf{7.4 \pm 1.5}$		*HST*+ground	[5]
0.64			$\boldsymbol{7.7 \pm 5.8}$	Pioneer 10/11	[8]
0.67	$6.7^{+1.3}_{-0.9}$			*HST*+ground	[6]
0.81	$8.0^{+1.6}_{-0.9}$			*HST*+ground	[6]
	8.1 ± 0.8	$\mathbf{9.3 \pm 1.6}$		*HST*+ground	[5]
0.814			57 ± 32	*HST*/WFPC2	[4]
1.1	$9.7^{+3.0}_{-1.9}$			*HST*+ground	[6]
1.25			$\boldsymbol{21 \pm 15}$	*COBE*/DIRBE	[10]
			54 ± 17	*COBE*/DIRBE	[11]
	10.9 ± 1.1	$\mathbf{11.5 \pm 1.3}$		*HST*+ground	[5]
	$11.7^{+5.6}_{-2.6}$			Subaru	[12]
1.4–4			$\sim 60 - 15$	*IRTS*	[13]
1.6	$9.0^{+2.6}_{-1.7}$			*HST*+ground	[6]
	$11.5^{+4.5}_{-1.5}$			Subaru	[12]
2.12	$10.0^{+2.8}_{-0.8}$			Subaru	[12]
2.2	$7.9^{+2.0}_{-1.2}$			*HST*+ground	[6]
	8.3 ± 0.8	$\mathbf{9.0 \pm 1.2}$		*HST*+ground	[5]
			$\boldsymbol{20 \pm 6}$	*COBE*/DIRBE	[10]
			28 ± 7	*COBE*/DIRBE	[11]
3.5			13.3 ± 2.8	*COBE*/DIRBE	[10]
			$\boldsymbol{13.8 \pm 3}$	*COBE*/DIRBE	[15]
3.6	5.4			*Spitzer*/IRAC	[16]
		$\mathbf{9.0^{+1.7}_{-0.9}}$		*Spitzer*/IRAC	[14]
4.5	**3.5**			*Spitzer*/IRAC	[16]
4.9			$\boldsymbol{22 \pm 12}$	*COBE*/DIRBE	[17]
5.8	**3.6**			*Spitzer*/IRAC	[16]
8.0	**2.6**			*Spitzer*/IRAC	[16]

ABS=absolute measurement; IGL=integrated galactic light; STK=lower limits from stacking analysis; EXT=extrapolated intensity from dN/dS

[1] Calculated for a 2.2 μm intensity of 20.0 nW m^{-2} sr^{-1} and the Kelsall et al. (1998) ZL model.

References:[1] Xu et al. (2005); [2] Gardner et al. (2000); [3] Milliard et al. (1992); [4] Bernstein (2007); [5] Totani et al. (2001); [6] Madau & Pozzetti (2000); [7] Mattila (1990),Leinert et al. (1998); [8] Matsuoka et al. (2011); [9] Dube et al. (1979),Leinert et al. (1998); [10] Levenson et al. (2007); [11] Cambrésy et al. (2001); [12] Keenan et al. (2010); [13] Matsumoto (2001); [14] Levenson & Wright (2008); [15] Dwek & Arendt (1998); [16] Fazio et al. (2004); [17] Arendt & Dwek (2003)

Table 4: Limits and detection of the extragalactic background light (EBL).

	$\nu\, I_\nu$ (nW m^{-2} sr^{-1})					
λ(μm)	IGL	STK	EXT	ABS	Comment	Reference
15	2.4 ± 0.5				*ISO*/ISOCAM	Elbaz et al. (2002)
	$\mathbf{2.7 \pm 0.6}$				*ISO*/ISOCAM	Metcalfe et al. (2003)
	1.9 ± 0.5				*Akari*	Hopwood et al. (2010)
16	2.2 ± 0.2				*Spitzer*	Teplitz et al. (2011)
24	1.9 ± 0.6		$2.7^{+1.1}_{-0.7}$		*Spitzer*/MIPS	Papovich et al. (2004)
	1.8 ± 0.2		2.0 ± 0.2		*Spitzer*/MIPS	Chary et al. (2004)
	$\mathbf{2.29 \pm 0.09}$		$2.86^{+0.19}_{-0.16}$		*Spitzer*/MIPS	Béthermin et al. (2010a)
60				$\boldsymbol{28.1{\pm}1.8{\pm}7}$	*COBE*/DIRBE	Finkbeiner et al. (2000)
65				$\boldsymbol{12.5{\pm}1.4{\pm}9.2}$	*Akari*	Matsuura et al. (2011)
70			7.4 ± 1.9		*Spitzer*/MIPS	Frayer et al. (2006)
		$\mathbf{7.1 \pm 1.0}$			*Herschel*/PACS	Dole et al. (2006)
	5.4 ± 0.4		$6.6^{+0.7}_{-0.6}$		*Spitzer*/MIPS	Béthermin et al. (2010a)
	4.52 ± 1.18				*Herschel*/PACS	Berta et al. (2011)
90				$\boldsymbol{22.3{\pm}1.7{\pm}4.7}$	*Akari*	Matsuura et al. (2011)
100				$< 34\,(22 \pm 6)$	*COBE*/DIRBE (D, KZL)	Hauser et al. (1998)
				12.5 ± 5	*COBE*/DIRBE (D, WZL)	Wright (2004)
				$24.6 \pm 2.5 \pm 8$	*COBE*/DIRBE	Finkbeiner et al. (2000)
				23.4 ± 6.3	*COBE*/DIRBE (D, KZL)	Lagache et al. (2000)
				$\boldsymbol{14.4{\pm}6.0}$	DIRBE (F, WZL)	Dole et al. (2006)
	8.35 ± 0.95	$\mathbf{9.4 \pm 1.1}$			*Herschel*/PACS	Berta et al. (2010)
				$6.6 \pm 1.8 \pm 2.1$	*Spitzer*/MIPS	Pénin et al. (2012)
140				25.0 ± 6.9	*COBE*/DIRBE (D, KZL)	Hauser et al. (1998)
				15.0 ± 5.9	*COBE*/DIRBE (F, KZL)	Odegard et al. (2007)
				32 ± 13	*COBE*/DIRBE	Schlegel et al. (1998)
				24.2 ± 11.6	*COBE*/DIRBE (D, KZL)	Lagache et al. (2000)
				22 ± 7	*COBE*/DIRBE (D, WZL)	Wright (2004)
				$20.1 \pm 3.4 \pm 1.1$	*Akari*	Matsuura et al. (2011)
				12.4 ± 6.9	*COBE*/DIRBE (F, WZL)	Dole et al. (2006)
				$\boldsymbol{12.6{\pm}6.0}$	*COBE*/FIRAS	Fixsen et al. (1998)

Table 5: Limits and detection of the extragalactic background light (EBL).

	νI_ν (nW m^{-2} sr^{-1})					
$\lambda(\mu$m)	IGL	STK	EXT	ABS	Comment	Reference
160		13.4 ± 1.7			*Herschel*/PACS	Dole et al. (2006)
				$13.7 \pm 3.9 \pm 0.8$	*Akari*	Matsuura et al. (2011)
	9.49 ± 0.59	11.4 ± 0.7			*Herschel*/PACS	Berta et al. (2010)
	8.9 ± 1.1		$14.6^{+7.1}_{-2.9}$		*Spitzer*/MIPS	Béthermin et al. (2010a)
				$14.4 \pm 0.8 \pm 2.3$	*Spitzer*/MIPS	Pénin et al. (2012)
				13.7±6.1	*COBE*/FIRAS	Fixsen et al. (1998)
170	$19.1 \pm 5.6 \pm 5.3$				ISOPHOT	Juvela et al. (2009)
240				13.6 ± 2.5	*COBE*/DIRBE (D, KZL)	Hauser et al. (1998)
				13 ± 2.5	*COBE*/DIRBE (D, WZL)	Wright (2004)
				12.7 ± 1.6	*COBE*/DIRBE (F, KZL)	Odegard et al. (2007)
				17 ± 4	*COBE*/DIRBE	Schlegel et al. (1998)
				11.0 ± 6.9	*COBE*/DIRBE (D, KZL)	Lagache et al. (2000)
				12.3 ± 2.5	*COBE*/DIRBE (F, WZL)	Dole et al. (2006)
				10.9±4.3	*COBE*/FIRAS	Fixsen et al. (1998)
250		8.6 ± 0.6			BLAST	Marsden et al. (2009)
	$0.24^{+0.18}_{-0.13}$	$5.0^{+2.5}_{-2.6}$			BLAST	Béthermin et al. (2010b)
	1.73 ± 0.33				*Herschel*/SPIRE	Oliver et al. (2010)
	1.55 ± 0.30	7.40 ± 1.42	$10.13^{+2.60}_{-2.33}$		*Herschel*/SPIRE	Béthermin et al. (2012)
				10.3±4.0	FIRAS	Fixsen et al. (1998)
350		4.93 ± 0.34			BLAST	Marsden et al. (2009)
	$0.06^{+0.05}_{-0.04}$	$2.8^{+1.8}_{-2.0}$			BLAST	Béthermin et al. (2010b)
	0.63 ± 0.18				*Herschel*/SPIRE	Oliver et al. (2010)
	0.77 ± 0.16	4.50 ± 0.90	$6.46^{+1.74}_{-1.57}$		*Herschel*/SPIRE	Béthermin et al. (2012)
				5.6±2.1	FIRAS	Fixsen et al. (1998)
500		2.27 ± 0.20			BLAST	Marsden et al. (2009)
	$0.01^{+0.01}_{-0.01}$	$1.4^{+2.1}_{-1.3}$			BLAST	Béthermin et al. (2010b)
	0.15 ± 0.07				*Herschel*/SPIRE	Oliver et al. (2010)
	0.14 ± 0.03	1.54 ± 0.34	$2.80^{+0.93}_{-0.81}$		*Herschel*/SPIRE	Béthermin et al. (2012)
				2.4±0.9	FIRAS	Fixsen et al. (1998)
850	0.12 ± 0.03				SCUBA	Coppin et al. (2006)
	0.24 ± 0.03				SCUBA	Zemcov et al. (2010)
				0.5±0.21	*COBE*/FIRAS	Fixsen et al. (1998)
200-1000				$a\left(\frac{\lambda_0}{\lambda}\right)^k \nu B_\nu(T)$	FIRAS	Fixsen et al. (1998)[1]

[1] $a = (1.3\pm = 0.4) \times 10^{-5};\ k = 0.64 \pm 0.12;\ T = (18.5 \pm 1.2)\ K;\ \lambda_0 = 100\ \mu$m

Table 6: Total EBL Intensity of Different Models (nW m^{-2} sr^{-1})

Model	Stars[1]	Dust[2]	Total
Franceschini et al. (2008)	25	40	65
Domínguez et al. (2011)	25	44	69
Gilmore et al. (2011)	25	23	48
Mazin & Raue (2007)	30	26	56
Finke et al. (2010)	27	20	47
Stecker et al. (2006)	61	35	96
Observations[3]	23–93	20–110	42–202
From CSFR[4]	–	–	21–66

[1] Integrated intensity from 0.1 to 10 μm.

[2] Integrated in tensity from 10 to 1000 μm.

3 From limits and detections of the EBL (Figure 7)

4 Total integrated intensity inferred from the CSFR (Fig.8)

References

Abdo, A. A., Ackermann, M., Agudo, I., Ajello, M., Aller, H. D., Aller, M. F., Angelakis, E., Arkharov, A. A., Axelsson, M., Bach, U., & et al. 2010a, ApJ, 716, 30

Abdo, A. A., Ackermann, M., Ajello, M., Allafort, A., Baldini, L., Ballet, J., Barbiellini, G., Baring, M. G., Bastieri, D., Bechtol, K., & et al. 2011a, ApJ, 727, 129

Abdo, A. A., Ackermann, M., Ajello, M., Asano, K., Baldini, L., Ballet, J., Barbiellini, G., Bastieri, D., Baughman, B. M., Bechtol, K., Bellazzini, R., Blandford, R. D., Bloom, E. D., Bonamente, E., Borgland, A. W., Bregeon, J., Brez, A., Brigida, M., Bruel, P., Burnett, T. H., Caliandro, G. A., Cameron, R. A., Caraveo, P. A., Casandjian, J. M., Cavazzuti, E., Cecchi, C., Celotti, A., Chekhtman, A., Cheung, C. C., Chiang, J., Ciprini, S., Claus, R., Cohen-Tanugi, J., Colafrancesco, S., Cominsky, L. R., Conrad, J., Costamante, L., Dermer, C. D., de Angelis, A., de Palma, F., Digel, S. W., Donato, D., do Couto e Silva, E., Drell, P. S., Dubois, R., Dumora, D., Farnier, C., Favuzzi, C., Finke, J., Focke, W. B., Frailis, M., Fukazawa, Y., Funk, S., Fusco, P., Gargano, F., Georganopoulos, M., Germani, S., Giebels, B., Giglietto, N., Giordano, F., Glanzman, T., Grenier, I. A., Grondin, M.-H., Grove, J. E., Guillemot, L., Guiriec, S., Hanabata, Y., Harding, A. K., Hartman, R. C., Hayashida, M., Hays, E., Hughes, R. E., Jóhannesson, G., Johnson, A. S., Johnson, R. P., Johnson, W. N., Kadler, M., Kamae, T., Kanai, Y., Katagiri, H., Kataoka, J., Kawai, N., Kerr, M., Knödlseder, J., Kuehn, F., Kuss, M., Latronico, L., Lemoine-Goumard, M., Longo, F., Loparco, F., Lott, B., Lovellette, M. N., Lubrano, P., Madejski, G. M., Makeev, A., Mazziotta, M. N., McEnery, J. E., Meurer, C., Michelson, P. F., Mitthumsiri, W., Mizuno, T., Moiseev, A. A., Monte, C., Monzani, M. E., Morselli, A., Moskalenko, I. V., Murgia, S., Nakamori, T., Nolan, P. L., Norris, J. P., Nuss, E., Ohsugi, T., Omodei, N., Orlando, E., Ormes, J. F., Paneque, D., Panetta, J. H., Parent, D., Pepe, M., Pesce-Rollins, M., Piron, F., Porter, T. A., Rainò, S., Razzano, M., Reimer, A., Reimer, O., Reposeur, T., Ritz, S., Rodriguez, A. Y., Romani, R. W., Ryde, F., Sadrozinski, H. F.-W., Sambruna, R., Sanchez, D., Sander, A., Sato, R., Parkinson, P. M. S., Sgrò, C., Smith, D. A., Smith, P. D., Spandre, G., Spinelli, P., Starck, J.-L., Strickman, M. S., Strong, A. W., Suson, D. J., Tajima, H., Takahashi, H., Takahashi, T., Tanaka, T., Taylor, G. B., Thayer, J. G., Thompson, D. J., Torres, D. F., Tosti, G., Uchiyama, Y., Usher, T. L., Vilchez, N., Vitale, V., Waite, A. P., Wood, K. S., Ylinen, T., Ziegler, M., Aller, H. D., Aller, M. F., Kellermann, K. I., Kovalev, Y. Y., Kovalev, Y. A., Lister, M. L., & Pushkarev, A. B. 2009, ApJ, 699, 31

Abdo, A. A., Ackermann, M., Ajello, M., Atwood, W. B., Axelsson, M., Baldini, L., Ballet, J., Barbiellini, G., Bastieri, D., Bechtol, K., Bellazzini, R., Berenji, B., Bloom, E. D., Bonamente, E., Borgland, A. W., Bregeon, J., Brez, A., Brigida, M., Bruel, P., Burnett, T. H., Caliandro, G. A., Cameron, R. A., Caraveo, P. A., Casandjian, J. M., Cavazzuti, E., Cecchi, C., Çelik, Ö., Charles, E., Chekhtman, A., Cheung, C. C., Chiang, J., Ciprini, S., Claus, R., Cohen-Tanugi, J., Conrad, J., Dermer, C. D., de Angelis, A., de Palma, F., Digel, S. W., Silva, E. d. C. e., Drell, P. S., Drlica-Wagner, A., Dubois, R., Dumora, D., Farnier, C., Favuzzi, C., Fegan, S. J., Focke, W. B., Foschini, L., Frailis, M., Fukazawa, Y., Funk, S., Fusco, P., Gargano, F., Gasparrini, D., Gehrels, N., Germani, S., Giebels, B., Giglietto, N., Giordano, F., Glanzman, T., Godfrey, G., Grenier, I. A., Grondin, M.-H., Grove, J. E., Guillemot, L., Guiriec, S., Hanabata, Y., Harding, A. K., Hayashida, M., Hays, E., Hughes, R. E., Jóhannesson, G., Johnson, A. S., Johnson, R. P., Johnson, W. N., Kamae, T., Katagiri, H., Kataoka, J., Kawai, N., Kerr, M., Knödlseder, J., Kocian, M. L., Kuss, M., Lande, J., Latronico, L., Lemoine-Goumard, M., Longo, F., Loparco, F., Lott, B., Lovellette, M. N., Lubrano, P., Madejski, G. M., Makeev, A., Mazziotta, M. N., McConville, W., McEnery, J. E., Meurer, C., Michelson, P. F., Mitthumsiri, W., Mizuno, T., Moiseev, A. A., Monte, C., Monzani, M. E., Morselli, A., Moskalenko, I. V., Murgia, S., Nakamori, T., Nolan, P. L., Norris, J. P., Nuss, E., Ohsugi, T., Omodei, N., Orlando, E., Ormes, J. F., Ozaki, M., Paneque, D., Panetta, J. H., Parent, D., Pelassa, V., Pepe, M., Pesce-Rollins, M., Piron, F., Porter, T. A., Rainò, S., Rando, R., Razzano, M., Reimer, A., Reimer, O., Reposeur, T., Ritz, S., Rodriguez, A. Y., Romani, R. W., Roth, M., Ryde, F., Sadrozinski, H. F.-W., Sander, A., Saz Parkinson, P. M., Scargle, J. D., Sellerholm, A., Sgrò, C., Shaw, M. S., Smith, D. A., Smith, P. D., Spandre, G., Spinelli, P., Strickman, M. S., Strong, A. W., Suson, D. J., Takahashi, H., Tanaka, T., Thayer, J. B., Thayer, J. G., Thompson, D. J., Tibaldo, L., Tibolla, O., Torres, D. F., Tosti, G., Tramacere, A., Uchiyama, Y., Usher, T. L., Vasileiou, V., Vilchez, N., Vitale, V., Waite, A. P., Wang, P., Winer, B. L., Wood, K. S., Ylinen, T., Ziegler, M., & Fermi LAT Collaboration. 2010b, ApJ, 709, L152

Abdo, A. A., Ackermann, M., Ajello, M., Atwood, W. B., Baldini, L., Ballet, J., Barbiellini, G., Bastieri, D., Baughman, B. M., Bechtol, K., Bellazzini, R., Berenji, B., Blandford, R. D., Bloom, E. D., Bonamente, E., Borgland, A. W., Bouvier, A., Brandt, T. J., Bregeon, J., Brez, A., Brigida, M., Bruel, P., Buehler, R., Buson, S., Caliandro, G. A., Cameron, R. A., Cannon, A., Caraveo, P. A., Carrigan, S., Casandjian, J. M., Cavazzuti, E., Cecchi, C., Çelik, Ö., Charles, E., Chekhtman, A., Cheung, C. C., Chiang, J., Ciprini, S., Claus, R., Cohen-Tanugi, J., Colafrancesco, S., Cominsky, L. R., Conrad, J., Costamante, L., Davis, D. S., Dermer, C. D., de Angelis, A., de Palma, F., Silva, E. d. C. e., Drell, P. S., Dubois, R., Dumora, D., Falcone, A., Farnier, C., Favuzzi, C., Fegan, S. J., Finke, J., Focke, W. B., Fortin, P., Frailis, M., Fukazawa, Y., Funk, S., Fusco, P., Gargano, F., Gasparrini, D., Gehrels, N., Georganopoulos, M., Germani, S., Giebels, B., Giglietto, N., Giommi, P., Giordano, F., Giroletti, M., Glanzman, T., Godfrey, G., Grandi, P., Grenier, I. A., Grondin, M.-H., Grove, J. E., Guillemot, L., Guiriec, S., Hadasch, D., Harding, A. K., Hase, H., Hayashida, M., Hays, E., Horan, D., Hughes, R. E., Itoh, R., Jackson, M. S., Jóhannesson, G., Johnson, A. S., Johnson, T. J., Johnson, W. N., Kadler, M., Kamae, T., Katagiri, H., Kataoka, J., Kawai, N., Kishishita, T., Knödlseder, J., Kuss, M., Lande, J., Latronico, L., Lee, S.-H., Lemoine-Goumard, M., Llena Garde, M., Longo, F., Loparco, F., Lott, B., Lovellette, M. N., Lubrano, P., Makeev, A., Mazziotta, M. N., McConville, W., McEnery, J. E., Michelson, P. F., Mitthumsiri, W., Mizuno, T., Moiseev, A. A., Monte, C., Monzani, M. E., Morselli, A., Moskalenko, I. V., Murgia, S., Müller, C., Nakamori, T., Naumann-Godo, M., Nolan, P. L., Norris, J. P., Nuss, E., Ohno, M., Ohsugi, T., Ojha, R., Okumura, A., Omodei, N., Orlando, E., Ormes, J. F., Ozaki, M., Pagani, C., Paneque, D., Panetta, J. H., Parent, D., Pelassa, V., Pepe, M., Pesce-Rollins, M., Piron, F., Plötz, C., Porter, T. A., Rainò, S., Rando, R., Razzano, M., Razzaque, S., Reimer, A., Reimer, O., Reposeur, T., Ripken, J., Ritz, S., Rodriguez, A. Y., Roth, M., Ryde, F., Sadrozinski, H. F.-W., Sanchez, D., Sander, A., Scargle, J. D., Sgrò, C., Siskind, E. J., Smith, P. D., Spandre, G., Spinelli, P., Starck, J.-L., Stawarz, L., Strickman, M. S., Suson, D. J., Tajima, H., Takahashi, H., Takahashi, T., Tanaka, T., Thayer, J. B., Thayer, J. G., Thompson, D. J., Tibaldo, L., Torres, D. F., Tosti, G., Tramacere, A., Uchiyama, Y., Usher, T. L., Vandenbroucke, J., Vasileiou, V., Vilchez, N., Vitale, V., Waite, A. P., Wang, P., Winer, B. L., Wood, K. S., Yang, Z., Ylinen, T., & Ziegler, M. 2010c, ApJ, 719, 1433

Abdo, A. A., Ackermann, M., Ajello, M., Atwood, W. B., Baldini, L., Ballet, J., Barbiellini, G., Bastieri, D., Baughman, B. M., Bechtol, K., Bellazzini, R., Berenji, B., Blandford, R. D., Bloom, E. D., Bonamente, E., Borgland, A. W., Bregeon, J., Brez, A., Brigida, M., Bruel, P., Burnett, T. H., Buson, S., Caliandro, G. A., Cameron, R. A., Caraveo, P. A., Casandjian, J. M., Cavazzuti, E., Cecchi, C., Çelik, Ö., Charles, E., Chekhtman, A., Cheung, C. C., Chiang, J., Ciprini, S., Claus, R., Cohen-Tanugi, J., Cominsky, L. R., Conrad, J., Cutini, S., Dermer, C. D., de Angelis, A., de Palma, F., Digel, S. W., di Bernardo, G., do Couto e Silva, E., Drell, P. S., Drlica-Wagner, A., Dubois, R., Dumora, D., Farnier, C., Favuzzi, C., Fegan, S. J., Focke, W. B., Fortin, P., Frailis, M., Fukazawa, Y., Funk, S., Fusco, P., Gaggero, D., Gargano, F., Gasparrini, D., Gehrels, N., Germani, S., Giebels, B., Giglietto, N., Giommi, P., Giordano, F., Glanzman, T., Godfrey, G., Grenier, I. A., Grondin, M.-H., Grove, J. E., Guillemot, L., Guiriec, S., Gustafsson, M., Hanabata, Y., Harding, A. K., Hayashida, M., Hughes, R. E., Itoh, R., Jackson, M. S., Jóhannesson, G., Johnson, A. S., Johnson, R. P., Johnson, T. J., Johnson, W. N., Kamae, T., Katagiri, H., Kataoka, J., Kawai, N., Kerr, M., Knödlseder, J., Kocian, M. L., Kuehn, F., Kuss, M., Lande, J., Latronico, L., Lemoine-Goumard, M., Longo, F., Loparco, F., Lott, B., Lovellette, M. N., Lubrano, P., Madejski, G. M., Makeev, A., Mazziotta, M. N., McConville, W., McEnery, J. E., Meurer, C., Michelson, P. F., Mitthumsiri, W., Mizuno, T., Moiseev, A. A., Monte, C., Monzani, M. E., Morselli, A., Moskalenko, I. V., Murgia, S., Nolan, P. L., Norris, J. P., Nuss, E., Ohsugi, T., Omodei, N., Orlando, E., Ormes, J. F., Paneque, D., Panetta, J. H., Parent, D., Pelassa, V., Pepe, M., Pesce-Rollins, M., Piron, F., Porter, T. A., Rainò, S., Rando, R., Razzano, M., Reimer, A., Reimer, O., Reposeur, T., Ritz, S., Rochester, L. S., Rodriguez, A. Y., Roth, M., Ryde, F., Sadrozinski, H. F.-W., Sanchez, D., Sander, A., Parkinson, P. M. S., Scargle, J. D., Sellerholm, A., Sgrò, C., Shaw, M. S., Siskind, E. J., Smith, D. A., Smith, P. D., Spandre, G., Spinelli, P., Starck, J.-L., Strickman, M. S., Strong, A. W., Suson, D. J., Tajima, H., Takahashi, H., Takahashi, T., Tanaka, T., Thayer, J. B., Thayer, J. G., Thompson, D. J., Tibaldo, L., Torres, D. F., Tosti, G., Tramacere, A., Uchiyama, Y., Usher, T. L., Vasileiou, V., Vilchez, N., Vitale, V., Waite, A. P., Wang, P., Winer, B. L., Wood,

K. S., Ylinen, T., Ziegler, M., & Fermi LAT Collaboration. 2010d, Physical Review Letters, 104, 101101

Abdo, A. A., Ackermann, M., Ajello, M., Baldini, L., Ballet, J., Barbiellini, G., Bastieri, D., Bechtol, K., Bellazzini, R., Berenji, B., & et al. 2011b, ApJ, 736, 131

Abdo, A. A. et al. 2010, ArXiv: 1110.0040

Abramowski, A., Acero, F., Aharonian, F., Akhperjanian, A. G., Anton, G., Balzer, A., Barnacka, A., Becherini, Y., Becker, J., Bernlöhr, K., Birsin, E., Biteau, J., Bochow, A., Boisson, C., Bolmont, J., Bordas, P., Brucker, J., Brun, F., Brun, P., Bulik, T., Büsching, I., Carrigan, S., Casanova, S., Cerruti, M., Chadwick, P. M., Charbonnier, A., Chaves, R. C. G., Cheesebrough, A., Cologna, G., Conrad, J., Couturier, C., Dalton, M., Daniel, M. K., Davids, I. D., Degrange, B., Deil, C., Dickinson, H. J., Djannati-Ataï, A., Domainko, W., O'C. Drury, L., Dubus, G., Dutson, K., Dyks, J., Dyrda, M., Egberts, K., Eger, P., Espigat, P., Fallon, L., Fegan, S., Feinstein, F., Fernandes, M. V., Fiasson, A., Fontaine, G., Förster, A., Füßling, M., Gajdus, M., Gallant, Y. A., Garrigoux, T., Gast, H., Gérard, L., Giebels, B., Glicenstein, J. F., Glück, B., Göring, D., Grondin, M.-H., Häffner, S., Hague, J. D., Hahn, J., Hampf, D., Harris, J., Hauser, M., Heinz, S., Heinzelmann, G., Henri, G., Hermann, G., Hillert, A., Hinton, J. A., Hofmann, W., Hofverberg, P., Holler, M., Horns, D., Jacholkowska, A., Jahn, C., Jamrozy, M., Jung, I., Kastendieck, M. A., Katarzyński, K., Katz, U., Kaufmann, S., Khélifi, B., Klochkov, D., Kluźniak, W., Kneiske, T., Komin, N., Kosack, K., Kossakowski, R., Krayzel, F., Laffon, H., Lamanna, G., Lenain, J.-P., Lennarz, D., Lohse, T., Lopatin, A., Lu, C.-C., Marandon, V., Marcowith, A., Masbou, J., Maurin, G., Maxted, N., Mayer, M., McComb, T. J. L., Medina, M. C., Méhault, J., Moderski, R., Mohamed, M., Moulin, E., Naumann, C. L., Naumann-Godo, M., de Naurois, M., Nedbal, D., Nekrassov, D., Nguyen, N., Nicholas, B., Niemiec, J., Nolan, S. J., Ohm, S., de Oña Wilhelmi, E., Opitz, B., Ostrowski, M., Oya, I., Panter, M., Paz Arribas, M., Pekeur, N. W., Pelletier, G., Perez, J., Petrucci, P.-O., Peyaud, B., Pita, S., Pühlhofer, G., Punch, M., Quirrenbach, A., Raue, M., Reimer, A., Reimer, O., Renaud, M., de los Reyes, R., Rieger, F., Ripken, J., Rob, L., Rosier-Lees, S., Rowell, G., Rudak, B., Rulten, C. B., Sahakian, V., Sanchez, D. A., Santangelo, A., Schlickeiser, R., Schulz, A., Schwanke, U., Schwarzburg, S., Schwemmer, S., Sheidaei, F., Skilton, J. L., Sol, H., Spengler, G., Stawarz, Ł., Steenkamp, R., Stegmann, C., Stinzing, F., Stycz, K., Sushch, I., Szostek, A., Tavernet, J.-P., Terrier, R., Tluczykont, M., Valerius, K., van Eldik, C., Vasileiadis, G., Venter, C., Viana, A., Vincent, P., Völk, H. J., Volpe, F., Vorobiov, S., Vorster, M., Wagner, S. J., Ward, M., White, R., Wierzcholska, A., Zacharias, M., Zajczyk, A., Zdziarski, A. A., Zech, A., & Zechlin, H.-S. 2012, ArXiv e-prints

Abramowski, A., Acero, F., Aharonian, F., Akhperjanian, A. G., Anton, G., Barnacka, A., Barres de Almeida, U., Bazer-Bachi, A. R., Becherini, Y., & et al. 2011, A&A, 533, A110

Acciari, V., Aliu, E., Arlen, T., Bautista, M., Beilicke, M., Benbow, W., Böttcher, M., Bradbury, S. M., Buckley, J. H., Bugaev, V., Butt, Y., Byrum, K., Cannon, A., Celik, O., Cesarini, A., Chow, Y. C., Ciupik, L., Cogan, P., Colin, P., Cui, W., Dickherber, R., Duke, C., Ergin, T., Falcone, A., Fegan, S. J., Finley, J. P., Finnegan, G., Fortin, P., Fortson, L., Furniss, A., Gall, D., Gibbs, K., Gillanders, G. H., Grube, J., Guenette, R., Gyuk, G., Hanna, D., Hays, E., Holder, J., Horan, D., Hui, C. M., Humensky, T. B., Imran, A., Kaaret, P., Karlsson, N., Kertzman, M., Kieda, D., Kildea, J., Konopelko, A., Krawczynski, H., Krennrich, F., Lang, M. J., LeBohec, S., Maier, G., McCann, A., McCutcheon, M., Millis, J., Moriarty, P., Mukherjee, R., Nagai, T., Ong, R. A., Otte, A. N., Pandel, D., Perkins, J. S., Petry, D., Pohl, M., Quinn, J., Ragan, K., Reyes, L. C., Reynolds, P. T., Roache, E., Rose, J., Schroedter, M., Sembroski, G. H., Smith, A. W., Steele, D., Swordy, S. P., Theiling, M., Toner, J. A., Valcarcel, L., Varlotta, A., Vassiliev, V. V., Wagner, R. G., Wakely, S. P., Ward, J. E., Weekes, T. C., Weinstein, A., White, R. J., Williams, D. A., Wissel, S., Wood, M., & Zitzer, B. 2009a, ApJ, 690, L126

Acciari, V. A., Aliu, E., Arlen, T., Aune, T., Bautista, M., Beilicke, M., Benbow, W., Boltuch, D., Bradbury, S. M., Buckley, J. H., Bugaev, V., Byrum, K., Cannon, A., Celik, O., Cesarini, A., Chow, Y. C., Ciupik, L., Cogan, P., Colin, P., Cui, W., Dickherber, R., Duke, C., Fegan, S. J., Finley, J. P., Finnegan, G., Fortin, P., Fortson, L., Furniss, A., Galante, N., Gall, D., Gibbs, K., Gillanders, G. H., Godambe, S., Grube, J., Guenette, R., Gyuk, G., Hanna, D., Holder, J., Horan, D., Hui, C. M., Humensky, T. B., Imran, A., Kaaret, P., Karlsson, N., Kertzman, M., Kieda, D., Kildea, J., Konopelko, A., Krawczynski, H., Krennrich, F., Lang, M. J., Lebohec, S., Maier, G., McArthur, S., McCann, A., McCutcheon, M., Millis, J., Moriarty, P., Mukherjee, R., Nagai, T., Ong, R. A., Otte, A. N., Pandel, D., Perkins, J. S., Pizlo, F., Pohl, M., Quinn, J., Ragan, K., Reyes, L. C., Reynolds, P. T., Roache, E., Rose, H. J., Schroedter, M., Sembroski, G. H., Smith, A. W., Steele, D., Swordy, S. P., Theiling, M., Thibadeau, S., Varlotta, A., Vassiliev, V. V., Vincent, S., Wagner, R. G., Wakely, S. P., Ward, J. E., Weekes, T. C., Weinstein, A., Weisgarber, T., Williams, D. A., Wissel, S., Wood, M., & Zitzer, B. 2009b, Nature, 462, 770

Acciari, V. A., Aliu, E., Arlen, T., Aune, T., Bautista, M., Beilicke, M., Benbow, W., Böttcher, M., Boltuch, D., Bradbury, S. M., & et al. 2010a, ApJ, 715, L49

Acciari, V. A., Aliu, E., Arlen, T., Aune, T., Beilicke, M., Benbow, W., Boltuch, D., Bradbury, S. M., Buckley, J. H., Bugaev, V., Byrum, K., Cannon, A., Cesarini, A., Chow, Y. C., Ciupik, L., Cogan, P., Cui, W., Dickherber, R., Duke, C., Finley, J. P., Finnegan, G., Fortin, P., Fortson, L., Furniss, A., Galante, N., Gall, D., Gillanders, G. H., Godambe, S., Grube, J., Guenette, R., Gyuk, G., Hanna, D., Holder, J., Hui, C. M., Humensky, T. B., Imran, A., Kaaret, P., Karlsson, N., Kertzman, M., Kieda, D., Konopelko, A., Krawczynski, H., Krennrich, F., Lang, M. J., LeBohec, S., Maier, G., McArthur, S., McCann, A., McCutcheon, M., Millis, J., Moriarty, P., Ong, R. A., Otte, A. N., Pandel, D., Perkins, J. S., Pichel, A., Pohl, M., Quinn, J., Ragan, K., Reyes, L. C., Reynolds, P. T., Roache, E., Rose, H. J., Rovero, A. C., Schroedter, M., Sembroski, G. H., Senturk, G. D., Smith, A. W., Steele, D., Swordy, S. P., Theiling, M., Thibadeau, S., Varlotta, A., Vincent, S., Wagner, R. G., Wakely, S. P., Ward, J. E., Weekes, T. C., Weinstein, A., Weisgarber, T., Williams, D. A., Wissel, S., Wood, M., Zitzer, B., Harris, D. E., & Massaro, F. 2010b, ApJ, 716, 819

Acciari, V. A., Aliu, E., Arlen, T., Aune, T., Beilicke, M., Benbow, W., Boltuch, D., Bradbury, S. M., Buckley, J. H., Bugaev, V., Byrum, K., Cannon, A., Cesarini, A., Ciupik, L., Cui, W., Dickherber, R., Duke, C., Falcone, A., Finley, J. P., Finnegan, G., Fortson, L., Furniss, A., Galante, N., Gall, D., Gillanders, G. H., Godambe, S., Grube, J., Guenette, R., Gyuk, G., Hanna, D., Holder, J., Hui, C. M., Humensky, T. B., Imran, A., Kaaret, P., Karlsson, N., Kertzman, M., Kieda, D., Konopelko, A., Krawczynski, H., Krennrich, F., Lang, M. J., Maier, G., McArthur, S., McCutcheon, M., Moriarty, P., Ong, R. A., Otte, A. N., Ouellette, M., Pandel, D., Perkins, J. S., Pichel, A., Pohl, M., Quinn, J., Ragan, K., Reyes, L. C., Reynolds, P. T., Roache, E., Rose, H. J., Rovero, A. C., Schroedter, M., Sembroski, G. H., Senturk, G. D., Steele, D., Swordy, S. P., Theiling, M., Thibadeau, S., Varlotta, A., Vassiliev, V. V., Vincent, S., Wagner, R. G., Wakely, S. P., Ward, J. E., Weekes, T. C., Weinstein, A., Weisgarber, T., Williams, D. A., Wissel, S., Wood, M., Zitzer, B., Garson, III, A., Lee, K., Sadun, A. C., Carini, M., Barnaby, D., Cook, K., Maune, J., Pease, A., Smith, S., Walters, R., Berdyugin, A., Lindfors, E., Nilsson, K., Pasanen, M., Sainio, J., Sillanpaa, A., Takalo, L. O., Villforth, C., Montaruli, T., Baker, M., Lahteenmaki, A., Tornikoski, M., Hovatta, T., Nieppola, E., Aller, H. D., & Aller, M. F. 2011a, ApJ, 738, 25

Acciari, V. A., Aliu, E., Arlen, T., Aune, T., Beilicke, M., Benbow, W., Boltuch, D., Bugaev, V., Cannon, A., Ciupik, L., Cogan, P., Colin, P., Dickherber, R., Falcone, A., Fegan, S. J., Finley, J. P., Fortin, P., Fortson, L. F., Furniss, A., Gall, D., Gillanders, G. H., Grube, J., Guenette, R., Gyuk, G., Hanna, D., Holder, J., Horan, D., Hui, C. M., Humensky, T. B., Imran, A., Kaaret, P., Karlsson, N., Kertzman, M., Kieda, D., Kildea, J., Konopelko, A., Krawczynski, H., Krennrich, F., Lang, M. J., LeBohec, S., Maier, G., Moriarty, P., Mukherjee, R., Ong, R. A., Otte, A. N., Pandel, D., Perkins, J. S., Pichel, A., Pohl, M., Quinn, J., Ragan, K., Reynolds, P. T., Rose, H. J., Schroedter, M., Sembroski, G. H., Smith, A. W., Steele, D., Swordy, S. P., Theiling, M., Toner, J. A., Varlotta, A., Vassiliev, V. V., Vincent, S., Wagner, R., Wakely, S. P., Ward, J. E., Weekes, T. C., Weinstein, A., Weisgarber, T., Williams, D. A., Wissel, S., Wood, M., & Zitzer, B. 2011b, ApJ, 738, 169

Acciari, V. A., Aliu, E., Arlen, T., Bautista, M., Beilicke, M., Benbow, W., Bradbury, S. M., Buckley, J. H., Bugaev, V., Butt, Y., & et al. 2009c, Science, 325, 444

Acciari, V. A., Aliu, E., Arlen, T., Beilicke, M., Benbow, W., Böttcher, M., Bradbury, S. M., Buckley, J. H., Bugaev, V., Butt, Y., Byrum, K., Cannon, A., Celik, O., Cesarini, A., Chow, Y. C., Ciupik, L., Cogan, P., Cui, W., Daniel, M. K., Dickherber, R., Ergin, T., Falcone, A., Fegan, S. J., Finley, J. P., Fortin, P., Fortson, L., Furniss, A., Gall, D., Gibbs, K., Gillanders, G. H., Godambe, S., Grube, J., Guenette, R., Gyuk, G., Hanna, D., Hays, E., Holder, J., Horan, D., Hui, C. M., Humensky, T. B., Imran, A., Kaaret, P., Karlsson, N., Kertzman, M., Kieda, D., Kildea, J., Konopelko, A., Krawczynski, H., Krennrich, F., Lang, M. J., LeBohec, S., Maier, G., McCann, A., McCutcheon, M., Millis, J., Moriarty, P., Mukherjee, R., Nagai, T., Ong, R. A., Otte, A. N., Pandel, D., Perkins, J. S., Petry, D., Pizlo, F., Pohl, M., Quinn, J., Ragan, K., Reyes, L. C., Reynolds, P. T., Roache, E., Rose, H. J., Schroedter, M., Sembroski, G. H., Smith, A. W., Steele, D., Swordy, S. P., Theiling, M., Toner, J. A., Varlotta, A., Vassiliev, V. V., Wagner, R. G., Wakely, S. P., Ward, J. E., Weekes, T. C., Weinstein, A., Williams, D. A., Wissel, S., Wood, M., & Zitzer, B. 2009d, ApJ, 693, L104

Acciari, V. A., Aliu, E., Aune, T., Beilicke, M., Benbow, W., Böttcher, M., Boltuch, D., Buckley, J. H., Bradbury, S. M., Bugaev, V., Byrum, K., Cannon, A., Cesarini, A., Ciupik, L., Cogan, P., Cui, W., Dickherber, R., Duke, C., Falcone, A., Finley, J. P., Fortin, P., Fortson, L., Furniss, A., Galante, N., Gall, D., Gibbs, K., Gillanders, G. H., Grube, J., Guenette, R., Gyuk, G., Hanna, D., Holder, J., Hui, C. M., Humensky, T. B., Kaaret, P., Karlsson, N., Kertzman, M., Kieda, D., Konopelko, A., Krawczynski, H., Krennrich, F., Lang, M. J., Le Bohec, S., Maier, G., McArthur, S., McCann, A., McCutcheon, M., Millis, J., Moriarty, P., Ong, R. A., Otte, A. N., Pandel, D., Perkins, J. S., Pichel, A., Pohl, M., Quinn, J., Ragan, K., Reyes, L. C., Reynolds, P. T., Roache, E., Rose, H. J., Sembroski, G. H., Smith, A. W., Steele, D., Theiling, M., Thibadeau, S., Varlotta, A., Vassiliev, V. V., Vincent, S., Wakely, S. P., Ward, J. E., Weekes, T. C., Weinstein, A., Weisgarber, T., Williams, D. A., Wissel, S., Wood, M., Pian, E., Vercellone, S., Donnarumma, I., D'Ammando, F., Bulgarelli, A., Chen, A. W., Giuliani, A., Longo, F., Pacciani, L., Pucella, G., Vittorini, V., Tavani, M., Argan, A., Barbiellini, G., Caraveo, P., Cattaneo, P. W., Cocco, V., Costa, E., Del Monte, E., De Paris, G., Di Cocco, G., Evangelista, Y., Feroci, M., Fiorini, M., Froysland, T., Frutti, M., Fuschino, F., Galli, M., Gianotti, F., Labanti, C., Lapshov, I., Lazzarotto, F., Lipari, P., Marisaldi, M., Mastropietro, M., Mereghetti, S., Morelli, E., Morselli, A., Pellizzoni, A., Perotti, F., Piano, G., Picozza, P., Pilia, M., Porrovecchio, G., Prest, M., Rapisarda, M., Rappoldi, A., Rubini, A., Sabatini, S., Soffitta, P., Trifoglio, M., Trois, A., Vallazza, E., Zambra, A., Zanello, D., Pittori, C., Santolamazza, P., Verrecchia, F., Giommi, P., Colafrancesco, S., Salotti, L., Villata, M., Raiteri, C. M., Aller, H. D., Aller, M. F., Arkharov, A. A., Efimova, N. V., Larionov, V. M., Leto, P., Ligustri, R., Lindfors, E., Pasanen, M., Kurtanidze, O. M., Tetradze, S. D., Lahteenmaki, A., Kotiranta, M., Cucchiara, A., Romano, P., Nesci, R., Pursimo, T., Heidt, J., Benitez, E., Hiriart, D., Nilsson, K., Berdyugin, A., Mujica, R., Dultzin, D., Lopez, J. M., Mommert, M., Sorcia, M., & de la Calle Perez, I. 2009e, ApJ, 707, 612

Acciari, V. A., Aliu, E., Beilicke, M., Benbow, W., Boltuch, D., Böttcher, M., Bradbury, S. M., Bugaev, V., Byrum, K., Cesarini, A., Ciupik, L., Cogan, P., Cui, W., Dickherber, R., Duke, C., Falcone, A., Finley, J. P., Finnegan, G., Fortson, L., Furniss, A., Galante, N., Gall, D., Gibbs, K., Guenette, R., Gillanders, G. H., Godambe, S., Grube, J., Hanna, D., Hui, C. M., Humensky, T. B., Imran, A., Kaaret, P., Karlsson, N., Kertzman, M., Kieda, D., Krawczynski, H., Krennrich, F., Lang, M. J., LeBohec, S., Maier, G., McArthur, S., McCann, A., Moriarty, P., Nagai, T., Ong, R. A., Otte, A. N., Pandel, D., Perkins, J. S., Pichel, A., Pohl, M., Quinn, J., Ragan, K., Reyes, L. C., Reynolds, P. T., Roache, E., Rose, H. J., Schroedter, M., Sembroski, G. H., Smith, A. W., Steele, D., Swordy, S. P., Theiling, M., Thibadeau, S., Vassiliev, V. V., Vincent, S., Wakely, S. P., Weekes, T. C., Weinstein, A., Weisgarber, T., Williams, D. A., & VERITAS Collaboration. 2010c, ApJ, 709, L163

Acciari, V. A., Aliu, E., Beilicke, M., Benbow, W., Böttcher, M., Bradbury, S. M., Buckley, J. H., Bugaev, V., Butt, Y., Celik, O., Cesarini, A., Ciupik, L., Chow, Y. C. K., Cogan, P., Colin, P., Cui, W., Daniel, M. K., Ergin, T., Falcone, A. D., Fegan, S. J., Finley, J. P., Finnegan, G., Fortin, P., Fortson, L. F., Furniss, A., Gall, D., Gillanders, G. H., Grube, J., Guenette, R., Gyuk, G., Hanna, D., Hays, E., Holder, J., Horan, D., Hui, C. M., Humensky, T. B., Imran, A., Kaaret, P., Karlsson, N., Kertzman, M., Kieda, D. B., Konopelko, A., Krawczynski, H., Krennrich, F., Lang, M. J., LeBohec, S., Lee, K., Maier, G., McCann, A., McCutcheon, M., Moriarty, P., Mukherjee, R., Nagai, T., Niemiec, J., Ong, R. A., Pandel, D., Perkins, J. S., Petry, D., Pohl, M., Quinn, J., Ragan, K., Reyes, L. C., Reynolds, P. T., Roache, E., Rose, H. J., Schroedter, M., Sembroski, G. H., Smith, A. W., Steele, D., Swordy, S. P., Toner, J. A., Vassiliev, V. V., Wagner, R., Wakely, S. P., Ward, J. E., Weekes, T. C., Weinstein, A., White, R. J., Williams, D. A., Wissel, S. A., Wood, M., & Zitzer, B. 2008, ApJ, 684, L73

Acero, F., Aharonian, F., Akhperjanian, A. G., Anton, G., Barres de Almeida, U., Bazer-Bachi, A. R., Becherini, Y., Behera, B., Bernlöhr, K., Bochow, A., Boisson, C., Bolmont, J., Borrel, V., Brucker, J., Brun, F., Brun, P., Bühler, R., Bulik, T., Büsching, I., Boutelier, T., Chadwick, P. M., Charbonnier, A., Chaves, R. C. G., Cheesebrough, A., Chounet, L.-M., Clapson, A. C., Coignet, G., Dalton, M., Daniel, M. K., Davids, I. D., Degrange, B., Deil, C., Dickinson, H. J., Djannati-Ataï, A., Domainko, W., Drury, L. O. ., Dubois, F., Dubus, G., Dyks, J., Dyrda, M., Egberts, K., Emmanoulopoulos, D., Espigat, P., Farnier, C., Fegan, S., Feinstein, F., Fiasson, A., Förster, A., Fontaine, G., Füßling, M., Gabici, S., Gallant, Y. A., Gérard, L., Gerbig, D., Giebels, B., Glicenstein, J. F., Glück, B., Goret, P., Göring, D., Hauser, D., Hauser, M., Heinz, S., Heinzelmann, G., Henri, G., Hermann, G., Hinton, J. A., Hoffmann, A., Hofmann, W., Hofverberg, P., Hoppe, S., Horns, D., Jacholkowska, A., de Jager, O. C., Jahn, C., Jung, I., Katarzyński, K., Katz, U., Kaufmann, S., Kerschhaggl, M., Khangulyan, D., Khélifi, B., Keogh, D., Klochkov, D., Kluźniak, W., Kneiske, T., Komin, N., Kosack, K., Kossakowski, R., Lamanna, G., Lenain, J.-P., Lohse, T., Marandon, V., Martineau-Huynh, O., Marcowith, A., Masbou, J., Maurin, D., McComb, T. J. L., Medina, M. C., Méhault, J., Moderski, R., Moulin, E., Naumann-Godo, M., de Naurois, M., Nedbal, D., Nekrassov, D., Nicholas, B., Niemiec, J., Nolan, S. J., Ohm, S., Olive, J.-F., Wilhelmi, E. d. O., Orford, K. J., Ostrowski, M., Panter, M., Arribas, M. P., Pedaletti, G., Pelletier, G., Petrucci, P.-O., Pita, S., Pühlhofer, G., Punch, M., Quirrenbach, A., Raubenheimer, B. C., Raue, M., Rayner, S. M., Reimer, O., Renaud, M., Rieger, F., Ripken, J., Rob, L., Rosier-Lees, S., Rowell, G., Rudak, B., Rulten, C. B., Ruppel, J., Sahakian, V., Santangelo, A., Schlickeiser, R., Schöck, F. M., Schwanke, U., Schwarzburg, S., Schwemmer, S., Shalchi, A., Sikora, M., Skilton, J. L., Sol, H., Stawarz, Ł., Steenkamp, R., Stegmann, C., Stinzing, F., Superina, G., Szostek, A., Tam, P. H., Tavernet, J.-P., Terrier, R., Tibolla, O., Tluczykont, M., van Eldik, C., Vasileiadis, G., Venter, C., Venter, L., Vialle, J. P., Vincent, P., Vivier, M., Völk, H. J., Volpe, F., Wagner, S. J., Ward, M., Zdziarski, A. A., & Zech, A. 2009, Science, 326, 1080

Ackermann, M., Ajello, M., Allafort, A., Antolini, E., Atwood, W. B., Axelsson, M., Baldini, L., Ballet, J., Barbiellini, G., Bastieri, D., Bechtol, K., Bellazzini, R., Berenji, B., Blandford, R. D., Bloom, E. D., Bonamente, E., Borgland, A. W., Bottacini, E., Bouvier, A., Bregeon, J., Brigida, M., Bruel, P., Buehler, R., Burnett, T. H., Buson, S., Caliandro, G. A., Cameron, R. A., Caraveo, P. A., Casandjian, J. M., Cavazzuti, E., Cecchi, C., Charles, E., Cheung, C. C., Chiang, J., Ciprini, S., Claus, R., Cohen-Tanugi, J., Conrad, J., Costamante, L., Cutini, S., de Angelis, A., de Palma, F., Dermer, C. D., Digel, S. W., Silva, E. d. C. e., Drell, P. S., Dubois, R., Escande, L., Favuzzi, C., Fegan, S. J., Ferrara, E. C., Finke, J., Focke, W. B., Fortin, P., Frailis, M., Fukazawa, Y., Funk, S., Fusco, P., Gargano, F., Gasparrini, D., Gehrels, N., Germani, S., Giebels, B., Giglietto, N., Giommi, P., Giordano, F., Giroletti, M., Glanzman, T., Godfrey, G., Grenier, I. A., Grove, J. E., Guiriec, S., Gustafsson, M., Hadasch, D., Hayashida, M., Hays, E., Healey, S. E., Horan, D., Hou, X., Hughes, R. E., Iafrate, G., Jóhannesson, G., Johnson, A. S., Johnson, W. N., Kamae, T., Katagiri, H., Kataoka, J., Knödlseder, J., Kuss, M., Lande, J., Larsson, S., Latronico, L., Longo, F., Loparco, F., Lott, B., Lovellette, M. N., Lubrano, P., Madejski, G. M., Mazziotta, M. N., McConville, W., McEnery, J. E., Michelson, P. F., Mitthumsiri, W., Mizuno, T., Moiseev, A. A., Monte, C., Monzani, M. E., Moretti, E., Morselli, A., Moskalenko, I. V., Murgia, S., Nakamori, T., Naumann-Godo, M., Nolan, P. L., Norris, J. P., Nuss, E., Ohno, M., Ohsugi, T., Okumura, A., Omodei, N., Orienti, M., Orlando, E., Ormes, J. F., Ozaki, M., Paneque, D., Parent, D., Pesce-Rollins, M., Pierbattista, M., Piranomonte, S., Piron, F., Pivato, G., Porter, T. A., Rainò, S., Rando, R., Razzano, M., Razzaque, S., Reimer, A., Reimer, O., Ritz, S., Rochester, L. S., Romani, R. W., Roth, M., Sanchez, D. A., Sbarra, C., Scargle, J. D., Schalk, T. L., Sgrò, C., Shaw, M. S., Siskind, E. J., Spandre, G., Spinelli, P., Strong, A. W., Suson, D. J., Tajima, H., Takahashi, H., Takahashi, T., Tanaka, T., Thayer, J. G., Thayer, J. B., Thompson, D. J., Tibaldo, L., Tinivella, M., Torres, D. F., Tosti, G., Troja, E., Uchiyama, Y., Vandenbroucke, J., Vasileiou, V., Vianello, G., Vitale, V., Waite, A. P., Wallace, E., Wang, P., Winer, B. L., Wood, D. L., Wood, K. S., & Zimmer, S. 2011, ApJ, 743, 171

Aharonian, F., Akhperjanian, A. G., Anton, G., de Almeida, U. B., Bazer-Bachi, A. R., Becherini, Y., Behera, B., Benbow, W., Bernlöhr, K., Boisson, C., Bochow, A., Borrel, V., Brion, E., Brucker, J., Brun, P., Bühler, R., Bulik, T., Büsching, I., Boutelier, T., Chadwick, P. M., Charbonnier, A., Chaves, R. C. G., Cheesebrough, A., Chounet, L.-M., Clapson, A. C., Coignet, G., Dalton, M., Daniel, M. K., Davids, I. D., Degrange, B., Deil, C., Dickinson, H. J., Djannati-Ataï, A., Domainko, W., Drury, L. O., Dubois, F., Dubus, G., Dyks, J., Dyrda, M., Egberts, K., Emmanoulopoulos, D., Espigat, P., Farnier, C., Feinstein, F., Fiasson, A., Förster, A., Fontaine, G., Füßling, M., Gabici, S., Gallant, Y. A., Gérard, L., Giebels, B., Glicenstein, J.-F., Glück, B., Goret, P., Göhring, D., Hauser, D., Hauser, M., Heinz, S., Heinzelmann, G., Henri, G., Hermann, G., Hinton, J. A., Hoffmann, A., Hofmann, W., Holleran, M., Hoppe, S., Horns, D., Jacholkowska, A., de Jager, O. C., Jahn, C., Jung, I., Katarzyński, K., Katz, U., Kaufmann, S., Kendziorra, E., Kerschhaggl, M., Khangulyan, D., Khélifi, B., Keogh, D., Kluźniak, W., Kneiske, T., Komin, N., Kosack, K., Lamanna, G., Latham, I. J., Lenain, J.-P., Lohse, T., Marandon, V., Martin, J. M., Martineau-Huynh, O., Marcowith, A., Maurin, D., McComb, T. J. L., Medina, M. C., Moderski, R., Moulin, E., Naumann-Godo, M., de Naurois, M., Nedbal, D., Nekrassov, D., Niemiec, J., Nolan, S. J., Ohm, S., Olive, J.-F., de Oña Wilhelmi, E., Orford, K. J., Ostrowski, M., Panter, M., Arribas, M. P., Pedaletti, G., Pelletier, G., Petrucci, P.-O., Pita, S., Pühlhofer, G., Punch, M., Quirrenbach, A., Raubenheimer, B. C., Raue, M., Rayner, S. M., Renaud, M., Rieger, F., Ripken, J., Rob, L., Rosier-Lees, S., Rowell, G., Rudak, B., Rulten, C. B., Ruppel, J., Sahakian, V., Santangelo, A., Schlickeiser, R., Schöck, F. M., Schröder, R., Schwanke, U., Schwarzburg, S., Schwemmer, S., Shalchi, A., Sikora, M., Skilton, J. L., Sol, H., Spangler, D., Stawarz, Ł., Steenkamp, R., Stegmann, C., Superina, G., Szostek, A., Tam, P. H., Tavernet, J.-P., Terrier, R., Tibolla, O., Tluczykont, M., van Eldik, C., Vasileiadis, G., Venter, C., Venter, L., Vialle, J. P., Vincent, P., Vink, J., Vivier, M., Völk, H. J., Volpe, F., Wagner, S. J., Ward, M., Zdziarski, A. A., & Zech, A. 2009, ApJ, 695, L40

Aharonian, F., Akhperjanian, A. G., Aye, K.-M., Bazer-Bachi, A. R., Beilicke, M., Benbow, W., Berge, D., Berghaus, P., Bernlöhr, K., Boisson, C., Bolz, O., Braun, I., Breitling, F., Brown, A. M., Bussons Gordo, J., Chadwick, P. M., Chounet, L.-M., Cornils, R., Costamante, L., Degrange, B., Djannati-Ataï, A., O'C. Drury, L., Dubus, G., Emmanoulopoulos, D., Espigat, P., Feinstein, F., Fleury, P., Fontaine, G., Fuchs, Y., Funk, S., Gallant, Y. A., Giebels, B., Gillessen, S., Glicenstein, J. F., Goret, P., Hadjichristidis, C., Hauser, M., Heinzelmann, G., Henri, G., Hermann, G., Hinton, J. A., Hofmann, W., Holleran, M., Horns, D., de Jager, O. C., Khélifi, B., Komin, N., Konopelko, A., Latham, I. J., Le Gallou, R., Lemière, A., Lemoine-Goumard, M., Leroy, N., Lohse, T., Martineau-

Huynh, O., Marcowith, A., Masterson, C., McComb, T. J. L., de Naurois, M., Nolan, S. J., Noutsos, A., Orford, K. J., Osborne, J. L., Ouchrif, M., Panter, M., Pelletier, G., Pita, S., Pühlhofer, G., Punch, M., Raubenheimer, B. C., Raue, M., Raux, J., Rayner, S. M., Redondo, I., Reimer, A., Reimer, O., Ripken, J., Rob, L., Rolland, L., Rowell, G., Sahakian, V., Saugé, L., Schlenker, S., Schlickeiser, R., Schuster, C., Schwanke, U., Siewert, M., Sol, H., Steenkamp, R., Stegmann, C., Tavernet, J.-P., Terrier, R., Théoret, C. G., Tluczykont, M., Vasileiadis, G., Venter, C., Vincent, P., Völk, H. J., & Wagner, S. J. 2005a, A&A, 436, L17

Aharonian, F., Akhperjanian, A. G., Aye, K.-M., Bazer-Bachi, A. R., Beilicke, M., Benbow, W., Berge, D., Berghaus, P., Bernlöhr, K., Bolz, O., Boisson, C., Borgmeier, C., Breitling, F., Brown, A. M., Bussons Gordo, J., Chadwick, P. M., Chitnis, V. R., Chounet, L.-M., Cornils, R., Costamante, L., Degrange, B., Djannati-Ataï, A., Drury, L. O., Ergin, T., Espigat, P., Feinstein, F., Fleury, P., Fontaine, G., Funk, S., Gallant, Y. A., Giebels, B., Gillessen, S., Goret, P., Guy, J., Hadjichristidis, C., Hauser, M., Heinzelmann, G., Henri, G., Hermann, G., Hinton, J. A., Hofmann, W., Holleran, M., Horns, D., de Jager, O. C., Jung I., Khélifi, B., Komin, N., Konopelko, A., Latham, I. J., Le Gallou, R., Lemoine, M., Lemière, A., Leroy, N., Lohse, T., Marcowith, A., Masterson, C., McComb, T. J. L., de Naurois, M., Nolan, S. J., Noutsos, A., Orford, K. J., Osborne, J. L., Ouchrif, M., Panter, M., Pelletier, G., Pita, S., Pohl, M., Pühlhofer, G., Punch, M., Raubenheimer, B. C., Raue, M., Raux, J., Rayner, S. M., Redondo, I., Reimer, A., Reimer, O., Ripken, J., Rivoal, M., Rob, L., Rolland, L., Rowell, G., Sahakian, V., Saugé, L., Schlenker, S., Schlickeiser, R., Schuster, C., Schwanke, U., Siewert, M., Sol, H., Steenkamp, R., Stegmann, C., Tavernet, J.-P., Théoret, C. G., Tluczykont, M., van der Walt, D. J., Vasileiadis, G., Vincent, P., Visser, B., Völk, H. J., & Wagner, S. J. 2005b, A&A, 430, 865

Aharonian, F., Akhperjanian, A. G., Barres de Almeida, U., Bazer-Bachi, A. R., Behera, B., Beilicke, M., Benbow, W., Bernlöhr, K., Boisson, C., Bolz, O., Borrel, V., Braun, I., Brion, E., Brown, A. M., Bühler, R., Bulik, T., Büsching, I., Boutelier, T., Carrigan, S., Chadwick, P. M., Chounet, L.-M., Clapson, A. C., Coignet, G., Cornils, R., Costamante, L., Dalton, M., Degrange, B., Dickinson, H. J., Djannati-Ataï, A., Domainko, W., O'C. Drury, L., Dubois, F., Dubus, G., Dyks, J., Egberts, K., Emmanoulopoulos, D., Espigat, P., Farnier, C., Feinstein, F., Fiasson, A., Förster, A., Fontaine, G., Funk, S., Füßling, M., Gallant, Y. A., Giebels, B., Glicenstein, J. F., Glück, B., Goret, P., Hadjichristidis, C., Hauser, D., Hauser, M., Heinzelmann, G., Henri, G., Hermann, G., Hinton, J. A., Hoffmann, A., Hofmann, W., Holleran, M., Hoppe, S., Horns, D., Jacholkowska, A., de Jager, O. C., Jung, I., Katarzyński, K., Kendziorra, E., Kerschhaggl, M., Khélifi, B., Keogh, D., Komin, N., Kosack, K., Lamanna, G., Latham, I. J., Lemière, A., Lemoine-Goumard, M., Lenain, J.-P., Lohse, T., Martin, J. M., Martineau-Huynh, O., Marcowith, A., Masterson, C., Maurin, D., Maurin, G., McComb, T. J. L., Moderski, R., Moulin, E., de Naurois, M., Nedbal, D., Nolan, S. J., Ohm, S., Olive, J.-P., de Oña Wilhelmi, E., Orford, K. J., Osborne, J. L., Ostrowski, M., Panter, M., Pedaletti, G., Pelletier, G., Petrucci, P.-O., Pita, S., Pühlhofer, G., Punch, M., Ranchon, S., Raubenheimer, B. C., Raue, M., Rayner, S. M., Renaud, M., Ripken, J., Rob, L., Rolland, L., Rosier-Lees, S., Rowell, G., Rudak, B., Ruppel, J., Sahakian, V., Santangelo, A., Schlickeiser, R., Schöck, F., Schröder, R., Schwanke, U., Schwarzburg, S., Schwemmer, S., Shalchi, A., Sol, H., Spangler, D., Stawarz, Ł., Steenkamp, R., Stegmann, C., Superina, G., Tam, P. H., Tavernet, J.-P., Terrier, R., van Eldik, C., Vasileiadis, G., Venter, C., Vialle, J. P., Vincent, P., Vivier, M., Völk, H. J., Volpe, F., Wagner, S. J., Ward, M., Zdziarski, A. A., & Zech, A. 2007a, A&A, 475, L9

Aharonian, F., Akhperjanian, A. G., Barrio, J. A., Bernlöhr, K., Bojahr, H., Calle, I., Contreras, J. L., Cortina, J., Daum, A., Deckers, T., Denninghoff, S., Fonseca, V., Gebauer, J., Gonzalez, J. C., Heinzelmann, G., Hemberger, M., Hermann, G., Hess, M., Heusler, A., Hofmann, W., Hohl, H., Horns, D., Ibarra, A., Kankanyan, R., Kestel, M., Kirstein, O., Köhler, C., Kornmayer, H., Kranich, D., Krawczynski, H., Lampeitl, H., Lindner, A., Lorenz, E., Magnussen, N., Meyer, H., Mirzoyan, R., Moralejo, A., Padilla, L., Panter, M., Petry, D., Plaga, R., Plyasheshnikov, A., Prahl, J., Pühlhofer, G., Rauterberg, G., Renault, C., Rhode, W., Röhring, A., Sahakian, V., Samorski, M., Schmele, D., Schröder, F., Stamm, W., Wiebel-Sooth, B., Wiedner, C., Willmer, M., Wirth, H., & Wittek, W. 1999, A&A, 349, 29

Aharonian, F., Akhperjanian, A. G., Bazer-Bachi, A. R., Behera, B., Beilicke, M., Benbow, W., Berge, D., Bernlöhr, K., Boisson, C., Bolz, O., Borrel, V., Boutelier, T., Braun, I., Brion, E., Brown, A. M., Bühler, R., Büsching, I., Bulik, T., Carrigan, S., Chadwick, P. M., Clapson, A. C., Chounet, L.-M., Coignet, G., Cornils, R., Costamante, L., Degrange, B., Dickinson, H. J., Djannati-Ataï, A., Domainko, W., Drury, L. O., Dubus, G., Dyks, J., Egberts, K., Emmanoulopoulos, D., Espigat, P., Farnier, C., Feinstein, F., Fiasson, A., Förster, A., Fontaine, G., Funk, S., Funk, S., Füßling, M., Gallant, Y. A., Giebels, B., Glicenstein, J. F., Glück, B., Goret, P., Hadjichristidis, C., Hauser, D., Hauser, M., Heinzelmann, G., Henri, G., Hermann, G., Hinton, J. A., Hoffmann, A., Hofmann, W., Holleran, M., Hoppe, S., Horns, D., Jacholkowska, A., de Jager, O. C., Kendziorra, E., Kerschhaggl, M., Khélifi, B., Komin, N., Kosack, K., Lamanna, G., Latham, I. J., Le Gallou, R., Lemière, A., Lemoine-Goumard, M., Lenain, J.-P., Lohse, T., Martin, J. M., Martineau-Huynh, O., Marcowith, A., Masterson, C., Maurin, G., McComb, T. J. L., Moderski, R., Moulin, E., de Naurois, M., Nedbal, D., Nolan, S. J., Olive, J.-P., Orford, K. J., Osborne, J. L., Ostrowski, M., Panter, M., Pedaletti, G., Pelletier, G., Petrucci, P.-O., Pita, S., Pühlhofer, G., Punch, M., Ranchon, S., Raubenheimer, B. C., Raue, M., Rayner, S. M., Renaud, M., Ripken, J., Rob, L., Rolland, L., Rosier-Lees, S., Rowell, G., Rudak, B., Ruppel, J., Sahakian, V., Santangelo, A., Saugé, L., Schlenker, S., Schlickeiser, R., Schröder, R., Schwanke, U., Schwarzburg, S., Schwemmer, S., Shalchi, A., Sol, H., Spangler, D., Stawarz, Ł., Steenkamp, R., Stegmann, C., Superina, G., Tam, P. H., Tavernet, J.-P., Terrier, R., van Eldik, C., Vasileiadis, G., Venter, C., Vialle, J. P., Vincent, P., Vivier, M., Völk, H. J., Volpe, F., Wagner, S. J., Ward, M., & Zdziarski, A. A. 2007b, ApJ, 664, L71

Aharonian, F., Akhperjanian, A. G., Bazer-Bachi, A. R., Beilicke, M., Benbow, W., Berge, D., Bernlöhr, K., Boisson, C., Bolz, O., Borrel, V., Braun, I., Breitling, F., Brown, A. M., Chadwick, P. M., Chounet, L.-M., Cornils, R., Costamante, L., Degrange, B., Dickinson, H. J., Djannati-Ataï, A., Drury, L. O., Dubus, G., Emmanoulopoulos, D., Espigat, P., Feinstein, F., Fontaine, G., Fuchs, Y., Funk, S., Gallant, Y. A., Giebels, B., Gillessen, S., Glicenstein, J. F., Goret, P., Hadjichristidis, C., Hauser, D., Hauser, M., Heinzelmann, G., Henri, G., Hermann, G., Hinton, J. A., Hofmann, W., Holleran, M., Horns, D., Jacholkowska, A., de Jager, O. C., Khélifi, B., Klages, S., Komin, N., Konopelko, A., Latham, I. J., Le Gallou, R., Lemière, A., Lemoine-Goumard, M., Leroy, N., Lohse, T., Martin, J. M., Martineau-Huynh, O., Marcowith, A., Masterson, C., McComb, T. J. L., de Naurois, M., Nolan, S. J., Noutsos, A., Orford, K. J., Osborne, J. L., Ouchrif, M., Panter, M., Pelletier, G., Pita, S., Pühlhofer, G., Punch, M., Raubenheimer, B. C., Raue, M., Raux, J., Rayner, S. M., Reimer, A., Reimer, O., Ripken, J., Rob, L., Rolland, L., Rowell, G., Sahakian, V., Saugé, L., Schlenker, S., Schlickeiser, R., Schuster, C., Schwanke, U., Siewert, M., Sol, H., Spangler, D., Steenkamp, R., Stegmann, C., Tavernet, J.-P., Terrier, R., Théoret, C. G., Tluczykont, M., van Eldik, C., Vasileiadis, G., Venter, C., Vincent, P., Völk, H. J., & Wagner, S. J. 2006a, Nature, 440, 1018

Aharonian, F., Akhperjanian, A. G., Bazer-Bachi, A. R., Beilicke, M., Benbow, W., Berge, D., Bernlöhr, K., Boisson, C., Bolz, O., Borrel, V., Braun, I., Brown, A. M., Bühler, R., Büsching, I., Carrigan, S., Chadwick, P. M., Chounet, L.-M., Coignet, G., Cornils, R., Costamante, L., Degrange, B., Dickinson, H. J., Djannati-Ataï, A., Drury, L. O., Dubus, G., Egberts, K., Emmanoulopoulos, D., Espigat, P., Feinstein, F., Ferrero, E., Fiasson, A., Fontaine, G., Funk, S., Funk, S., Füßling, M., Gallant, Y. A., Giebels, B., Glicenstein, J. F., Goret, P., Hadjichristidis, C., Hauser, D., Hauser, M., Heinzelmann, G., Henri, G., Hermann, G., Hinton, J. A., Hoffmann, A., Hofmann, W., Holleran, M., Hoppe, S., Horns, D., Jacholkowska, A., de Jager, O. C., Kendziorra, E., Kerschhaggl, M., Khélifi, B., Komin, N., Konopelko, A., Kosack, K., Lamanna, G., Latham, I. J., Le Gallou, R., Lemière, A., Lemoine-Goumard, M., Lenain, J.-P., Lohse, T., Martin, J. M., Martineau-Huynh, O., Marcowith, A., Masterson, C., Maurin, G., McComb, T. J. L., Moulin, E., de Naurois, M., Nedbal, D., Nolan, S. J., Noutsos, A., Orford, K. J., Osborne, J. L., Ouchrif, M., Panter, M., Pelletier, G., Pita, S., Pühlhofer, G., Punch, M., Ranchon, S., Raubenheimer, B. C., Raue, M., Rayner, S. M., Reimer, A., Ripken, J., Rob, L., Rolland, L., Rosier-Lees, S., Rowell, G., Sahakian, V., Santangelo, A., Saugé, L., Schlenker, S., Schlickeiser, R., Schröder, R., Schwanke, U., Schwarzburg, S., Schwemmer, S., Shalchi, A., Sol, H., Spangler, D., Spanier, F., Steenkamp, R., Stegmann, C., Superina, G., Tam, P. H., Tavernet, J.-P., Terrier, R., Tluczykont, M., van Eldik, C., Vasileiadis, G., Venter, C., Vialle, J. P., Vincent, P., Völk, H. J., Wagner, S. J., & Ward, M. 2006b, Science, 314, 1424

Aharonian, F., Essey, W., Kusenko, A., & Prosekin, A. 2012, ArXiv e-prints

Aharonian, F. A., Khangulyan, D., & Costamante, L. 2008, MNRAS, 387, 1206

Albert, J., Aliu, E., Anderhub, H., Antoranz, P., Armada, A., Asensio, M., Baixeras, C., Barrio, J. A., Bartko, H., Bastieri, D., Becker, J., Bednarek, W., Berger, K., Bigongiari, C., Biland, A., Bisesi, E., Bock, R. K., Bordas, P., Bosch-Ramon, V., Bretz, T., Britvitch, I., Camara, M., Carmona, E., Chilingarian, A., Ciprini, S., Coarasa, J. A., Commichau, S., Contreras, J. L., Cortina, J., Curtef, V., Danielyan, V., Dazzi, F., De Angelis, A., de los Reyes, R., De Lotto, B., Domingo-Santamaría, E., Dorner, D., Doro, M., Errando, M., Fagiolini, M., Ferenc, D., Fernández, E., Firpo, R., Flix, J., Fonseca, M. V., Font, L., Fuchs, M., Galante, N., Garczarczyk, M., Gaug, M., Giller, M., Goebel, F., Hakobyan, D., Hayashida, M., Hengstebeck, T., Höhne, D., Hose, J., Hsu, C. C., Jacon, P., Kalekin, O., Kosyra, R., Kranich, D., Laatiaoui, M., Laille, A., Lenisa, T., Liebing, P., Lindfors, E., Lombardi, S., Longo, F., López, J., López, M., Lorenz, E., Majumdar, P., Maneva, G., Mannheim, K., Mansutti, O., Mariotti, M., Martínez, M., Mazin, D., Merck, C., Meucci, M., Meyer, M., Miranda, J. M., Mirzoyan, R., Mizobuchi, S., Moralejo, A., Nilsson, K., Ninkovic, J., Oña-Wilhelmi, E., Orduña, R., Otte, N., Oya, I., Paneque, D., Paoletti, R., Paredes, J. M., Pasanen, M., Pascoli, D., Pauss, F., Pegna, R., Persic, M., Peruzzo, L., Piccioli, A., Poller, M., Prandini, E., Raymers, A., Rhode, W., Ribó, M., Rico, J., Riegel, B., Rissi, M., Robert, A., Rügamer, S., Saggion, A., Sánchez, A., Sartori, P., Scalzotto, V., Scapin, V., Schmitt, R., Schweizer, T., Shayduk, M., Shinozaki, K., Shore, S. N., Sidro, N., Sillanpää, A., Sobczynska, D., Stamerra, A., Stark, L. S., Takalo, L., Temnikov, P., Tescaro, D., Teshima, M., Tonello, N., Torres, A., Torres, D. F., Turini, N., Vankov, H., Vitale, V., Wagner, R. M., Wibig, T., Wittek, W., Zanin, R., & Zapatero, J. 2006a, ApJ, 648, L105

Albert, J., Aliu, E., Anderhub, H., Antoranz, P., Armada, A., Asensio, M., Baixeras, C., Barrio, J. A., Bartko, H., Bastieri, D., Bednarek, W., Berger, K., Bigongiari, C., Biland, A., Bisesi, E., Bock, R. K., Bretz, T., Britvitch, I., Camara, M., Chilingarian, A., Ciprini, S., Coarasa, J. A., Commichau, S., Contreras, J. L., Cortina, J., Danielyan, V., Dazzi, F., De Angelis, A., de los Reyes, R., De Lotto, B., Domingo-Santamaría, E., Dorner, D., Doro, M., Errando, M., Ferenc, D., Fernández, E., Firpo, R., Flix, J., Fonseca, M. V., Font, L., Galante, N., Garczarczyk, M., Gaug, M., Gebauer, J., Giannitrapani, R., Giller, M., Goebel, F., Hakobyan, D., Hayashida, M., Hengstebeck, T., Höhne, D., Hose, J., Jacon, P., Kalekin, O., Kranich, D., Laille, A., Lenisa, T., Liebing, P., Lindfors, E., Longo, F., López, J., López, M., Lorenz, E., Lucarelli, F., Majumdar, P., Maneva, G., Mannheim, K., Mariotti, M., Martínez, M., Mase, K., Mazin, D., Merck, C., Merck, M., Meucci, M., Meyer, M., Miranda, J. M., Mirzoyan, R., Mizobuchi, S., Moralejo, A., Nilsson, K., Oña-Wilhelmi, E., Orduña, R., Otte, N., Oya, I., Paneque, D., Paoletti, R., Pasanen, M., Pascoli, D., Pauss, F., Pavel, N., Pegna, R., Peruzzo, L., Piccioli, A., Pin, M., Prandini, E., Rico, J., Rhode, W., Riegel, B., Rissi, M., Robert, A., Rossato, G., Rügamer, S., Saggion, A., Sánchez, A., Sartori, P., Scalzotto, V., Schmitt, R., Schweizer, T., Shayduk, M., Shinozaki, K., Sidro, N., Sillanpää, A., Sobczynska, D., Stamerra, A., Stark, L., Takalo, L., Temnikov, P., Tescaro, D., Teshima, M., Tonello, N., Torres, A., Torres, D. F., Turini, N., Vankov, H., Vitale, V., Wagner, R. M., Wibig, T., Wittek, W., & Zapatero, J. 2006b, ApJ, 639, 761

Albert, J., Aliu, E., Anderhub, H., Antoranz, P., Armada, A., Baixeras, C., Barrio, J. A., Bartko, H., Bastieri, D., Becker, J. K., Bednarek, W., Berger, K., Bigongiari, C., Biland, A., Bock, R. K., Bordas, P., Bosch-Ramon, V., Bretz, T., Britvitch, I., Camara, M., Carmona, E., Chilingarian, A., Coarasa, J. A., Commichau, S., Contreras, J. L., Cortina, J., Costado, M. T., Curtef, V., Danielyan, V., Dazzi, F., De Angelis, A., Delgado, C., de los Reyes, R., De Lotto, B., Domingo-Santamaría, E., Dorner, D., Doro, M., Errando, M., Fagiolini, M., Ferenc, D., Fernández, E., Firpo, R., Flix, J., Fonseca, M. V., Font, L., Fuchs, M., Galante, N., García-López, R., Garczarczyk, M., Gaug, M., Giller, M., Goebel, F., Hakobyan, D., Hayashida, M., Hengstebeck, T., Herrero, A., Höhne, D., Hose, J., Hsu, C. C., Jacon, P., Jogler, T., Kosyra, R., Kranich, D., Kritzer, R., Laille, A., Lindfors, E., Lombardi, S., Longo, F., López, J., López, M., Lorenz, E., Majumdar, P., Maneva, G., Mannheim, K., Mansutti, O., Mariotti, M., Martínez, M., Mazin, D., Merck, C., Meucci, M., Meyer, M., Miranda, J. M., Mirzoyan, R., Mizobuchi, S., Moralejo, A., Nilsson, K., Ninkovic, J., Oña-Wilhelmi, E., Otte, N., Oya, I., Paneque, D., Panniello, M., Paoletti, R., Paredes, J. M., Pasanen, M., Pascoli, D., Pauss, F., Pegna, R., Persic, M., Peruzzo, L., Piccioli, A., Poller, M., Prandini, E., Puchades, N., Raymers, A., Rhode, W., Ribó, M., Rico, J., Rissi, M., Robert, A., Rügamer, S., Saggion, A., Sánchez, A., Sartori, P., Scalzotto, V., Scapin, V., Schmitt, R., Schweizer, T., Shayduk, M., Shinozaki, K., Shore, S. N., Sidro, N., Sillanpää, A., Sobczynska, D., Stamerra, A., Stark, L. S., Takalo, L., Temnikov, P., Tescaro, D., Teshima, M., Tonello, N., Torres, D. F., Turini, N., Vankov, H., Vitale, V., Wagner, R. M., Wibig, T., Wittek, W., Zandanel, F., Zanin, R., & Zapatero, J. 2007a, ApJ, 666, L17

Albert, J., Aliu, E., Anderhub, H., Antoranz, P., Armada, A., Baixeras, C., Barrio, J. A., Bartko, H., Bastieri, D., Becker, J. K., Bednarek, W., Berger, K., Bigongiari, C., Biland, A., Bock, R. K., Bordas, P., Bosch-Ramon, V., Bretz, T., Britvitch, I., Camara, M., Carmona, E., Chilingarian, A., Coarasa, J. A., Commichau, S., Contreras, J. L., Cortina, J., Costado, M. T., Curtef, V., Danielyan, V., Dazzi, F., De Angelis, A., Delgado, C., de los Reyes, R., De Lotto, B., Domingo-Santamaría, E., Dorner, D., Doro, M., Errando, M., Fagiolini, M., Ferenc, D., Fernández, E., Firpo, R., Flix, J., Fonseca, M. V., Font, L., Fuchs, M., Galante, N., García-López, R. J., Garczarczyk, M., Gaug, M., Giller, M., Goebel, F., Hakobyan, D., Hayashida, M., Hengstebeck, T., Herrero, A., Höhne, D., Hose, J., Hsu, C. C., Jacon, P., Jogler, T., Kosyra, R., Kranich, D., Kritzer, R., Laille, A., Lindfors, E., Lombardi, S., Longo, F., López, J., López, M., Lorenz, E., Majumdar, P., Maneva, G., Mannheim, K., Mansutti, O., Mariotti, M., Martínez, M., Mazin, D., Merck, C., Meucci, M., Meyer, M., Miranda, J. M., Mirzoyan, R., Mizobuchi, S., Moralejo, A., Nieto, D., Nilsson, K., Ninkovic, J., Oña-Wilhelmi, E., Otte, N., Oya, I., Paneque, D., Panniello, M., Paoletti, R., Paredes, J. M., Pasanen, M., Pascoli, D., Pauss, F., Pegna, R., Perlman, E., Persic, M., Peruzzo, L., Piccioli, A., Prandini, E., Puchades, N., Raymers, A., Rhode, W., Ribó, M., Rico, J., Rissi, M., Robert, A., Rügamer, S., Saggion, A., Saito, T., Sánchez, A., Sartori, P., Scalzotto, V., Scapin, V., Schmitt, R., Schweizer, T., Shayduk, M., Shinozaki, K., Shore, S. N., Sidro, N., Sillanpää, A., Sobczynska, D., Stamerra, A., Stark, L. S., Takalo, L., Tavecchio, F., Temnikov, P., Tescaro, D., Teshima, M., Torres, D. F., Turini, N., Vankov, H., Vitale, V., Wagner, R. M., Wibig, T., Wittek, W., Zandanel, F., Zanin, R., & Zapatero, J. 2007b, ApJ, 667, L21

Aleksic, J., Alvarez, E. A., Antonelli, L. A., Antoranz, P., Asensio, M., Backes, M., Barrio, J. A., Bastieri, D., Becerra Gonzalez, J., Bednarek, W., Berdyugin, A., Berger, K., Bernardini, E., Biland, A., Blanch, O., Bock, R. K., Boller, A., Bonnoli, G., Borla Tridon, D., Braun, I., Bretz, T., Canellas, A., Carmona, E., Carosi, A., Colin, P., Colombo, E., Contreras, J. L., Cortina, J., Cossio, L., Covino, S., Dazzi, F., De Angelis, A., De Caneva, G., De Cea del Pozo, E., De Lotto, B., Delgado Mendez, C., Diago Ortega, A., Doert, M., Dominguez1, A., Dominis Prester, D., Dorner, D., Doro, M., Elsaesser, D., Ferenc, D., Fonseca, M. V., Font, L., Fruck, C., Garcia Lopez, R. J., Garczarczyk, M., Garrido, D., Giavitto, G., Godinovic, N., Hadasch, D., Häfner, D., Herrero, A., Hildebrand, D., Höhne-Mönch, D., Hose, J., Hrupec, D., Huber, B., Jogler, T., Kellermann, H., Klepser, S., Krahenbuh, T., Krause, J., La Barbera, A., Lelas, D., Leonardo, E., Lindfors, E., Lombardi, S., Lopez, A., Lopez, M., Lorenz, E., Makariev, M., Maneva, G., Mankuzhiyil, N., Mannheim, K., Maraschi, L., Mariotti, M., Martinez, M., Mazin, D., Meucci, M., Miranda, J. M., Mirzoyan, R., Miyamoto, H., Moldon, J., Moralejo, A., Munar-Adrover, P., Nieto, D., Nilsson, K., Orito, R., Oya, I., Paneque, D., Paoletti, R., Pardo, S., Paredes, J. M., Partini, S., Pasanen, M., Pauss, F., Perez-Torres, M. A., Persic, M., Peruzzo, L., Pilia, M., Pochon, J., Prada, F., Prada Moroni, P. G., Prandini, E., Puljak, I., Reichardt, I., Reinthal, R., Rhode, W., Ribo, M., Rico, J., Rügamer, S., Saggion, A., Saito, K., Saito, T. Y., Salvati, M., Satalecka, K., Scalzotto, V., Scapin, V., Schultz, C., Schweizer, T., Shayduk, M., Shore, S. N., Sillanpaa, A., Sitarek, J., Sobczynska, D., Spanier, F., Spiro, S., Stamerra, A., Steinke, B., Storz, J., Strah, N., Suric, T., Takalo, L., Takami, H., Tavecchio, F., Temnikov, P., Terzic, T., Tescaro, D., Teshima, M., Tibolla, O., Torres, D. F., Treves, A., Uellenbeck, M., Vankov, H., Vogler, P., Wagner, R. M., Weitzel, Q., Zabalza, V., Zandanel, F., & Zanin, R. 2011, ArXiv: 1589

Aleksić, J., Anderhub, H., Antonelli, L. A., Antoranz, P., Backes, M., Baixeras, C., Balestra, S., Barrio, J. A., Bastieri, D., Becerra González, J., Becker, J. K., Bednarek, W., Berdyugin, A., Berger, K., Bernardini, E., Biland, A., Bock, R. K., Bonnoli, G., Bordas, P., Borla Tridon, D., Bosch-Ramon, V., Bose, D., Braun, I., Bretz, T., Britzger, D., Camara, M., Carmona, E., Carosi, A., Colin, P., Commichau, S., Contreras, J. L., Cortina, J., Costado, M. T., Covino, S., Dazzi, F., de Angelis, A., de Cea Del Pozo, E., de Los Reyes, R., de Lotto, B., de Maria, M., de Sabata, F., Delgado Mendez, C., Doert, M., Domínguez, A., Dominis Prester, D., Dorner, D., Doro, M., Elsaesser, D., Errando, M., Ferenc, D., Fonseca, M. V., Font, L., García López, R. J., Garczarczyk, M., Gaug, M., Godinovic, N., Hadasch, D., Herrero, A., Hildebrand, D., Höhne-Mönch, D., Hose, J., Hrupec, D., Hsu, C. C., Jogler, T., Klepser, S., Krähenbühl, T., Kranich, D., La Barbera, A., Laille, A., Leonardo, E., Lindfors, E., Lombardi, S., Longo, F., López, M., Lorenz, E., Majumdar, P., Maneva, G., Mankuzhiyil, N., Mannheim, K., Maraschi, L., Mariotti, M., Martínez, M., Mazin, D., Meucci, M., Miranda, J. M., Mirzoyan, R., Miyamoto, H., Moldón, J., Moles, M., Moralejo, A., Nieto, D., Nilsson, K., Ninkovic, J., Orito, R., Oya, I., Paoletti, R., Paredes, J. M., Partini, S., Pasanen, M., Pascoli, D., Pauss, F., Pegna, R. G., Perez-Torres, M. A., Persic, M., Peruzzo, L., Prada, F., Prandini, E., Puchades, N., Puljak, I., Reichardt, I., Rhode, W., Ribó, M., Rico, J., Rissi, M., Rügamer, S., Saggion, A., Saito, T. Y., Salvati, M., Sánchez-Conde, M., Satalecka, K., Scalzotto, V., Scapin, V., Schweizer, T., Shayduk, M., Shore, S. N., Sierpowska-Bartosik, A., Sillanpää, A., Sitarek, J., Sobczynska, D., Spanier, F., Spiro, S., Stamerra, A., Steinke, B., Strah, N., Struebig, J. C., Suric, T., Takalo, L., Tavecchio, F., Temnikov, P., Tescaro, D., Teshima, M., Torres, D. F., Vankov, H., Wagner, R. M., Zabalza, V., Zandanel, F., Zanin, R., & MAGIC Collaboration. 2010a, A&A, 519, A32

Aleksić, J., Antonelli, L. A., Antoranz, P., Backes, M., Barrio, J. A., Bastieri, D., Becerra González, J., Bednarek, W., Berdyugin, A., Berger, K., Bernardini, E., Biland, A., Blanch, O., Bock, R. K., Boller, A., Bonnoli, G., Bordas, P., Borla Tridon, D., Bosch-Ramon, V., Bose, D., Braun, I., Bretz, T., Camara, M., Cañellas, A., Carmona, E., Carosi, A., Colin, P., Colombo, E., Contreras, J. L., Cortina, J., Cossio, L., Covino, S., Dazzi, F., De Angelis, A., De Cea del Pozo, E., De Lotto, B., De Maria, M., De Sabata, F., Delgado Mendez, C., Diago Ortega, A., Doert, M., Domínguez, A., Dominis Prester, D., Dorner, D., Doro, M., Elsaesser, D., Errando, M., Ferenc, D., Fonseca, M. V., Font, L., García López, R. J., Garczarczyk, M., Giavitto, G., Godinović, N., Hadasch, D., Herrero, A., Hildebrand, D., Höhne-Mönch, D., Hose, J., Hrupec, D., Jogler, T., Klepser, S., Krähenbühl, T., Kranich, D., Krause, J., La Barbera, A., Leonardo, E., Lindfors, E., Lombardi, S., Longo, F., López, M., Lorenz, E., Majumdar, P., Makariev, M., Maneva, G., Mankuzhiyil, N., Mannheim, K., Maraschi, L., Mariotti, M., Martínez, M., Mazin, D., Meucci, M., Miranda, J. M., Mirzoyan, R., Miyamoto, H., Moldón, J., Moralejo, A., Nieto, D., Nilsson, K., Orito, R., Oya, I., Paoletti, R., Paredes, J. M., Partini, S., Pasanen, M., Pauss, F., Pegna, R. G., Perez-Torres, M. A., Persic, M., Peruzzo, L., Pochon, J., Prada, F., Prada Moroni, P. G., Prandini, E., Puchades, N., Puljak, I., Reichardt, I., Reinthal, R., Rhode, W., Ribó, M., Rico, J., Rügamer, S., Saggion, A., Saito, K., Saito, T. Y., Salvati, M., Sánchez-Conde, M., Satalecka, K., Scalzotto, V., Scapin, V., Schultz, C., Schweizer, T., Shayduk, M., Shore, S. N., Sierpowska-Bartosik, A., Sillanpää, A., Sitarek, J., Sobczynska, D., Spanier, F., Spiro, S., Stamerra, A., Steinke, B., Storz, J., Strah, N., Struebig, J. C., Suric, T., Takalo, L., Tavecchio, F., Temnikov, P., Terzić, T., Tescaro, D., Teshima, M., Torres, D. F., Vankov, H., Wagner, R. M., Weitzel, Q., Zabalza, V., Zandanel, F., Zanin, R., Neronov, A., Pfrommer, C., Pinzke, A., Semikoz, D. V., & MAGIC Collaboration. 2010b, ApJ, 723, L207

Aleksić, J., Antonelli, L. A., Antoranz, P., Backes, M., Barrio, J. A., Bastieri, D., Becerra González, J., Bednarek, W., Berdyugin, A., Berger, K., Bernardini, E., Biland, A., Blanch, O., Bock, R. K., Boller, A., Bonnoli, G., Borla Tridon, D., Braun, I., Bretz, T., Cañellas, A., Carmona, E., Carosi, A., Colin, P., Colombo, E., Contreras, J. L., Cortina, J., Cossio, L., Covino, S., Dazzi, F., De Angelis, A., De Cea del Pozo, E., De Lotto, B., Delgado Mendez, C., Diago Ortega, A., Doert, M., Domínguez, A., Dominis Prester, D., Dorner, D., Doro, M., Elsaesser, D., Ferenc, D., Fonseca, M. V., Font, L., Fruck, C., García López, R. J., Garczarczyk, M., Garrido, D., Giavitto, G., Godinović, N., Hadasch, D., Häfner, D., Herrero, A., Hildebrand, D., Höhne-Mönch, D., Hose, J., Hrupec, D., Huber, B., Jogler, T., Klepser, S., Krähenbühl, T., Krause, J., La Barbera, A., Lelas, D., Leonardo, E., Lindfors, E., Lombardi, S., López, M., Lorenz, E., Makariev, M., Maneva, G., Mankuzhiyil, N., Mannheim, K., Maraschi, L., Mariotti, M., Martínez, M., Mazin, D., Meucci, M., Miranda, J. M., Mirzoyan, R., Miyamoto, H., Moldón, J., Moralejo, A., Nieto, D., Nilsson, K., Orito, R., Oya, I., Paneque, D., Paoletti, R., Pardo, S., Paredes, J. M., Partini, S., Pasanen, M., Pauss, F., Perez-Torres, M. A., Persic, M., Peruzzo, L., Pilia, M., Pochon, J., Prada, F., Prada Moroni, P. G., Prandini, E., Puljak, I., Reichardt, I., Reinthal, R., Rhode, W., Ribó, M., Rico, J., Rügamer, S., Saggion, A., Saito, K., Saito, T. Y., Salvati, M., Satalecka, K., Scalzotto, V., Scapin, V., Schultz, C., Schweizer, T., Shayduk, M., Shore, S. N., Sillanpää, A., Sitarek, J., Sobczynska, D., Spanier, F., Spiro, S., Stamerra, A., Steinke, B., Storz, J., Strah, N., Surić, T., Takalo, L., Tavecchio, F., Temnikov, P., Terzić, T., Tescaro, D., Teshima, M., Thom, M., Tibolla, O., Torres, D. F., Treves, A., Vankov, H., Vogler, P., Wagner, R. M., Weitzel, Q., Zabalza, V., Zandanel, F., Zanin, R., MAGIC Collaboration, Tanaka, Y. T., Wood, D. L., & Buson, S. 2011a, ApJ, 730, L8

Aleksić, J., Antonelli, L. A., Antoranz, P., Backes, M., Barrio, J. A., Bastieri, D., Becerra González, J., Bednarek, W., Berdyugin, A., Berger, K., Bernardini, E., Biland, A., Blanch, O., Bock, R. K., Boller, A., Bonnoli, G., Borla Tridon, D., Braun, I., Bretz, T., Cañellas, A., Carmona, E., Carosi, A., Colin, P., Colombo, E., Contreras, J. L., Cortina, J., Cossio, L., Covino, S., Dazzi, F., de Angelis, A., de Cea Del Pozo, E., de Lotto, B., Delgado Mendez, C., Diago Ortega, A., Doert, M., Domínguez, A., Dominis Prester, D., Dorner, D., Doro, M., Elsaesser, D., Ferenc, D., Fonseca, M. V., Font, L., Fruck, C., García López, R. J., Garczarczyk, M., Garrido, D., Giavitto, G., Godinović, N., Hadasch, D., Häfner, D., Herrero, A., Hildebrand, D., Hose, J., Hrupec, D., Huber, B., Jogler, T., Klepser, S., Krähenbühl, T., Krause, J., La Barbera, A., Lelas, D., Leonardo, E., Lindfors, E., Lombardi, S., López, M., Lorenz, E., Majumdar, P., Makariev, M., Maneva, G., Mankuzhiyil, N., Mannheim, K., Maraschi, L., Mariotti, M., Martínez, M., Mazin, D., Meucci, M., Miranda, J. M., Mirzoyan, R., Miyamoto, H., Moldón, J., Moralejo, A., Nieto, D., Nilsson, K., Orito, R., Oya, I., Paoletti, R., Pardo, S., Paredes, J. M., Partini, S., Pasanen, M., Pauss, F., Perez-Torres, M. A., Persic, M., Peruzzo, L., Pilia, M., Pochon, J., Prada, F., Prada Moroni, P. G., Prandini, E., Puljak, I., Reichardt, I., Reinthal, R., Rhode, W., Ribó, M., Rico, J., Rügamer, S., Rüger, M., Saggion, A., Saito, K., Saito, T. Y., Salvati, M., Satalecka, K., Scalzotto, V., Scapin, V., Schultz, C., Schweizer, T., Shayduk, M., Shore, S. N., Sillanpää, A., Sitarek, J., Sobczynska, D., Spanier, F., Spiro, S., Stamerra, A., Steinke, B., Storz, J., Strah, N., Surić, T., Takalo, L., Tavecchio, F., Temnikov, P., Terzić, T., Tescaro, D., Teshima, M., Thom, M., Tibolla, O., Torres, D. F., Treves, A., Vankov, H., Vogler, P., Wagner, R. M., Weitzel, Q., Zabalza, V., Zandanel, F., & Zanin, R. 2011b, A&A, 530, A4

Anderhub, H., Antonelli, L. A., Antoranz, P., Backes, M., Baixeras, C., Balestra, S., Barrio, J. A., Bastieri, D., Becerra González, J., Becker, J. K., Bednarek, W., Berdyugin, A., Berger, K., Bernardini, E., Biland, A., Bock, R. K., Bonnoli, G., Bordas, P., Borla Tridon, D., Bosch-Ramon, V., Bose, D., Braun, I., Bretz, T., Britzger, D., Camara, M., Carmona, E., Carosi, A., Colin, P., Commichau, S., Contreras, J. L., Cortina, J., Costado, M. T., Covino, S., Dazzi, F., De Angelis, A., de Cea del Pozo, E., De los Reyes, R., De Lotto, B., De Maria, M., De Sabata, F., Delgado Mendez, C., Domínguez, A., Dominis Prester, D., Dorner, D., Doro, M., Elsaesser, D., Errando, M., Ferenc, D., Fernández, E., Firpo, R., Fonseca, M. V., Font, L., Galante, N., García López, R. J., Garczarczyk, M., Gaug, M., Godinovic, N., Goebel, F., Hadasch, D., Herrero, A., Hildebrand, D., Höhne-Mönch, D., Hose, J., Hrupec, D., Hsu, C. C., Jogler, T., Klepser, S., Kranich, D., La Barbera, A., Laille, A., Leonardo, E., Lindfors, E., Lombardi, S., Longo, F., López, M., Lorenz, E., Majumdar, P., Maneva, G., Mankuzhiyil, N., Mannheim, K., Maraschi, L., Mariotti, M., Martínez, M., Mazin, D., Meucci, M., Miranda, J. M., Mirzoyan, R., Miyamoto, H., Moldón, J., Moles, M., Moralejo, A., Nieto, D., Nilsson, K., Ninkovic, J., Orito, R., Oya, I., Paoletti, R., Paredes, J. M., Pasanen, M., Pascoli, D., Pauss, F., Pegna, R. G., Perez-Torres, M. A., Persic, M., Peruzzo, L., Prada, F., Prandini, E., Puchades, N., Puljak, I., Reichardt, I., Rhode, W., Ribó, M., Rico, J., Rissi, M., Robert, A., Rügamer, S., Saggion, A., Sainio, J., Saito, T. Y., Salvati, M., Sánchez-Conde, M., Satalecka, K., Scalzotto, V., Scapin, V., Schweizer, T., Shayduk, M., Shore, S. N., Sierpowska-Bartosik, A., Sillanpää, A., Sitarek, J., Sobczynska, D., Spanier, F., Spiro, S., Stamerra, A., Stark, L. S., Suric, T., Takalo, L., Tavecchio, F., Temnikov, P., Tescaro, D., Teshima, M., Torres, D. F., Turini, N., Vankov, H., Wagner, R. M., Villforth, C., Zabalza, V., Zandanel, F., Zanin, R., & Zapatero, J. 2009, ApJ, 704, L129

Arendt, R. G. & Dwek, E. 2003, ApJ, 585, 305

Audouze, J. & Tinsley, B. M. 1976, ARA&A, 14, 43

Ballantyne, D. R., Shi, Y., Rieke, G. H., Donley, J. L., Papovich, C., & Rigby, J. R. 2006, ApJ, 653, 1070

Beacom, J. F. 2010, Annual Review of Nuclear and Particle Science, 60, 439

Beacom, J. F. & Vagins, M. R. 2004, Physical Review Letters, 93, 171101

Benbow, W. 2011, arXiv: 1110.0040, L3003

Benbow, W. et al. 2011, ArXiv: 1110.0040

Berger, K., Dominis Prester, D., Tavecchio, F., Terzić, T., & for the MAGIC Collaboration. 2011a, ArXiv: 1109.5879

Berger, K., Giavitto, G., Lindfors, E., Takalo, L., Paneque, D., Stamerra, A., & On behalf of the MAGIC Collaboration. 2011b, ArXiv: 1110.6368

Bernstein, R. A. 2007, ApJ, 666, 663

Bernstein, R. A., Freedman, W. L., & Madore, B. F. 2002, ApJ, 571, 56

Berta, S., Magnelli, B., Lutz, D., Altieri, B., Aussel, H., Andreani, P., Bauer, O., Bongiovanni, A., Cava, A., Cepa, J., Cimatti, A., Daddi, E., Dominguez, H., Elbaz, D., Feuchtgruber, H., Förster Schreiber, N. M., Genzel, R., Gruppioni, C., Katterloher, R., Magdis, G., Maiolino, R., Nordon, R., Pérez García, A. M., Poglitsch, A., Popesso, P., Pozzi, F., Riguccini, L., Rodighiero, G., Saintonge, A., Santini, P., Sanchez-Portal, M., Shao, L., Sturm, E., Tacconi, L. J., Valtchanov, I., Wetzstein, M., & Wieprecht, E. 2010, A&A, 518, L30+

Berta, S., Magnelli, B., Nordon, R., Lutz, D., Wuyts, S., Altieri, B., Andreani, P., Aussel, H., Castañeda, H., Cepa, J., Cimatti, A., Daddi, E., Elbaz, D., Förster Schreiber, N. M., Genzel, R., Le Floc'h, E., Maiolino, R., Pérez-Fournon, I., Poglitsch, A., Popesso, P., Pozzi, F., Riguccini, L., Rodighiero, G., Sanchez-Portal, M., Sturm, E., Tacconi, L. J., & Valtchanov, I. 2011, A&A, 532, A49+

Béthermin, M., Dole, H., Beelen, A., & Aussel, H. 2010a, A&A, 512, A78+

Béthermin, M., Dole, H., Cousin, M., & Bavouzet, N. 2010b, A&A, 516, A43+

Béthermin, M., Le Floc'h, E., Ilbert, O., Conley, A., Lagache, G., Amblard, A., Arumugam, V., Aussel, H., Berta, S., Bock, J., Boselli, A., Buat, V., Casey, C. M., Castro-Rodríguez, N., Cava, A., Clements, D. L., Cooray, A., Dowell, C. D., Eales, S., Farrah, D., Franceschini, A., Glenn, J., Griffin, M., Hatziminaoglou, E., Heinis, S., Ibar, E., Ivison, R. J., Kartaltepe, J. S., Levenson, L., Magdis, G., Marchetti, L., Marsden, G., Nguyen, H. T., O'Halloran, B., Oliver, S. J., Omont, A., Page, M. J., Panuzzo, P., Papageorgiou, A., Pearson, C. P., Pérez-Fournon, I., Pohlen, M., Rigopoulou, D., Roseboom, I. G., Rowan-Robinson, M., Salvato, M., Schulz, B., Scott, D., Seymour, N., Shupe, D. L., Smith, A. J., Symeonidis, M., Trichas, M., Tugwell, K. E., Vaccari, M., Valtchanov, I., Vieira, J. D., Viero, M., Wang, L., Xu, C. K., & Zemcov, M. 2012, A&A, 542, A58

Biller, S. D., Akerlof, C. W., Buckley, J., Cawley, M. F., Chantell, M., Fegan, D. J., Fennell, S., Gaidos, J. A., Hillas, A. M., Kerrick, A. D., Lamb, R. C., Lewis, D. A., Meyer, D. I., Mohanty, G., O'Flaherty, K. S., Punch, M., Reynolds, P. T., Rose, H. J., Rovero, A. C., Schubnell, M. S., Sembroski, G., Weekes, T. C., & Wilson, C. 1995, ApJ, 445, 227

Biller, S. D., Buckley, J., Burdett, A., Bussons Gordo, J., Carter-Lewis, D. A., Fegan, D. J., Finley, J., Gaidos, J. A., Hillas, A. M., Krennrich, F., Lamb, R. C., Lessard, R., McEnery, J. E., Mohanty, G., Quinn, J., Rodgers, A. J., Rose, H. J., Samuelson, F., Sembroski, G., Skelton, P., Weekes, T. C., & Zweerink, J. 1998, Phys. Rev. Lett., 80, 2992

Boettcher, M. 2010, ArXiv: 1006.5048

Böttcher, M., Dermer, C. D., & Finke, J. D. 2008, ApJ, 679, L9

Bromm, V. & Loeb, A. 2002, ApJ, 575, 111

Bruzual, G. & Charlot, S. 2003, MNRAS, 344, 1000

Şentürk, G. D., for the VERITAS Collaboration, Fortin, P., Horan, D., & for the Fermi-LAT Collaboration. 2011, ArXiv: 1109.6035

Cambrésy, L., Reach, W. T., Beichman, C. A., & Jarrett, T. H. 2001, ApJ, 555, 563

Catanese, M., Bradbury, S. M., Breslin, A. C., Buckley, J. H., Carter-Lewis, D. A., Cawley, M. F., Dermer, C. D., Fegan, D. J., Finley, J. P., Gaidos, J. A., Hillas, A. M., Johnson, W. N., Krennrich, F., Lamb, R. C., Lessard, R. W., Macomb, D. J., McEnery, J. E., Moriarty, P., Quinn, J., Rodgers, A. J., Rose, H. J., Samuelson, F. W., Sembroski, G. H., Srinivasan, R., Weekes, T. C., & Zweerink, J. 1997, ApJ, 487, L143

Cerruti, M. for the H.E.S.S. Collaboration . 2011, ArXiv; 1110.2119

Chary, R., Casertano, S., Dickinson, M. E., Ferguson, H. C., Eisenhardt, P. R. M., Elbaz, D., Grogin, N. A., Moustakas, L. A., Reach, W. T., & Yan, H. 2004, ApJS, 154, 80

Chary, R. & Elbaz, D. 2001, ApJ, 556, 562

Colin, P., Becerra Gonzalez, J., Lindfors, E., Lombardi, S., Sitarek, J., Stamera, A., & for the MAGIC Collaboration. 2011, ArXiv: 1110.0236

Condon, J. J., Anderson, M. L., & Helou, G. 1991, ApJ, 376, 95

Coppin, K., Chapin, E. L., Mortier, A. M. J., Scott, S. E., Borys, C., Dunlop, J. S., Halpern, M., Hughes, D. H., Pope, A., Scott, D., Serjeant, S., Wagg, J., Alexander, D. M., Almaini, O., Aretxaga, I., Babbedge, T., Best, P. N., Blain, A., Chapman, S., Clements, D. L., Crawford, M., Dunne, L., Eales, S. A., Edge, A. C., Farrah, D., Gaztañaga, E., Gear, W. K., Granato, G. L., Greve, T. R., Fox, M., Ivison, R. J., Jarvis, M. J., Jenness, T., Lacey, C., Lepage, K., Mann, R. G., Marsden, G., Martinez-Sansigre, A., Oliver, S., Page, M. J., Peacock, J. A., Pearson, C. P., Percival, W. J., Priddey, R. S., Rawlings, S., Rowan-Robinson, M., Savage, R. S., Seigar, M., Sekiguchi, K., Silva, L., Simpson, C., Smail, I., Stevens, J. A., Takagi, T., Vaccari, M., van Kampen, E., & Willott, C. J. 2006, MNRAS, 372, 1621

Dermer, C. D. 2012, ArXiv e-prints

Djannati-Atai , A., Piron, F., Barrau, A., Iacoucci, L., Punch, M., Tavernet, J.-P., Bazer-Bachi, R., Cabot, H., Chounet, L.-M., Debiais, G., Degrange, B., Dezalay, J.-P., Dumora, D., Espigat, P., Fabre, B., Fleury, P., Fontaine, G., Ghesquière, C., Goret, P., Gouiffes, C., Grenier, I. A., Le Bohec, S., Malet, I., Meynadier, C., Mohanty, G., Nuss, E., Paré, E., Québert, J., Ragan, K., Renault, C., Rivoal, M., Rob, L., Schahmaneche, K., & Smith, D. A. 1999, A&A, 350, 17

Dole, H., Lagache, G., Puget, J.-L., Caputi, K. I., Fernández-Conde, N., Le Floc'h, E., Papovich, C., Pérez-González, P. G., Rieke, G. H., & Blaylock, M. 2006, A&A, 451, 417

Dole, H., Rieke, G. H., Lagache, G., Puget, J., Alonso-Herrero, A., Bai, L., Blaylock, M., Egami, E., Engelbracht, C. W., Gordon, K. D., Hines, D. C., Kelly, D. M., Le Floc'h, E., Misselt, K. A., Morrison, J. E., Muzerolle, J., Papovich, C., Perez-Gonzalez, P. G., Rieke, M. J., Rigby, J. R., Neugebauer, G., Stansberry, J. A., Su, K. Y. L., Young, E. T., Beichman, C. A., & Richards, P. L. 2004, ArXiv Astrophysics e-prints

Domínguez, A., Primack, J. R., Rosario, D. J., Prada, F., Gilmore, R. C., Faber, S. M., Koo, D. C., Somerville, R. S., Pérez-Torres, M. A., Pérez-González, P., Huang, J.-S., Davis, M., Guhathakurta, P., Barmby, P., Conselice, C. J., Lozano, M., Newman, J. A., & Cooper, M. C. 2011, MNRAS, 410, 2556

Donnarumma, I., Pucella, G., Vittorini, V., D'Ammando, F., Vercellone, S., Raiteri, C. M., Villata, M., Perri, M., Chen, W. P., Smart, R. L., Kataoka, J., Kawai, N., Mori, Y., Tosti, G., Impiombato, D., Takahashi, T., Sato, R., Tavani, M., Bulgarelli, A., Chen, A. W., Giuliani, A., Longo, F., Pacciani, L., Argan, A., Barbiellini, G., Boffelli, F., Caraveo, P., Cattaneo, P. W., Cocco, V., Contessi, T., Costa, E., Del Monte, E., De Paris, G., Di Cocco, G., Evangelista, Y., Feroci, M., Ferrari, A., Fiorini, M., Froysland, T., Frutti, M., Fuschino, F., Galli, M., Gianotti, F., Labanti, C., Lapshov, I., Lazzarotto, F., Lipari, P., Marisaldi, M., Mastropietro, M., Mereghetti, S., Morelli, E., Moretti, E., Morselli, A., Pellizzoni, A., Perotti, F., Piano, G., Picozza, P., Pilia, M., Porrovecchio, G., Prest, M., Rapisarda, M., Rappoldi, A., Rubini, A., Sabatini, S., Scalise, E., Soffitta, P., Striani, E., Trifoglio, M., Trois, A., Vallazza, E., Zambra, A., Zanello, D., Pittori, C., Santolamazza, P., Verrecchia, F., Giommi, P., Antonelli, L. A., Colafrancesco, S., & Salotti, L. 2009, ApJ, 707, 1115

Draper, A. R. & Ballantyne, D. R. 2009, ApJ, 707, 778

Dube, R. R., Wickes, W. C., & Wilkinson, D. T. 1979, ApJ, 232, 333

Dunne, L., Eales, S., Edmunds, M., Ivison, R., Alexander, P., & Clements, D. L. 2000, MNRAS, 315, 115

Dwek, E. & Arendt, R. G. 1998, ApJ, 508, L9

Dwek, E., Arendt, R. G., Hauser, M. G., Fixsen, D., Kelsall, T., Leisawitz, D., Pei, Y. C., Wright, E. L., Mather, J. C., Moseley, S. H., Odegard, N., Shafer, R., Silverberg, R. F., & Weiland, J. L. 1998, ApJ, 508, 106

Dwek, E., Arendt, R. G., & Krennrich, F. 2005a, ApJ, 635, 784

Dwek, E. & Barker, M. K. 2002, ApJ, 575, 7

Dwek, E. & Krennrich, F. 2005, ApJ, 618, 657

Dwek, E., Krennrich, F., & Arendt, R. G. 2005b, ApJ, 634, 155

Dwek, E. & Slavin, J. 1994, ApJ, 436, 696

Dwek, E., Staguhn, J. G., Arendt, R. G., Capak, P. L., Kovacs, A., Benford, D. J., Fixsen, D., Karim, A., Leclercq, S., Maher, S. F., Moseley, S. H., Schinnerer, E., & Sharp, E. H. 2011, ApJ, 738, 36

Elbaz, D., Cesarsky, C. J., Chanial, P., Aussel, H., Franceschini, A., Fadda, D., & Chary, R. R. 2002, A&A, 384, 848

Errando, M. et al. 2011, ArXiv: 1111.1209

Fazio, G. G., Ashby, M. L. N., Barmby, P., Hora, J. L., Huang, J.-S., Pahre, M. A., Wang, Z., Willner, S. P., Arendt, R. G., Moseley, S. H., Brodwin, M., Eisenhardt, P., Stern, D., Tollestrup, E. V., & Wright, E. L. 2004, ApJS, 154, 39

Finkbeiner, D. P., Davis, M., & Schlegel, D. J. 2000, ApJ, 544, 81

Finke, J. D. & Razzaque, S. 2009, ApJ, 698, 1761

Finke, J. D., Razzaque, S., & Dermer, C. D. 2010, ApJ, 712, 238

Fioc, M. & Rocca-Volmerange, B. 1997, A&A, 326, 950

Fixsen, D. J., Dwek, E., Mather, J. C., Bennett, C. L., & Shafer, R. A. 1998, ApJ, 508, 123

Fontanot, F. & Somerville, R. S. 2011, MNRAS, 416, 2962

Fontanot, F., Somerville, R. S., Silva, L., Monaco, P., & Skibba, R. 2009, MNRAS, 392, 553

Fossati, G., Buckley, J. H., Bond, I. H., Bradbury, S. M., Carter-Lewis, D. A., Chow, Y. C. K., Cui, W., Falcone, A. D., Finley, J. P., Gaidos, J. A., Grube, J., Holder, J., Horan, D., Horns, D., Jordan, M. M., Kieda, D. B., Kildea, J., Krawczynski, H., Krennrich, F., Lang, M. J., LeBohec, S., Lee, K., Moriarty, P., Ong, R. A., Petry, D., Quinn, J., Sembroski, G. H., Wakely, S. P., & Weekes, T. C. 2008, ApJ, 677, 906

Fossati, G., Maraschi, L., Celotti, A., Comastri, A., & Ghisellini, G. 1998, MNRAS, 299, 433

Franceschini, A., Fadda, D., Cesarsky, C. J., Elbaz, D., Flores, H., & Granato, G. L. 2002, ApJ, 568, 470

Franceschini, A., Rodighiero, G., & Vaccari, M. 2008, A&A, 487, 837

Frayer, D. T., Huynh, M. T., Chary, R., Dickinson, M., Elbaz, D., Fadda, D., Surace, J. A., Teplitz, H. I., Yan, L., & Mobasher, B. 2006, ApJ, 647, L9

Fumagalli, M., Furniss, A., O'Meara, J. M., Prochaska, J. X., Williams, D. A., & Farina, E. P. 2012, ArXiv e-prints

Funk, B., Magnussen, N., Meyer, H., Rhode, W., Westerhoff, S., & Wiebel-Sooth, B. 1998, Astroparticle Physics, 9, 97

Gaidos, J. A., Akerlof, C. W., Biller, S., Boyle, P. J., Breslin, A. C., Buckley, J. H., Carter-Lewis, D. A., Catanese, M., Cawley, M. F., Fegan, D. J., Finley, J. P., Gordo, J. B., Hillas, A. M., Krennrich, F., Lamb, R. C., Lessard, R. W., McEnery, J. E., Masterson, C., Mohanty, G., Moriarty, P., Quinn, J., Rodgers, A. J., Rose, H. J., Samuelson, F., Schubnell, M. S., Sembroski, G. H., Srinivasan, R., Weekes, T. C., Wilson, C. L., & Zweerink, J. 1996, Nature, 383, 319

Gandhi, P. & Fabian, A. C. 2003, MNRAS, 339, 1095

Gardner, J. P., Brown, T. M., & Ferguson, H. C. 2000, ApJ, 542, L79

Gardner, J. P., Mather, J. C., Clampin, M., Doyon, R., Greenhouse, M. A., Hammel, H. B., Hutchings, J. B., Jakobsen, P., Lilly, S. J., Long, K. S., Lunine, J. I., McCaughrean, M. J., Mountain, M., Nella, J., Rieke, G. H., Rieke, M. J., Rix, H.-W., Smith, E. P., Sonneborn, G., Stiavelli, M., Stockman, H. S., Windhorst, R. A., & Wright, G. S. 2006, Space Sci. Rev., 123, 485

Georganopoulos, M., Sambruna, R. M., Kazanas, D., Cillis, A. N., Cheung, C. C., Perlman, E. S., Blundell, K. M., & Davis, D. S. 2008, ApJ, 686, L5

Georganopoulos, M., Sambruna, R. M., Kazanas, D., Davis, D. S., Cillis, A. N., Cheung, C. C., Perlman, E. S., & Blundell, K. M. 2010, in Astronomical Society of the Pacific Conference Series, Vol. 427, Accretion and Ejection in AGN: a Global View, ed. L. Maraschi, G. Ghisellini, R. Della Ceca, & F. Tavecchio, 177

Gilmore, R. C., Somerville, R. S., Primack, J. R., & Domínguez, A. 2011, ArXiv: 1104.0671

Gordon, K. D., Misselt, K. A., Witt, A. N., & Clayton, G. C. 2001, ApJ, 551, 269

Guy, J., Renault, C., Aharonian, F. A., Rivoal, M., & Tavernet, J.-P. 2000, A&A, 359, 419

Haarsma, D. B. & Partridge, R. B. 1998, ApJ, 503, L5

Haarsma, D. B., Partridge, R. B., Windhorst, R. A., & Richards, E. A. 2000, ApJ, 544, 641

Hainline, L. J., Blain, A. W., Smail, I., Frayer, D. T., Chapman, S. C., Ivison, R. J., & Alexander, D. M. 2009, ApJ, 699, 1610

Hauser, M. G., Arendt, R. G., Kelsall, T., Dwek, E., Odegard, N., Weiland, J. L., Freudenreich, H. T., Reach, W. T., Silverberg, R. F., Moseley, S. H., Pei, Y. C., Lubin, P., Mather, J. C., Shafer, R. A., Smoot, G. F., Weiss, R., Wilkinson, D. T., & Wright, E. L. 1998, ApJ, 508, 25

Hauser, M. G. & Dwek, E. 2001, ARA&A, 39, 249

Helgason, K., Ricotti, M., & Kashlinsky, A. 2012, ApJ, 752, 113

Hildebrand, D., Lombardi, S., Colin, P., Sitarek, J., Zandanel, F., Prada, F., for the MAGIC Collaboration, Pfrommer, C., & Pinzke, A. 2011, ArXiv: 1110.5358

Hinshaw, G., Weiland, J. L., Hill, R. S., Odegard, N., Larson, D., Bennett, C. L., Dunkley, J., Gold, B., Greason, M. R., Jarosik, N., Komatsu, E., Nolta, M. R., Page, L., Spergel, D. N., Wollack, E., Halpern, M., Kogut, A., Limon, M., Meyer, S. S., Tucker, G. S., & Wright, E. L. 2009, ApJS, 180, 225

Hinton, J. A. & Hofmann, W. 2009, ARA&A, 47, 523

Hopkins, A. M. & Beacom, J. F. 2006, ApJ, 651, 142

Hopwood, R., Serjeant, S., Negrello, M., Pearson, C., Egami, E., Im, M., Kneib, J.-P., Ko, J., Lee, H. M., Lee, M. G., Matsuhara, H., Nakagawa, T., Smail, I., & Takagi, T. 2010, ApJ, 716, L45

Horiuchi, S., Beacom, J. F., & Dwek, E. 2009, Phys. Rev. D, 79, 083013

Kampert, K.-H. f. 2012, ArXiv e-prints

Kashlinsky, A. 2005, Phys. Rep., 409, 361

Kashlinsky, A., Arendt, R. G., Ashby, M. L. N., Fazio, G. G., Mather, J., & Moseley, S. H. 2012, ApJ, 753, 63

Kashlinsky, A., Mather, J. C., Odenwald, S., & Hauser, M. G. 1996, ApJ, 470, 681

Katarzyński, K., Ghisellini, G., Tavecchio, F., Gracia, J., & Maraschi, L. 2006, MNRAS, 368, L52

Keenan, R. C., Barger, A. J., Cowie, L. L., & Wang, W.-H. 2010, ApJ, 723, 40

Kelsall, T., Weiland, J. L., Franz, B. A., Reach, W. T., Arendt, R. G., Dwek, E., Freudenreich, H. T., Hauser, M. G., Moseley, S. H., Odegard, N. P., Silverberg, R. F., & Wright, E. L. 1998, ApJ, 508, 44

Kennicutt, Jr., R. C. 1998, ApJ, 498, 541

Krawczynski, H., Hughes, S. B., Horan, D., Aharonian, F., Aller, M. F., Aller, H., Boltwood, P., Buckley, J., Coppi, P., Fossati, G., Götting, N., Holder, J., Horns, D., Kurtanidze, O. M., Marscher, A. P., Nikolashvili, M., Remillard, R. A., Sadun, A., & Schröder, M. 2004, ApJ, 601, 151

Krennrich, F., Bond, I. H., Bradbury, S. M., Buckley, J. H., Carter-Lewis, D. A., Cui, W., de la Calle Perez, I., Fegan, D. J., Fegan, S. J., Finley, J. P., Gaidos, J. A., Gibbs, K., Gillanders, G. H., Hall, T. A., Hillas, A. M., Holder, J., Horan, D., Jordan, M., Kertzman, M., Kieda, D., Kildea, J., Knapp, J., Kosack, K., Lang, M. J., LeBohec, S., Moriarty, P., Müller, D., Ong, R. A., Pallassini, R., Petry, D., Quinn, J., Reay, N. W., Reynolds, P. T., Rose, H. J., Sembroski, G. H., Sidwell, R., Stanton, N., Swordy, S. P., Vassiliev, V. V., Wakely, S. P., & Weekes, T. C. 2002, ApJ, 575, L9

Krennrich, F., Dwek, E., & Imran, A. 2008, ApJ, 689, L93

Kronberg, P. P. 1994, Reports on Progress in Physics, 57, 325

—. 2010, ArXiv e-prints

Kusenko, A. 2012, ArXiv e-prints

Kutyrev, A. S., Arendt, R., Dwek, E., Moseley, S. H., Rapchun, D., & Silverberg, R. F. 2008, in Society of Photo-Optical Instrumentation Engineers (SPIE) Conference Series, Vol. 7014, Society of Photo-Optical Instrumentation Engineers (SPIE) Conference Series

Kutyrev, A. S., Bennett, C. L., Moseley, S. H., Rapchun, D., & Stewart, K. P. 2004, in Society of Photo-Optical Instrumentation Engineers (SPIE) Conference Series, Vol. 5492, Society of Photo-Optical Instrumentation Engineers (SPIE) Conference Series, ed. A. F. M. Moorwood & M. Iye, 1172–1178

Lagache, G., Bavouzet, N., Fernandez-Conde, N., Ponthieu, N., Rodet, T., Dole, H., Miville-Deschênes, M.-A., & Puget, J.-L. 2007, ApJ, 665, L89

Lagache, G., Dole, H., & Puget, J.-L. 2003, MNRAS, 338, 555

Lagache, G., Haffner, L. M., Reynolds, R. J., & Tufte, S. L. 2000, A&A, 354, 247

Lagache, G. & Puget, J. L. 2000, A&A, 355, 17

Lagache, G., Puget, J.-L., & Dole, H. 2005, ARA&A, 43, 727

Landt, H. 2012, MNRAS, 423, L84

Lefa, E., Rieger, F. M., & Aharonian, F. A. 2011, ApJ, 740, 64

Leinert, C., Bowyer, S., Haikala, L. K., Hanner, M. S., Hauser, M. G., Levasseur-Regourd, A.-C., Mann, I., Mattila, K., Reach, W. T., Schlosser, W., Staude, H. J., Toller, G. N., Weiland, J. L., Weinberg, J. L., & Witt, A. N. 1998, A&AS, 127, 1

Leitherer, C., Schaerer, D., Goldader, J. D., González Delgado, R. M., Robert, C., Kune, D. F., de Mello, D. F., Devost, D., & Heckman, T. M. 1999, ApJS, 123, 3

Levenson, L. R. & Wright, E. L. 2008, ApJ, 683, 585

Levenson, L. R., Wright, E. L., & Johnson, B. D. 2007, ApJ, 666, 34

Lin, Y. C., Bertsch, D. L., Chiang, J., Fichtel, C. E., Hartman, R. C., Hunter, S. D., Kanbach, G., Kniffen, D. A., Kwok, P. W., Mattox, J. R., Mayer-Hasselwander, H. A., Michelson, P. F., von Montigny, C., Nolan, P. L., Pinkau, K., Schneid, E., Sreekumar, P., & Thompson, D. J. 1992, ApJ, 401, L61

Lisenfeld, U., Voelk, H. J., & Xu, C. 1996, A&A, 306, 677

MacMinn, D. & Primack, J. R. 1996, Space Sci. Rev., 75, 413

Madau, P., Ferguson, H. C., Dickinson, M. E., Giavalisco, M., Steidel, C. C., & Fruchter, A. 1996, MNRAS, 283, 1388

Madau, P. & Pozzetti, L. 2000, MNRAS, 312, L9

Malkov, M. A. & O'C Drury, L. 2001, Reports on Progress in Physics, 64, 429

Mankuzhiyil, N., Persic, M., & Tavecchio, F. 2010, ApJ, 715, L16

Mannheim, K. 1993, A&A, 269, 67

—. 1998, Science, 279, 684

Maraston, C. & Strömbäck, G. 2011, MNRAS, 1817

Marsden, G., Ade, P. A. R., Bock, J. J., Chapin, E. L., Devlin, M. J., Dicker, S. R., Griffin, M., Gundersen, J. O., Halpern, M., Hargrave, P. C., Hughes, D. H., Klein, J., Mauskopf, P., Magnelli, B., Moncelsi, L., Netterfield, C. B., Ngo, H., Olmi, L., Pascale, E., Patanchon, G., Rex, M., Scott, D., Semisch, C., Thomas, N., Truch, M. D. P., Tucker, C., Tucker, G. S., Viero, M. P., & Wiebe, D. V. 2009, ApJ, 707, 1729

Matsumoto, T. 2001, in IAU Symposium, Vol. 204, The Extragalactic Infrared Background and its Cosmological Implications, ed. M. Harwit & M. G. Hauser, 87

Matsumoto, T., Matsuura, S., Murakami, H., Tanaka, M., Freund, M., Lim, M., Cohen, M., Kawada, M., & Noda, M. 2005, ApJ, 626, 31

Matsuoka, Y., Ienaka, N., Kawara, K., & Oyabu, S. 2011, ApJ, 736, 119

Matsuura, S., Shirahata, M., Kawada, M., Takeuchi, T. T., Burgarella, D., Clements, D. L., Jeong, W.-S., Hanami, H., Khan, S. A., Matsuhara, H., Nakagawa, T., Oyabu, S., Pearson, C. P., Pollo, A., Serjeant, S., Takagi, T., & White, G. J. 2011, ApJ, 737, 2

Mattila, K. 1990, in IAU Symposium, Vol. 139, The Galactic and Extragalactic Background Radiation, ed. S. Bowyer & C. Leinert, 257–268

Maurer, A., Raue, M., Kneiske, T., Horns, D., Elsässer, D., & Hauschildt, P. H. 2012, ApJ, 745, 166

Mazin, D. & Raue, M. 2007, A&A, 471, 439

Metcalfe, L., Kneib, J.-P., McBreen, B., Altieri, B., Biviano, A., Delaney, M., Elbaz, D., Kessler, M. F., Leech, K., Okumura, K., Ott, S., Perez-Martinez, R., Sanchez-Fernandez, C., & Schulz, B. 2003, A&A, 407, 791

Michałowski, M., Hjorth, J., & Watson, D. 2010, A&A, 514, A67

Milliard, B., Donas, J., Laget, M., Armand, C., & Vuillemin, A. 1992, A&A, 257, 24

Mo, H., van den Bosch, F. C., & White, S. 2010, Galaxy Formation and Evolution

Mushotzky, R. F., Cowie, L. L., Barger, A. J., & Arnaud, K. A. 2000, Nature, 404, 459

Nenkova, M., Ivezić, Ž., & Elitzur, M. 2000, Thermal Emission Spectroscopy and Analysis of Dust, Disks, and Regoliths, 196, 77

Neronov, A., Semikoz, D., & Vovk, I. 2010, A&A, 519, L6

Nieppola, E., Tornikoski, M., & Valtaoja, E. 2006, A&A, 445, 441

Odegard, N., Arendt, R. G., Dwek, E., Haffner, L. M., Hauser, M. G., & Reynolds, R. J. 2007, ApJ, 667, 11

Oliver, S. J., Wang, L., Smith, A. J., Altieri, B., Amblard, A., Arumugam, V., Auld, R., Aussel, H., Babbedge, T., Blain, A., Bock, J., Boselli, A., Buat, V., Burgarella, D., Castro-Rodríguez, N., Cava, A., Chanial, P., Clements, D. L., Conley, A., Conversi, L., Cooray, A., Dowell, C. D., Dwek, E., Eales, S., Elbaz, D., Fox, M., Franceschini, A., Gear, W., Glenn, J., Griffin, M., Halpern, M., Hatziminaoglou, E., Ibar, E., Isaak, K., Ivison, R. J., Lagache, G., Levenson, L., Lu, N., Madden, S., Maffei, B., Mainetti, G., Marchetti, L., Mitchell-Wynne, K., Mortier, A. M. J., Nguyen, H. T., O'Halloran, B., Omont, A., Page, M. J., Panuzzo, P., Papageorgiou, A., Pearson, C. P., Pérez-Fournon, I., Pohlen, M., Rawlings, J. I., Raymond, G., Rigopoulou, D., Rizzo, D., Roseboom, I. G., Rowan-Robinson, M., Sánchez Portal, M., Savage, R., Schulz, B., Scott, D., Seymour, N., Shupe, D. L., Stevens, J. A., Symeonidis, M., Trichas, M., Tugwell, K. E., Vaccari, M., Valiante, E., Valtchanov, I., Vieira, J. D., Vigroux, L., Ward, R., Wright, G., Xu, C. K., & Zemcov, M. 2010, A&A, 518, L21+

Orr, M. R., Krennrich, F., & Dwek, E. 2011, ApJ, 733, 77

Pagel, B. E. J. 2001, PASP, 113, 137

Papovich, C., Dole, H., Egami, E., Le Floc'h, E., Pérez-González, P. G., Alonso-Herrero, A., Bai, L., Beichman, C. A., Blaylock, M., Engelbracht, C. W., Gordon, K. D., Hines, D. C., Misselt, K. A., Morrison, J. E., Mould, J., Muzerolle, J., Neugebauer, G., Richards, P. L., Rieke, G. H., Rieke, M. J., Rigby, J. R., Su, K. Y. L., & Young, E. T. 2004, ApJS, 154, 70

Pei, Y. C. & Fall, S. M. 1995, ApJ, 454, 69

Pei, Y. C., Fall, S. M., & Hauser, M. G. 1999, ApJ, 522, 604

Pénin, A., Lagache, G., Noriega-Crespo, A., Grain, J., Miville-Deschênes, M.-A., Ponthieu, N., Martin, P., Blagrave, K., & Lockman, F. J. 2012, A&A, 543, A123

Petry, D., Bond, I. H., Bradbury, S. M., Buckley, J. H., Carter-Lewis, D. A., Cui, W., Duke, C., de la Calle Perez, I., Falcone, A., Fegan, D. J., Fegan, S. J., Finley, J. P., Gaidos, J. A., Gibbs, K., Gammell, S., Hall, J., Hall, T. A., Hillas, A. M., Holder, J., Horan, D., Jordan, M., Kertzman, M., Kieda, D., Kildea, J., Knapp, J., Kosack, K., Krennrich, F., LeBohec, S., Moriarty, P., Müller, D., Nagai, T. N., Ong, R., Page, M., Pallassini, R., Power-Mooney, B., Quinn, J., Reay, N. W., Reynolds, P. T., Rose, H. J., Schroedter, M., Sembroski, G. H., Sidwell, R., Stanton, N., Swordy, S. P., Vassiliev, V. V., Wakely, S. P., Walker, G., & Weekes, T. C. 2002, ApJ, 580, 104

Ponente, P. P., Ascasibar, Y., & Diego, J. M. 2011, MNRAS, 418, 1467

Punch, M., Akerlof, C. W., Cawley, M. F., Chantell, M., Fegan, D. J., Fennell, S., Gaidos, J. A., Hagan, J., Hillas, A. M., Jiang, Y., Kerrick, A. D., Lamb, R. C., Lawrence, M. A., Lewis, D. A., Meyer, D. I., Mohanty, G., O'Flaherty, K. S., Reynolds, P. T., Rovero, A. C., Schubnell, M. S., Sembroski, G., Weekes, T. C., & Wilson, C. 1992, Nature, 358, 477

Raue, M., Kneiske, T., & Mazin, D. 2009, A&A, 498, 25

Razzaque, S., Dermer, C. D., & Finke, J. D. 2009, ApJ, 697, 483

Renault, C., Barrau, A., Lagache, G., & Puget, J.-L. 2001, A&A, 371, 771

Rodighiero, G., Vaccari, M., Franceschini, A., Tresse, L., Le Fevre, O., Le Brun, V., Mancini, C., Matute, I., Cimatti, A., Marchetti, L., Ilbert, O., Arnouts, S., Bolzonella, M., Zucca, E., Bardelli, S., Lonsdale, C. J., Shupe, D., Surace, J., Rowan-Robinson, M., Garilli, B., Zamorani, G., Pozzetti, L., Bondi, M., de la Torre, S., Vergani, D., Santini, P., Grazian, A., & Fontana, A. 2010, A&A, 515, A8

Rowan-Robinson, M. 2001, New A Rev., 45, 631

—. 2009, MNRAS, 394, 117

Salvaterra, R. & Ferrara, A. 2003, MNRAS, 339, 973

Samuelson, F. W., Biller, S. D., Bond, I. H., Boyle, P. J., Bradbury, S. M., Breslin, A., Buckley, J. H., Burdett, A. M., Buss'ons Gordo, J., Carter-Lewis, D. A., Cantanese, M., Cawley, M. F., Fegan, D. J., Finley, J. P., Gaidos, J. A., Hall, T., Hillas, A. M., Krennrich, F., Lamb, R. C., Lessard, R. W., McEnery, J. E., Masterson, C., Quinn, J., Rodgers, A. J., Rose, H. J., Sembroski, G. H., Srinivasan, R., Vassiliev, V. V., Weekes, T. C., & Zweerink, J. 1998, ApJ, 501, L17

Sánchez-Conde, M. A., Paneque, D., Bloom, E., Prada, F., & Domínguez, A. 2009, Phys. Rev. D, 79, 123511

Saunders, W., Rowan-Robinson, M., Lawrence, A., Efstathiou, G., Kaiser, N., Ellis, R. S., & Frenk, C. S. 1990, MNRAS, 242, 318

Schlegel, D. J., Finkbeiner, D. P., & Davis, M. 1998, ApJ, 500, 525

Schroedter, M., Badran, H. M., Buckley, J. H., Bussons Gordo, J., Carter-Lewis, D. A., Duke, C., Fegan, D. J., Fegan, S. F., Finley, J. P., Gillanders, G. H., Grube, J., Horan, D., Kenny, G. E., Kertzman, M., Kosack, K., Krennrich, F., Kieda, D. B., Kildea, J., Lang, M. J., Lee, K., Moriarty, P., Quinn, J., Quinn, M., Power-Mooney, B., Sembroski, G. H., Wakely, S. P., Vassiliev, V. V., Weekes, T. C., & Zweerink, J. 2005, ApJ, 634, 947

Shang, C., Haiman, Z., Knox, L., & Oh, S. P. 2012, MNRAS, 421, 2832

Shectman, S. A. 1973, ApJ, 179, 681

—. 1974, ApJ, 188, 233

Silva, L., Granato, G. L., Bressan, A., & Danese, L. 1998, ApJ, 509, 103

Soifer, B. T., Helou, G., & Werner, M. 2008, ARA&A, 46, 201

Soifer, B. T. & Neugebauer, G. 1991, AJ, 101, 354

Sokolsky, P. & for the HiRes Collaboration. 2010, ArXiv e-prints

Somerville, R. S., Gilmore, R. C., Primack, J. R., & Dominguez, A. 2011, arXiv: 1104.0669

Stanev, T., Engel, R., Mücke, A., Protheroe, R. J., & Rachen, J. P. 2000, Phys. Rev. D, 62, 093005

Stanev, T. & Franceschini, A. 1998, ApJ, 494, L159

Stecker, F. W., Baring, M. G., & Summerlin, E. J. 2007, ApJ, 667, L29

Stecker, F. W. & de Jager, O. C. 1993, ApJ, 415, L71

Stecker, F. W., Malkan, M. A., & Scully, S. T. 2006, ApJ, 648, 774

Stecker, F. W. & Scully, S. T. 2006, ApJ, 652, L9

Teplitz, H. I., Chary, R., Elbaz, D., Dickinson, M., Bridge, C., Colbert, J., Le Floc'h, E., Frayer, D. T., Howell, J. H., Koo, D. C., Papovich, C., Phillips, A., Scarlata, C., Siana, B., Spinrad, H., & Stern, D. 2011, AJ, 141, 1

Tinsley, B. M. 1981, ApJ, 250, 758

Totani, T., Yoshii, Y., Maihara, T., Iwamuro, F., & Motohara, K. 2001, ApJ, 559, 592

Treister, E., Urry, C. M., Van Duyne, J., Dickinson, M., Chary, R.-R., Alexander, D. M., Bauer, F., Natarajan, P., Lira, P., & Grogin, N. A. 2006, ApJ, 640, 603

Vassiliev, V. V. 2000, Astroparticle Physics, 12, 217

Völk, H. J., Aharonian, F. A., & Breitschwerdt, D. 1996, Space Sci. Rev., 75, 279

Volpe, F., Ohm, S., Hauser, M., Kaufmann, S., Gérard, L., Costamante, L., Fegan, S., & Ajello, M. 2011, ArXiv: 1105.5114

Weekes, T. C. 2008, in American Institute of Physics Conference Series, Vol. 1085, American Institute of Physics Conference Series, ed. F. A. Aharonian, W. Hofmann, & F. Rieger, 3–17

Wehrle, A. E., Pian, E., Urry, C. M., Maraschi, L., McHardy, I. M., Lawson, A. J., Ghisellini, G., Hartman, R. C., Madejski, G. M., Makino, F., Marscher, A. P., Wagner, S. J., Webb, J. R., Aldering, G. S., Aller, M. F., Aller, H. D., Backman, D. E., Balonek, T. J., Boltwood, P., Bonnell, J., Caplinger, J., Celotti, A., Collmar, W., Dalton, J., Drucker, A., Falomo, R., Fichtel, C. E., Freudling, W., Gear, W. K., Gonzalez-Perez, N., Hall, P., Inoue, H., Johnson, W. N., Kazanas, D., Kidger, M. R., Kii, T., Kollgaard, R. I., Kondo, Y., Kurfess, J., Lin, Y. C., McCollum, B., McNaron-Brown, K., Nagase, F., Nair, A. D., Penton, S., Pesce, J. E., Pohl, M., Raiteri, C. M., Renda, M., Robson, E. I., Sambruna, R. M., Schirmer, A. F., Shrader, C., Sikora, M., Sillanpaeae, A., Smith, P. S., Stevens, J. A., Stocke, J., Takalo, L. O., Teraesranta, H., Thompson, D. J., Thompson, R., Tornikoski, M., Tosti, G., Treves, A., Turcotte, P., Unwin, S. C., Valtaoja, E., Villata, M., Xu, W., Yamashita, A., & Zook, A. 1998, ApJ, 497, 178

Wright, E. L. 2004, New A Rev., 48, 465

Xu, C. K., Donas, J., Arnouts, S., Wyder, T. K., Seibert, M., Iglesias-Páramo, J., Blaizot, J., Small, T., Milliard, B., Schiminovich, D., Martin, D. C., Barlow, T. A., Bianchi, L., Byun, Y.-I., Forster, K., Friedman, P. G., Heckman, T. M., Jelinsky, P. N., Lee, Y.-W., Madore, B. F., Malina, R. F., Morrissey, P., Neff, S. G., Rich, R. M., Siegmund, O. H. W., Szalay, A. S., & Welsh, B. Y. 2005, ApJ, 619, L11

Younger, J. D. & Hopkins, P. F. 2011, MNRAS, 410, 2180

Zacharopoulou, O., Khangulyan, D., Aharonian, F. A., & Costamante, L. 2011, ApJ, 738, 157

Zech, A., Behera, B., Becherini, Y., Boisson, C., Giebels, B., Hauser, M., Kastendieck, M., Kaufmann, S., Kosack, K., Lenain, J. ., de Naurois, M., Punch, M., Raue, M., Sol, H., Wagner, S., & the H. E. S. S. collaboration. 2011, ArXiv: 1105.0840

Zemcov, M., Blain, A., Halpern, M., & Levenson, L. 2010, ApJ, 721, 424